

POLITECNICO DI TORINO

MASTER's Degree in Energy and Nuclear Engineer



MASTER's Degree Thesis

Development of a tool for the energy feasibility analysis of a floating city

Supervisors

Prof.ssa Giuliana MATTIAZZO

Prof. Sergej Antonello SIRIGU

Dr.Ing. Beatrice FENU

Candidate

Ludovica Maria GULLO

A.Y. 2021/2022

Summary

Seventy-one percent of our planet is covered by sea: it is better to call it an ocean planet than planet earth. The challenge of our time is undoubtedly to curb climate change: it is well known that global warming and rising sea levels are among the most discussed environmental issues. It is estimated that by 2050, 90 percent of the world's largest cities will be exposed to sea level rise (UN-Habitat). The leading causes lie in the concomitant of various environmental phenomena: such as global warming of the atmosphere, melting of glaciers at the poles, coastal erosion, and increasingly frequent flooding. The sea, like plants, produces 50 percent of the oxygen and captures 25 percent of the carbon dioxide: thus, it alone lends us a big hand in coping with climate change. The sea has constantly recreated a vital role in our lives, but why not try to give it an even more important one, namely housing us? Why not shift our daily lives to the water as we live on land? Life on water could be the answer to land scarcity and the impact of climate change. So, the constraint is that the new "floating cities" be designed to be autonomous, carbon-neutral, and support marine environments. On the other hand, from the energy point of view, the offshore sector seems to be increasingly promising: consider all the new projects and research funding for the construction of offshore wind farms, floating solar, tidal energy, and wave energy converters. Floating cities growing in the sea would thus have a close relationship with these types of renewable energy. The share of electricity generated from renewable energy sources (RES) is rising, and energy communities (ECs) are one of the options to increase self-consumption in aggregate systems. The type of electricity grid of ECs must be designed to manage the variability of RES and zero inertia of technologies. This work aims to propose a methodology and develop a tool based on MatLab software that can furnish the energy pre-feasibility analysis of a possible floating community as autonomous from land.

Acknowledgements

Essendo questa una tesi scientifica, vorrei provare ad emozionarvi con un codice MatLAB, consapevole, però, che potrei riuscirci solo con pochi, con un pochino di furbizia, cerco di semplificarvi il compito provando a commuovervi tramite i ringraziamenti.

Non è stato un percorso sempre facile e guardandomi indietro, penso sia bellissimo poter affermare “sono arrivata fino a qua grazie alle mie capacità” ma credo sia molto più saggio e più realistico riconoscere che “sono arrivata fino a qua perché mi sono impegnata ma soprattutto perché lungo la mia strada ho incontrato alcune persone”.

Di seguito voglio quindi ringraziare queste persone:

A Mia mamma e mio papà, per avermi insegnato come scrivere la mia rotta nella vita: senza avermi mai imposto alcun giro di boa mi hanno sempre incoraggiato a navigare dove il vento soffiava più forte.

A mio fratello, per essere la persona che ogni giorno mi motiva sempre ad essere da esempio.

Ad i miei 6 angeli, perché definirli nonni sarebbe riduttivo: coloro che indubbiamente sono i miei più grandi fan, che lodano la mia vita mettendola al pari dell’odissea, che hanno sempre creduto in me, più di me stessa e forse più del dovuto.

Ai miei tre zii ed a tutto il resto della ciurma, complici e amici da sempre.

Un ringraziamento speciale va alla professoressa Giuliana Mattiazzo che mi ha permesso, non solo di sviluppare questa tesi, ma soprattutto di vivere quella che indubbiamente resterà l’esperienza universitaria che più mi ha fatto crescere. Ringrazio Sergio Sergey e Beatrice Fenu che mi hanno guidato nella stesura della tesi, essendo per me una guida fondamentale. Un ringraziamento anche ad Enrico Giglio ed Alice Rosiello ed ai membri del MORE energy lab, che hanno assunto un ruolo fondamentale per questo lavoro.

Ai miei colleghi del cuore, che sono stati la mia più grande fortuna in questi anni: un aiuto costante, senza rivalità, che mi ha protetta quando non l'ho chiesto ma ne avevo bisogno e che ogni volta che ne ho avuto bisogno si è fatto trovare lì, pronto. Qualcuno di voi si è lasciato convincere da me a svegliarsi all'alba mentre qualcun'altro mi ha fatto studiare fino alle 4 di notte. A Marco, Ginevra, Gabriel, Valerio, Francesco, Beatrice, Vittorio, Danilo e tutti coloro con cui ho condiviso le aule universitarie.

A Sofia, Marta, Caterina, Francesca, Filippo, Claudio, Andrea e tutti i miei amici "di giù" che hanno sempre provato, invano, a placare le mie ansie.

Ai miei amici del Polito Sailing Team: la mia famiglia torinese in cui ho trovato dei veri e propri genitori, fratelli, cugini e figli. Menziono solo Leo perché senza di lui, non potreste proprio leggere questo documento.

A coloro che hanno riscaldato i $-9\text{ }^{\circ}\text{C}$ costanti durante il mio Erasmus Norvegese, e che con me hanno visto l'aurora boreale ed hanno scalato cime innevate.

Ai miei bambini della scuola vela, che mi ricordano sempre quanto sia importante fare qualsiasi cosa con passione, altrimenti la gratificazione è nulla. Questa tesi è simile a quei sogni di cui tanto mi avete raccontato, sono sicura che vi piacerà.

ALLORA, per concludere: con questo lavoro termina la mia esperienza universitaria, che porterò sempre con me come un punto felice della mia vita. Ci sono stati momenti bellissimi ed altri difficili: entrambi, per un motivo o per un altro (consapevole di essere molto fortunata nel poterlo dire) li ricorderò con piacere e col sorriso.

"Un punto!... così passeggero,
che in vero passò non raggiunto,
ma bello così, che molto ero
felice, felice, quel punto!"
G.Pascoli

In memoria di Clio,

Table of Contents

| | |
|--|-------|
| List of Tables | XII |
| List of Figures | XIII |
| Acronyms | XVIII |
| 1 Introduction | 1 |
| 1.1 Motivation | 1 |
| 1.2 Thesis structure | 2 |
| 2 State of the art of living floating platforms | 3 |
| 2.1 Floating village existing | 3 |
| 2.2 Living Floating platform projects | 4 |
| 2.2.1 Oceanix City | 5 |
| 2.2.2 Maldive Floating City | 6 |
| 2.2.3 Oxagon City | 6 |
| 2.2.4 Schoon Schip | 7 |
| 2.2.5 Urban Rigger | 8 |
| 2.2.6 Ocean Builders | 9 |
| 2.3 SeaForm Project | 10 |
| 3 Technical Background | 11 |
| 4 Methodology | 13 |
| 4.1 Typical Meteorological Year | 15 |
| 4.2 Resource Analysis | 18 |
| 4.2.1 Solar Resource | 18 |
| 4.2.2 Wind Resource | 19 |
| 4.2.3 Wave Resource | 20 |
| 4.3 Estimation of consumption | 26 |
| 4.3.1 Thermal load | 32 |

| | | |
|----------|--|------------|
| 4.3.2 | Electric device load | 38 |
| 4.3.3 | Lighting load | 42 |
| 4.3.4 | Total load | 44 |
| 4.4 | Productivity Analysis | 47 |
| 4.4.1 | PV productivity | 48 |
| 4.4.2 | WT productivity | 50 |
| 4.5 | Storage | 52 |
| 4.6 | Techno-economic analysis | 56 |
| 4.7 | Critical issues of the model and future improvements | 60 |
| 5 | Case study: Venice | 62 |
| 5.1 | Venice overview | 62 |
| 5.1.1 | Depopulation | 63 |
| 5.1.2 | Sea Level | 64 |
| 5.2 | Venice energy consumption | 64 |
| 5.3 | SeaForm | 67 |
| 6 | Results | 69 |
| 6.1 | Typical meteorologic year | 69 |
| 6.2 | Resource Analysis | 74 |
| 6.2.1 | Sun | 74 |
| 6.2.2 | Wind | 77 |
| 6.2.3 | Wave | 83 |
| 6.2.4 | Renewable Resource | 85 |
| 6.3 | Estimation of consumption | 86 |
| 6.3.1 | External Temperature | 86 |
| 6.3.2 | Thermal load | 87 |
| 6.3.3 | Electronic devices load | 90 |
| 6.3.4 | Lighting load | 91 |
| 6.3.5 | Six uniform platforms case | 92 |
| 6.3.6 | Total load | 93 |
| 6.4 | Productivity Analysis | 95 |
| 6.4.1 | PV productivity | 95 |
| 6.4.2 | WT productivity | 96 |
| 6.4.3 | Renewable production | 97 |
| 6.5 | Storage and presentation of energy scenario | 99 |
| 6.6 | Techno-economic analysis | 104 |
| 7 | Conclusion and future work | 106 |

| | |
|-----------------------------|-----|
| A Appendix | 108 |
| A.1 TMY parameter | 109 |
| A.2 Other cases | 110 |
| Bibliography | 116 |

List of Tables

| | | |
|------|---|-----|
| 4.1 | Weighting values for Sandia Method | 16 |
| 4.2 | Models and databases for the solar resource | 19 |
| 4.3 | Models and databases for the wind resource | 20 |
| 4.4 | Models and databases for the wave resource | 21 |
| 4.5 | Italian Climatic Zones | 29 |
| 4.6 | Climatic data input for load | 30 |
| 4.7 | Dimensional data input for thermal loads | 32 |
| 4.8 | Heat gain for the different applications | 35 |
| 4.9 | Confort Condition in Summer | 36 |
| 4.10 | Confort Condition in Winter | 36 |
| 4.11 | Typical daily consumption for residential application with 4 people | 46 |
| 4.12 | Storage property | 53 |
| 4.13 | Investment Cost per kW for each component of the system [46] [47] | 58 |
| 4.14 | Operation and maintenance per kW for each component of the system [43] | 59 |
| 6.1 | Sensors of ISMAR | 70 |
| 6.2 | Building Parameters | 87 |
| 6.3 | PV Technical Data | 95 |
| 6.4 | WT Technical Data | 96 |
| 6.5 | Battery bank specification: Li-ion [61] | 99 |
| 6.6 | Panoramic of energy scenario | 101 |
| 6.7 | Panoramic of energy percentage | 101 |
| 6.8 | Investment Cost per kW for each component of the system [46] [47] | 105 |
| 6.9 | KPs of the different cases | 105 |
| A.1 | Panoramic of energy scenarios | 115 |
| A.2 | Panoramic of energy percentages | 115 |

List of Figures

| | | |
|------|--|----|
| 1.1 | Agenda 2030 | 2 |
| 2.1 | Kampong Ayer | 4 |
| 2.2 | Makoko | 4 |
| 2.3 | Mahuli | 4 |
| 2.4 | Floating city projects in the world | 4 |
| 2.5 | Oceanix City | 5 |
| 2.6 | Oceanix Village | 5 |
| 2.7 | Oceanix Neighborhood | 6 |
| 2.8 | Oxagon Project | 7 |
| 2.9 | Main features of Oxagon | 7 |
| 2.10 | Schoon schip | 8 |
| 2.11 | Urban rigger | 9 |
| 3.1 | General sketch of a Microgrid [12] | 12 |
| 4.1 | Tool's flowchart | 14 |
| 4.2 | Platform base | 26 |
| 4.3 | Modular building | 26 |
| 4.4 | Platform Building | 27 |
| 4.5 | Piece model | 27 |
| 4.6 | Italian Climatic Zones | 29 |
| 4.7 | Occurrence in living space | 31 |
| 4.8 | Occurrence in living space | 31 |
| 4.9 | Internal Temperature set point for living space heating [25] | 37 |
| 4.10 | Internal Temperature set point for living space cooling [25] | 37 |
| 4.11 | Internal Temperature set point for office space [25] | 38 |
| 4.12 | Use fraction of device load for residential [25] [30] | 40 |
| 4.13 | Use fraction of device load for office [25] [30] | 41 |
| 4.14 | Use fraction of lighting in residential | 43 |
| 4.15 | Use fraction of lighting in office | 44 |

| | | |
|------|--|----|
| 4.16 | Algorithm consumption estimation | 45 |
| 4.17 | Algorithm RES productivity | 47 |
| 4.18 | Air Temperature influence on PV efficiency | 49 |
| 4.19 | Power Curve of wind turbines | 50 |
| 4.20 | Power Coefficient of wind turbines | 51 |
| 4.21 | Battery charging algorithm | 54 |
| 4.22 | Ocean Battery | 61 |
| | | |
| 5.1 | Venice from the top | 62 |
| 5.2 | Births | 63 |
| 5.3 | Deaths | 63 |
| 5.4 | Natural balance | 63 |
| 5.5 | Mosè in Venice | 64 |
| 5.6 | kWh per abitant | 65 |
| 5.7 | Venice energy production and request | 65 |
| 5.8 | Energy consumption per sector | 66 |
| 5.9 | Pavillon exposition | 67 |
| 5.10 | Six platform configuration | 68 |
| | | |
| 6.1 | ISMAR platform | 69 |
| 6.2 | TMY | 70 |
| 6.3 | TMY Parameters profile | 71 |
| 6.4 | Comparison between Solar irradiation profile of TMW and the real years | 72 |
| 6.5 | Comparison between Air Temperature profile of TMW and the real years | 72 |
| 6.6 | Comparison between Humidity profile of TMW and the real years | 73 |
| 6.7 | Comparison between Wind Speed profile of TMW and the real years | 73 |
| 6.8 | Sensor solar | 74 |
| 6.9 | Monthly average | 75 |
| 6.10 | Solar power density TDAY | 75 |
| 6.11 | Daily irradiance | 76 |
| 6.12 | Wind speed sensor | 77 |
| 6.13 | Wind direction sensor | 77 |
| 6.14 | Wind rose | 78 |
| 6.15 | Monthly average daily wind speed | 79 |
| 6.16 | Monthly energy density | 79 |
| 6.17 | Daily average wind speed | 80 |
| 6.18 | Daily average wind power density | 81 |
| 6.19 | Wind power density TDAY | 82 |
| 6.20 | Wave sensor | 83 |

| | | |
|------|--|-----|
| 6.21 | Wave occurrence scatter | 83 |
| 6.22 | Energy wave scatter | 83 |
| 6.23 | Wave rose | 84 |
| 6.24 | Monthly power density of wave | 84 |
| 6.25 | Montly renewable energy density | 85 |
| 6.26 | Renewable energy density of TDAYS | 85 |
| 6.27 | Temperature sensor | 86 |
| 6.28 | Thermal load profiles for residential piece in a Typical winter Day . | 88 |
| 6.29 | Thermal load profiles for residential piece in a Typical summer Day | 88 |
| 6.30 | Thermal load profile for office piece in a Typical winter Day | 88 |
| 6.31 | Thermal load profile for office piece in a Typical summer Day . . . | 89 |
| 6.32 | Thermal load profile for support piece in a Typical winter Day . . . | 89 |
| 6.33 | Thermal load profile for support piece in a Typical summer Day . . | 89 |
| 6.34 | Electronic devices load profiles for residential piece in a Typical Day weekly | 90 |
| 6.35 | Electronic devices load profiles for residential piece in a Typical Day holiday | 90 |
| 6.36 | Electronic devices load profile for office piece in a Typical Day weekly | 90 |
| 6.37 | Lighting load profile for residential piece in a Typical Day weekly . | 91 |
| 6.38 | Lighting load profile for office piece in a Typical Day weekly | 91 |
| 6.39 | Dark hours in Venice 2022 [60] | 92 |
| 6.40 | Configuration with pieces with different applications | 92 |
| 6.41 | Total loads | 93 |
| 6.42 | TDAY load case | 94 |
| 6.43 | Montly PV productivty | 95 |
| 6.44 | Annual production of wind turbines | 96 |
| 6.45 | Monthly WT productivity | 97 |
| 6.46 | Monthly RES productivity | 97 |
| 6.47 | Daily RES productivity | 98 |
| 6.48 | TDAYS renewable productivity | 98 |
| 6.49 | Comparison between renewable power and consumption in hour resolution | 99 |
| 6.50 | Monthly comparison between renewable power and consumption . . | 100 |
| 6.51 | Caracteristic spring weekly profile | 100 |
| 6.52 | Waste energy profile | 101 |
| | | |
| A.1 | TMY Water temperature | 109 |
| A.2 | TMY Rain profile | 109 |
| A.3 | Comparison between renewable power and consumption in hour resolution | 110 |
| A.4 | Load consumption for typical days | 110 |

| | | |
|------|--|-----|
| A.5 | Monthly load consumption | 111 |
| A.6 | Monthly comparison between renewable power and consumption . . | 111 |
| A.7 | Characteristic spring weekly profile | 111 |
| A.8 | Waste energy profile | 112 |
| A.9 | Comparison between renewable power and consumption in hour resolution | 112 |
| A.10 | Load consumption for typical days | 113 |
| A.11 | Monthly load consumption | 113 |
| A.12 | Monthly comparison between renewable power and load consumption | 114 |
| A.13 | Characteristic spring weekly profile | 114 |
| A.14 | Waste energy profile | 114 |

Acronyms

EC

Energy Communities

TMY

Typical Meteorological Year

STC

Standard Temperature Condition

ISMAR

Istituto delle Scienze Marine

TD

Typical Day

RES

Renewable Energy Systems

PV

Photovoltaic Panel

WT

Wind Turbine

KPs

Key Performance Indicators

NPV

Net Present Value

LCOE

Levelised Cost of Energy

Chapter 1

Introduction

1.1 Motivation

It would be shortsighted not to design cities without considering the climatic and environmental changes already underway: "making cities and human settlements inclusive, safe, resilient and sustainable" is, in fact, one of the objectives of the 2030 Agenda. Cities near the sea currently need more space to build on, and it is also essential that they improve their defenses against coastal erosion. In some areas, solutions are already in place to bring water to life. The spread of cities over water has occurred for centuries in low countries such as the Netherlands, where about 17% of the country's current territory has been reclaimed from the sea or lakes. The objective of the new projects that intend to bring life to the water is to promote a sustainable lifestyle that is as independent as possible from the mainland. One of the most recent projects in this area is the foundation of the SeaForm Start-up: a reality that tries to fit into this research area by proposing an 'Italian' solution.

This thesis work was therefore born within this project to start a study from the energy point of view for the structure to be built. It will technically verify the feasibility that the floating city is self-sustaining or determine the limit of autonomy it can reach by proposing alternative solutions.



Figure 1.1: Agenda 2030

1.2 Thesis structure

The thesis is structured into six chapters. The thesis forms by showing the state of the art of floating cities in the world: the aim is to explain how although this "life revolution" may seem like a utopia, it is getting closer and closer and more and more treated. Then, in the second paragraph, a little background of projects that, from the energy point of view, can be treated likewise is presented.

The most powerful chapter of the thesis is the third: here, the methodology chosen to carry out the energy pre-feasibility analysis is presented in detail. The objective of this part is to provide as generic a procedure as possible for dealing with a study of this kind: trying to be as generic as possible, the tools are provided to be able to carry out the analysis of the resource at any chosen site, the estimation of consumption, the calculation of energy productivity, and the sizing and type of storage to be provided.

Chapter 4 illustrates the case study of the Venice site, the first place where SeaForm started moving to install a prototype. Chapter 5 reports the results obtained from the energy feasibility investigation of the case study.

Finally, the main results are resumed, and some tips are made for possible next steps to continue this work.

Chapter 2

State of the art of living floating platforms

2.1 Floating village existing

On the planet, it is estimated that about 13 thousand people already live in structures such as stilts and settlements partly built on the water. Although this problem has only recently developed, man's relationship with water has very ancient origins. Source of life and sustenance, this element has been, for some communities, the element with which to share their daily lives. This is the case of Majuli, a river island in India where its inhabitants have always adapted their lifestyle to the river's moods. This implies adjusting the crops to flood cycles, filling artificial ponds for water storage, and living in boats and stilts houses. This adaptation to environmental conditions also applies to Makoko, a floating slum in Lagos in, Nigeria. Also known as Venice of Africa, this vast neighborhood was born naturally due to the need to expand the city in the face of the exhaustion of the area available on the mainland led to the construction of stilts and boats for transport and trade. Kampong Ayer in Brunei comprises neighborhoods of houses, schools, and mosques built on stilts above the Brunei River near the capital's city center. It has an area of about 10 square kilometers (3.9 sq mi); the total population was 10,250 in 2016. The community of Makoko of Lagos, in Nigeria, also called Black Venice or Venice of Africa is a slum located on the outskirts of Lagos, Nigeria. Today the population is estimated to be 30,000 to 250,000.



Figure 2.1: Kampong Ayer



Figure 2.2: Makoko



Figure 2.3: Mahuli

2.2 Living Floating platform projects

The challenge of our time is to stem climate change, at least it would be short-sighted not to design cities without taking into account the climate and environmental changes already underway.



Figure 2.4: Floating city projects in the world

2.2.1 Oceanix City

The American company Oceanix in collaboration with the Center for Ocean Engineering of MIT, the city of Busan, and UN-Habita, has decided to build the world's first prototype of a modular floating city on the coasts of Busan in South Korea. The project involves the construction of 75 hectares to accommodate 10,000 people and will cost around 600 million.

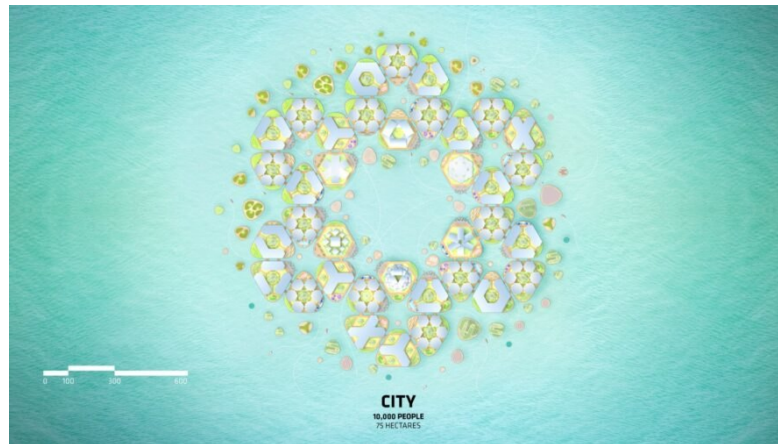


Figure 2.5: Oceanix City

The city will be divided into single villages of 12.2 hectares for 1650 people, each with a triangular neighborhood of 2 hectares to accommodate about 300 residents. The construction of the first neighborhood is scheduled to begin in 2023. conceived as a "modular maritime metropolis," Oceanix City is engineered for self-sufficiency with features from net-zero energy and zero-waste systems to sharing culture.



Figure 2.6: Oceanix Village

Precisely because the goal is the generation of a city, modular triangular floating platforms are used which, grouped in 6 to 6, generate a hexagon of 1 hectare of surface, equal to 3.5 football fields. Each aggregation can accommodate about 300 people, and it is possible to increase the size of the city by adding other agglomerations from 6 platforms until the desired dimension is reached. Every single island is anchored to the ocean floor and allowing it to withstand even Category 5 hurricanes with winds exceeding 250 km/h. The housing units and the individual islands are totally eco-sustainable, built with local materials such as wood and bamboo, with wind and solar plants in profusion, and with greenhouses and gardens for the cultivation of fruit and vegetables. [1]



Figure 2.7: Oceanix Neighborhood

2.2.2 Maldivé Floating City

Maldives Floating City is another example of the same goal of building a new city on water. Located 10 minutes by boat from the capital of the Maldives, Male, this city wants to respond to the problem of rising seas that will soon overwhelm this wonderful area. The masterplan, which recalls the shapes of the coral reef and includes homes, shops, and industries, is the only vision at the present moment of the project, which, however, bases its strength on its government's support. [2]

2.2.3 Oxagon City

A pilot project for the "floating islands" is that of OXAGON by NEOM, which aims to be the largest floating structure in the world. It will contribute to Saudi Arabia's regional trade and trade (Suez Canal) and support the creation of a new focal point for global trade flows. This new city, built around innovative new industries, aims to accommodate a population of 90 people and 70 jobs by 2030.M. Also part

of this vision is OXAGON, an octagonal-shaped area of a floating city on the sea with a diameter of 7km and hosting up to 90000 people by 2030. Rather than a habitable city, it is mainly an industrial pole with the aim of establishing a new hub for clean and innovative manufacturing and allowing easy trade with the rest of the world through the strategic location. [3]



Figure 2.8: Oxagon Project

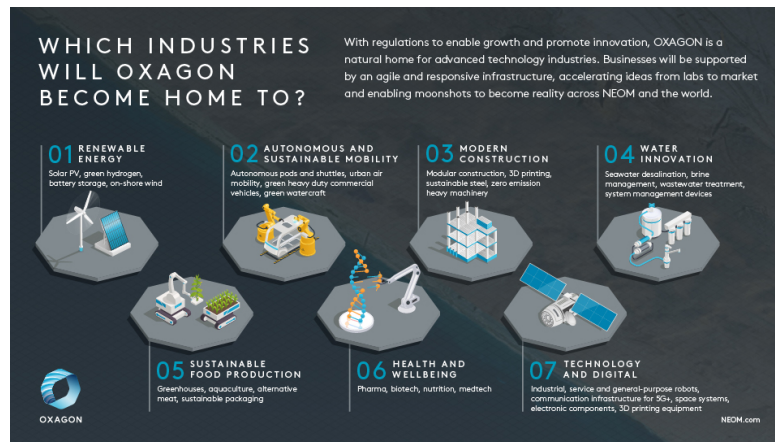


Figure 2.9: Main features of Oxagon

2.2.4 Schoon Schip

Shoon Ship is a floating residential area in the Johan van Hasselt canal, a side canal of the IJ in Buiksloterham, Amsterdam North. The feature of the structure is that it is ecologically and socially sustainable. Since 2020, 46 families have lived in the district, meaning 144 residents. The water houses are very well insulated ($EPC =$

maximum 0) and are not connected to the natural gas network. About 30 heat pumps extract heat from the water in the canal (equatorial) and provide heating using passive solar heat as much as possible. Electricity is produced with about 516 photovoltaic solar panels, and each house has a large battery where temporary surpluses can be stored. All the houses are connected to a common smart grid. This grid allows us to exchange electricity intelligently. With 46 families, we have only one connection to the national energy grid. There is a separate flow for draining gray water (from the dishwasher and washing machine) and black water (from the toilet). One goal is to transport black water to a bio refinery, ferment it, and convert it into energy. All houses have a green roof covering at least one third of the area. Electric cars, electric cargo bikes, and e-bikes are shared. [4]

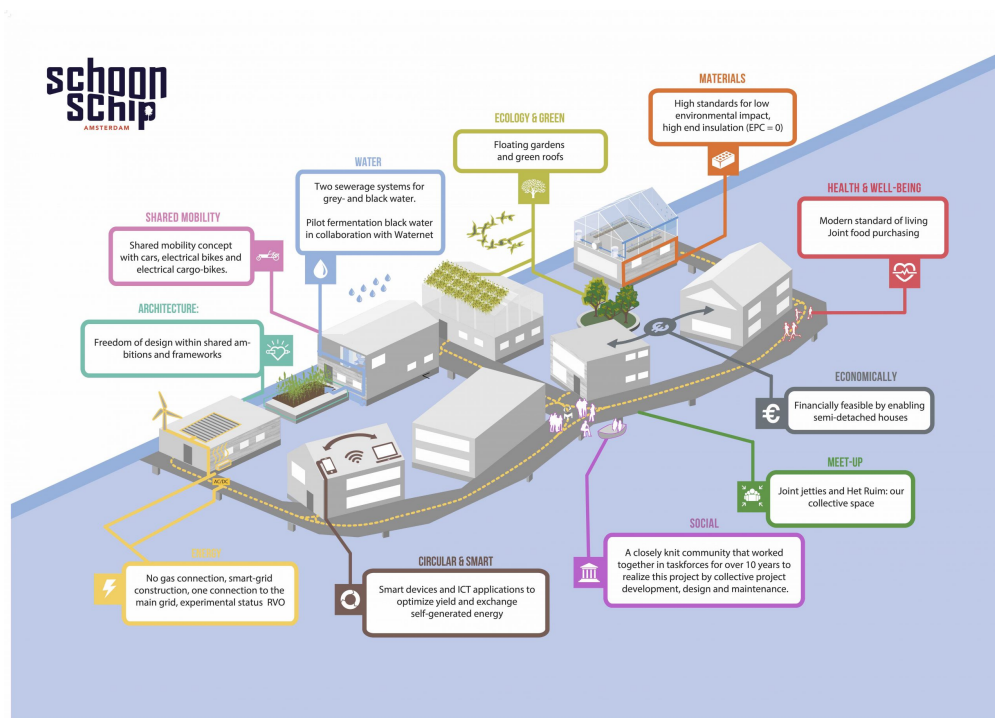


Figure 2.10: Schoon schip

2.2.5 Urban Rigger

Urban Rigger is currently working on different projects in the hope of bringing sustainable accommodation to harbours around the world: Copenhagen, Cork and San Francisco. Urban Rigger is a sustainable housing concept, designed by BIG (Bjarke Ingels Group), with the purpose of changing how we build and live ecocentrically with respect to nature, organic live and the climate. It is the

future of water housing, developed to help cities and municipalities becoming more sustainable by building Doughnut-inspired communities floating on water. By combining the most sustainable building materials with a unique approach to circular economy and sharing economy, Urban Rigger offers an affordable housing concept, that is inspired by industrial environments and the creative urban scene. [5]



Figure 2.11: Urban rigger

2.2.6 Ocean Builders

It is remarkable the project by Ocean Builders for Seapods in the water, luxury floating accommodations in the waters of Panama that use air-filled steel tubes and designed as exclusive homes or vacation destinations. This project has not yet been realised and focuses on a high-profile clientele, therefore on profits, rather than on contingent needs for which life on the water represents a concrete solution. [6]

2.3 SeaForm Project

The founding principle of SeaForm is to offer a solution to the problem of sea level rise, which in the future will lead to the disappearance of most of the coasts, especially of small islands. This goal is parallel to allowing current cities to expand not by consuming more land but by intelligently using the resource of the sea. Therefore, the central theme is sustainability and social commitment, helping to build a new sustainable model capable of responding to urgent climatic and demographic questions. The final goal of the Start-up is to create a real floating community made up of the interconnection of floating hexagonal platforms. The project is very ambitious and also very recent. At the first design stage, we are concentrating on two aspects: the actual design of a first module and the creation of a prototype on a reduced scale to be exhibited at the Venice Biennale in 2024. The sizing and feasibility study of the first module (the subject of this thesis) is currently being developed, the substructure of which can become the "basic module." The platform's substructure is hexagonal, with a diameter of 57 meters and an area of 2,107 square meters; it will be made of reinforced concrete for a total volume of 12,661 cubic meters. Its maximum dimensions were dictated by construction constraints, given the maximum dimensions of the construction sites in which it can be built. The project is currently in an initial phase and can be divided into two main parts: the substructure and the superstructure. The first guarantees the structure and stability of the one above, dedicated to congress, recreational, and living spaces. This thesis focuses on the energetic dimension of the upper structure. The goal is to develop a method to be followed in order to quickly determine the energy limits and advantages of a design configuration in a given place.

Chapter 3

Technical Background

A pre-feasibility study is a rough screening aiming at identifying the most promising idea(s) and discard the unattractive options. This reduces the number of options that is chosen to proceed with a more detailed feasibility study and eventually with business development, ultimately saving time and money. The aim of the thesis is to investigate the creation of an Energy Community. Energy communities are an increasingly present reality today: an association of people, commercial and non-commercial activities, who decide to join forces to equip themselves with one or more shared plants for the production and self-consumption of energy from renewable sources (solar, wind, geothermal, ocean, waste-to-energy, etc.). Generally speaking, this is an energy scenario based on distributed generation, which favors the development of zero-kilometer energy and smart grids. The goal is to make the floating community as independent as possible from an energy point of view from the border town to which it stands. The objective is, therefore, to search for methods to produce clean energy in order to meet the energy needs of the project and to search for the configuration of proposed activities that have the energy needs most satisfied with hybrid renewable energy systems. Energy communities represent one of the primary constituent elements of intelligent grids, both in typical applications connected to the public grid, and in off-grid cases, in the absence of electricity distribution. The motivations for the design of this kind of system can be technological, economic, environmental, and social. There is also concern about the fundamentals of energy policies, such as the decentralization of energy systems and energy self-sufficiency [7]. Factors with positive effects are environmental awareness and intention of energy independence. Currently, the most popular applications for the development of microgrids are island communities and rural villages. Precisely because of their difficulty in being connected to the city electricity grid. So, for this thesis's elaboration, reference was made to microgrid and energy community projects reported in the literature of island communities or conceptually similar offshore communities [8] and rural villages [9].

To the electricity system, the energy communities (or energy communities) can be classified as:

- Off-grid: isolated networks, not connected to the public electricity grid
- "Isolable" on-grid: grids completely interconnected to the public electricity grid, capable of bi-directional exchange of electricity and self-sustaining for a the specific period of time in the event of unavailability of the electricity grid
- "Asynchronous" on-grid: grids connected to the public electricity grid, which can only draw energy from the grid in case of need but cannot supply it.

The categories of users interested in forming part of an EC are many. In particular, users can be identified in the residential area, such as condominiums and residential complexes, and the tertiary sector, such as shopping, logistic centers, and hospital complexes.[10] Microgrids are a part of a more extensive system that allows the smart grid to become a reality. They constitute a local distribution system made up of generators and accumulation systems, capable of operating either autonomously ("off-grid") or in connection with the national electricity system. It operates as a single controllable system in order to provide electricity and heat to the local area, exploiting energy from renewable sources, storing them, and making them available to internal users. The components of a micro-grid are five [11]:

- Distribution generation
- Loads
- Energy Storage
- Control device
- Point of common coupling: is a single point in the electrical circuit which connects the micro-grid to the utility

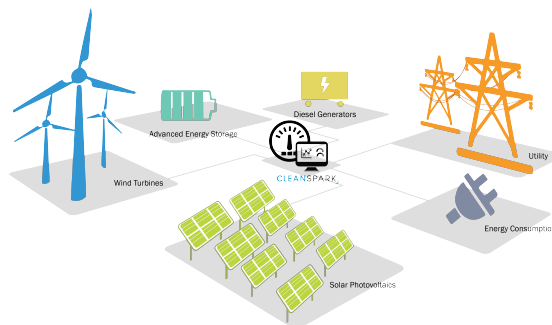


Figure 3.1: General sketch of a Microgrid [12]

Chapter 4

Methodology

In this chapter, the methodology followed for elaborating the work of the thesis is reported. Since this is an energy feasibility study, the starting point of the analysis is the recovery of the site's meteorological data. The data are post-processed in order to obtain them in an hourly resolution. The tool has the objective of proceeding with data in hourly resolution: both the part relating to the resource and energy production and the part of the estimation of loads. Generally, working in hourly resolution, thermal and electrical transients can be neglected. Through a statistical procedure, the typical meteorological year must be obtained, which helps to proceed with analyzing the renewable resources on-site and the consumption of the platform utilities. The study continues with the energy resource and the plate data of the different technologies as input used to determine the energy that can be produced. The next step is to compare the consumption of users with the energy that can be produced from renewable sources to determine the size of the storage to be proposed. In conclusion, a techno-economic analysis is proposed. The methodology on which the tool is developed can be summarized as follows in 5 steps:

1. Determination of the typical meteorologic year
2. Renewable resource analysis
3. Estimation of the energy loads of platform utilities.
4. Developed an energy production mix and a storage system to guarantee reliable and effective electricity production from RES.
5. Techno-economic analysis to determine its energy and commercial feasibility.

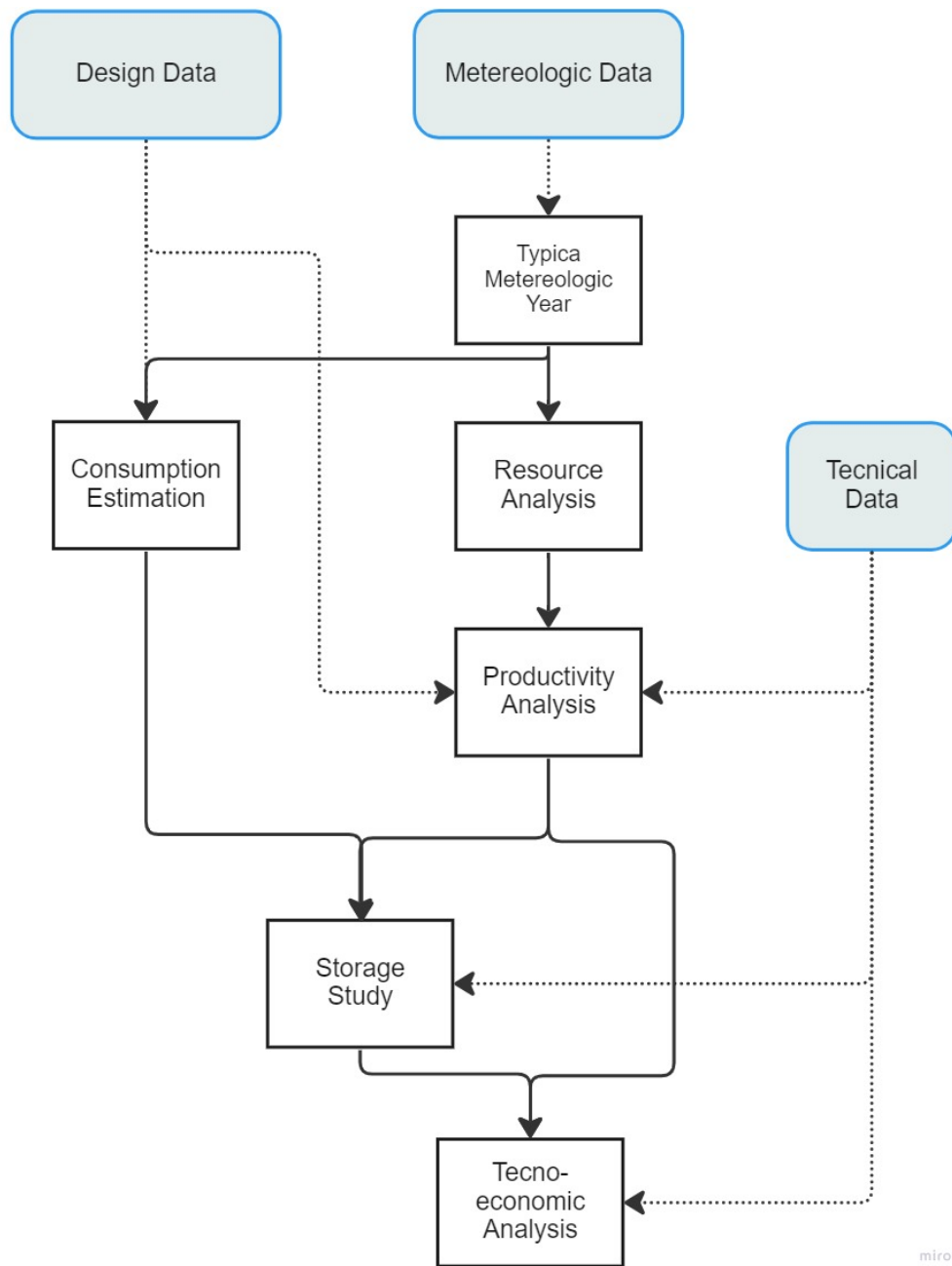


Figure 4.1: Tool's flowchart

4.1 Typical Meteorological Year

The goal is to find a methodology to process the climatic data to be provided as input for the determination of energy production and energy needs for the heating and cooling of buildings following the standard (UNI TS 11300-1, UNI TS 11300-2, UNI TS 11300-3, UNI EN ISO 13788:2003, UNI EN 12831:2006, UNI EN 15255:2008, UNI EN ISO 13791:2005, UNI EN ISO 13792:2005, UNI EN ISO 10375:1995). [13]

The typical year consists of 12 characteristic months (January through December) chosen by a meteorological database of a period that should be, according to the procedure described in EN ISO 15927-4, at least ten years long. The characteristic year must represent the most typical values of the most essential climatic parameters, and it must:

- be as close as possible to the average values calculated over a long period.
- be characterized by realistic dynamics: time sequences and variations during days and series of days typical of the climatic zone.
- exhibit a real correlation between different parameters, in particular temperature and global solar irradiance on a horizontal plane. [14]

There is more than one method to obtain the Typical Weather Year (TWY). This thesis generated the TWY by implementing the Sandia method on MatLab.

The Sandia method is a practical technique that selects individual months from several years of the registration period. For example, in the case containing ten years of data, all of the ten Januarys are reviewed, and the one considered the most typical is chosen to be included in the TMY. The other months of the year are dealt with similarly. Then the selected typical 12 months are concatenated to form an entire year.

Alternatively, software, such as Meteonorm and Weathergenerator, could have been used, but nevertheless, from a long-term comparison, they revealed comparable results. [15]

Precisely, in order to determine which year is the most typical for each month, a statistical procedure is followed. That kind of procedure takes as a reference the climatic values. The Sandia method selects a typical month based on nine daily indices consisting of maximum, minimum, and half dry bulb and dew point temperatures, the maximum and average wind speed, and the global total horizontal solar radiation. In this work only four indexes are considered without requiring a very high degree of precision, however the possible implementation procedure is simple. Specifically, those chosen in this work are:

- Solar Global Radiation;

- Air Temperature
- Humidity (that is linked with the user dew temperature according to the Magnus-Tetens Approximation)
- Wind Speed

These elements are considered the most important for simulating solar energy conversion systems and building systems. If any data were missing from the key fields (solar, temperature, humidity, station pressure, wind speed, aerosols, and precipitable water), the station received a Class III designation. The algorithm distinguishes between Class I and Class II stations by examining the uncertainty for each hourly modeled value in the global field. If less than 25% of the data for the examination period of record exceeds an uncertainty of 11%, the station received a Class I designation.[13] Starting from a meteorological record of hourly data, the daily values of the four selected parameters are calculated for each month of all available years. In particular, the daily average of the air temperature, humidity and wind speed and the total daily solar irradiation are calculated. For leap years, February is truncated to 28 days. The values found are compared with the long-term mean measured daily data of the same parameter using RMSE (root mean square error):

$$RMSE = \sqrt{(x - x_{av})^2} \quad (4.1)$$

with:

- x : daily value
- x_{av} : the daily mean long-term average

The monthly RMSE values (SRMSE) of the four parameters are calculated each month. The annual average of the sum of the monthly values (MRMSE) of RMSE is then calculated. Each year whose month is the most typical is chosen concerning the minimum value of ERMSE, determined as follows. As some indices are considered more important, a weighted sum (WS) of the FS statistics was used to select the five candidate months with the lowest weighted sums.

| Climatic Data | Weight for Sandia Method |
|-----------------------|--------------------------|
| Global Radiation | 12/24 |
| Dry Bulb Temperature | 4/24 |
| Dew Point Temperature | 4/24 |
| Wind Speed | 4/24 |

Table 4.1: Weighting values for Sandia Method

The final goal is to determine which year is the most typical for each month. To do this, for each month, the years are ranked in ascending order with respect to the ERSME parameter, defined below:

$$ERSME^i = \left(\frac{1}{2}\right) \frac{SRMRE_1^i}{MRMSE_1} + \left(\frac{1}{6}\right) \frac{SRMRE_2^i}{MRMSE_2} + \left(\frac{1}{6}\right) \frac{SRMRE_3^i}{MRMSE_3} + \left(\frac{1}{6}\right) \frac{SRMRE_4^i}{MRMSE_4} \quad (4.2)$$

with:

- i: month number
- SRMSE: the sum monthly values of RMSE for each of the four parameter in month i
- MRMSE: the mean yearly of sum monthly values of RMSE for the four parameters

It is important to note that the weightings of the four parameters chosen are not the same, but were determined according to their relevance. The highest candidate month in ascending order of ERSME values meeting the persistence criterion is used in the TMY. Then, the selected 12 months were chained to obtain a complete year and to smooth out discontinuities at the interfaces of the months for six hours per side using curve fitting techniques.[16]

4.2 Resource Analysis

The first step for the energy feasibility analysis is to study the renewable resource in the chosen site. Renewable energy has been defined as "any form of energy from solar, geophysical or biological sources that are replenished by natural processes at a rate that equals or exceeds its rate of use" [17]. Two major factors determine the possibilities for integration of these sources into existing power systems:

- the temporal variability of the output power from renewable power plants
- the accuracy of forecasts for the variable generation processes at a rate that equals or exceeds its rate of use [18]

The research on the different renewable energy resources is at different stages in developing methods for assessing the temporal variability and has focused, at least partly, on different time scales and different models and methods. The following analysis is a preliminary approximation, but given the promising results obtained, we will continue by exploring the energy production technologies, exploring their benefits and limiting factors. Identifying the potential of renewable energy sources is of interest to energy planning. The exploitation of sustainable resources is linked to the particular characteristics of the local environment. Many coastal zones of the world are suitable for using a number of power sources (wind, solar, wave, and tidal) to reduce variability and lower the costs associated with the renewable integration system [18]. In fact, several studies have examined combinations of resources and how they correlate and complement each other. Most of the studies have been conducted for the combination of wind and solar resources [19],[20],[21], and these have found that the complementary is high, especially on a seasonal basis. The hypothetical combination between wind and waves has also been studied, which only sometimes seems to be an exciting combination but rather an excellent way to provide a more constant production and reduce the risk of zero potential[19] [22]. This chapter aims to explain how it is possible to determine the density of renewable energy extracted from the site. A small overview is made exclusively regarding the solar, windy, and wave resource as these, at the current state of the art, are the main energy sources that can be exploited in off-shore mode. For each analyzed resource, some possible databases from which it is possible to obtain meteorological information when there is no available experimental data extrapolated from field sensors are reported.

4.2.1 Solar Resource

The global irradiance that reaches the earth is given by the sum of the three components: direct, diffuse, and reflected.

$$E_{density,sun}[kWh/m^2] = I_{global} = I_{direct} + I_{diffuse} + I_{reflected} \quad (4.3)$$

Various measurements are required to evaluate the energy that a photovoltaic system can use in the available area. Solar energy depends on many factors, such as the conditions of the atmosphere, the distance between the Sun and the Earth, the tilt of the Earth, and the installation place. It is noted that seasonality plays a less decisive role in the variability of the solar resource than diurnal cycles and other effects, such as clouds or precipitation, among others. [23].

Forecasting and Reanalysis models and database for solar resource

One category of databases consists of collections of ground-measured irradiances typically provided by national meteorological services. Another category consists of models that combine data from solar irradiance monitoring networks with physical models to generate solar irradiance data for an arbitrary site. Two examples of such models are Meteonorm and PVGIS. Another broad category is satellite-based models, where recordings of Earth radiances from weather satellites are used to determine cloud cover and global irradiance at the Earth’s surface. These models may range from physically based ones, involving detailed modeling of the radiative transfer through the atmosphere, to purely empirical ones, using regression between satellite data and surface monitoring data. Semiempirical models use simple models combined with data fitting and include the SolarAnywhere and SolarGIS models. There are also more physically rigorous models and databases like SSE.

| Name | Producer | Temporal resolution | Spatial resolution |
|---------------|----------------|---------------------|--------------------|
| Meteonorm | Meteotest | 1 min | any point |
| PVGIS | EU JRC | Daily | 1km/2km |
| SolarGIS | GeoModel solar | 15-30 min | 250 m |
| SSE | NASA | Month avg. on 1day | 1° |
| SolarAnywhere | CPR | 30-60 min | 1km/10 km |

Table 4.2: Models and databeses for the solar resource

4.2.2 Wind Resource

Wind energy uses the kinetic energy of the air. In summary, the wind arises from thermal contrasts generated as the Sun does not heat the Earth’s surface uniformly. Therefore hot air columns (which generate a low-pressure zone) and columns of cold air (which generate a high-pressure area) are created. The resulting baric gradient, therefore, creates a movement of the air mass from high to low pressure. The wind energy desity is calculated as the following equation:

$$E_{density,wind} = \frac{1}{2}\rho v^3 [kWh/m^2] \quad (4.4)$$

Forecasting and Reanalysis models and database for wind resource

In order to promote and guide the development of wind power, many countries have produced maps of a wind speed or power content. Global maps of coarser resolution are also available. The maps are produced by averaging and possibly long-term correct time series from NWP models. To reduce computational time, a statistical representative of weather situations could be modeled instead of continuous time series. In park optimization, a further increase of the horizontal resolution, down to 10 m, is necessary. For this purpose, local CFD calculations or simplified methods such as Wind Atlas Analysis and Application Program (WAsP) could be used.

| Name | Producer | Temporal resolution | Spatial resolution |
|-------------------|---------------|---------------------|--------------------|
| Global Wind Atlas | DTU,IRENA | mean | 3 km |
| MERRA | NASA | 1h | 0.5x 2/3° |
| JRA-55 | JMR | 3/6h | 1.25 ° |
| ERA Interim | ECMWF | 6h | 0.75 ° |
| IFS | ECMWF | 1h | 16 km |
| GFS | NCEP | 3h | 27 km |
| WRF | Collaboration | 1h | few km |

Table 4.3: Models and databases for the wind resource

4.2.3 Wave Resource

Waves are formed by wind blowing over water (which transfers its kinetic energy to the waves). The climate of the waves depends on the fetch (the length of the sea over which the wind blows) and the duration time of the wind. The wind first causes small capillary waves on the water surface, held together by the weak surface tension force, whose typical wavelength is 17.3 mm. When the capillary waves form, they provide a rougher surface on which the wind can blow, transferring more energy, and the waves grow in height, forming ripples. The waves grow, forming chops (low wavelength) waves, and then the sea fully develops. As the waves continue to grow, their height increases faster than their wavelength until the critical rapidity (wave height/wavelength) of 1:7 is reached; at this value, the waves break, generating the phenomenon of white capping.

$$E_{density,wave} = 0.49Hs^2Te[kWh/m] \quad (4.5)$$

with:

- Hs: wave height [m]
- Te: wave period [s]

Forecasting and Reanalysis models and database for wave resource

In order to give an overview on the wave resource worldwide, global maps and databases have been created. Typically, the spatial resolution is higher close to the coast (0.251) and smaller offshore (1.5–31). With the purpose of evaluating the wave conditions and generating the previously mentioned databases, in-situ and satellite measurements are integrated with model simulations. The reason why wave climate estimates have to rely on wave models is that variability on all time scales makes the resource difficult and costly to measure.

| Name | Producer | Temporal resolution | Spatial resolution |
|-------------|------------|---------------------|--------------------|
| ERA Interim | ECMWF | 6h | 0.75 ° |
| WERATLAS | EU project | 6h | 85 datapoints |
| AVISO | Aviso | 6h | 1/3 ° |
| ONDATLAS | INETI | 6h | 10 km |
| World waves | OCEANOR | 6h | 0.5 ° |

Table 4.4: Models and databases for the wave resource

In order to give an overview of the wave resource worldwide, global maps and databases have been created. Typically, the spatial resolution is higher close to the coast (0.251) and smaller offshore (1.5–31). With the purpose of evaluating the wave conditions and generating the previously mentioned databases, in-situ and satellite measurements are integrated with model simulations. The reason why wave climate estimates have to rely on wave models is that variability on all time scales makes the resource difficult and costly to measure

!

4.3 Estimation of consumption

The main feature of the design of the upper structure is that it must be light and easy to build. Specifically, the main concepts are modularity and the dry-construction. The buildings that will be built will, therefore, overlap two standard pieces (one square and one trapezoidal) that are easy to assemble together. In this way, it is possible to adapt multiple configurations to a specific hexagonal platform; in particular, an easy construction is associated with an easy disassembly that facilitates recycling and reuse.

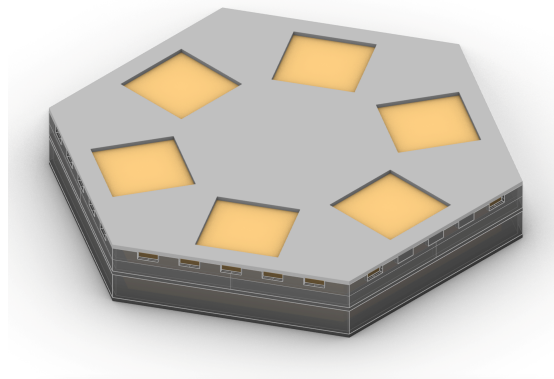


Figure 4.2: Platform base

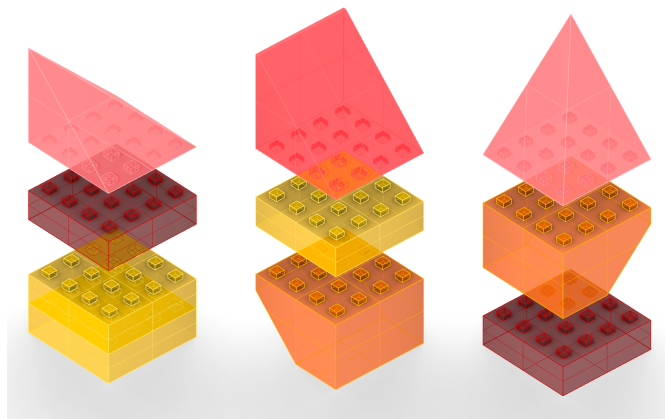


Figure 4.3: Modular building

The objective of this chapter is to provide an estimate of the consumption of the platform's users. The buildings intended to install fall within the net zero emission typology, so for the estimate of their consumption, reference was made to the legislation [24]. Specifically, the annual and daily consumption profile is sought in addition to the total consumption. In particular, four "standard" days are considered concerning daily consumption, one for each season and for each of the days. It is shown how the profile varies according to the type of day considered (weekday or holiday). Specifically, typical profiles have been identified for heating and cooling needs, which make it possible to view the main characteristics and trends of the thermal loads for the ten building types selected. This type of analysis aims to highlight the high dependence of the dynamics of the load profiles on internal inputs and plant management profiles.

Each building, as explained, is modular: therefore, made up of several pieces. Each piece is assumed to be the same size regardless of its relative position in the building, and the activity carried out inside it. Being a preliminary study, the buildings are treated in this way to simplify the treatment. These assumptions are made to go and identify those configurations closest to energy independence by going quickly and efficiently to change the configuration of the platforms. However, they will be responsible for an overall overestimation of consumption. These assumptions are made to keep the results of the obtained loads conservative.

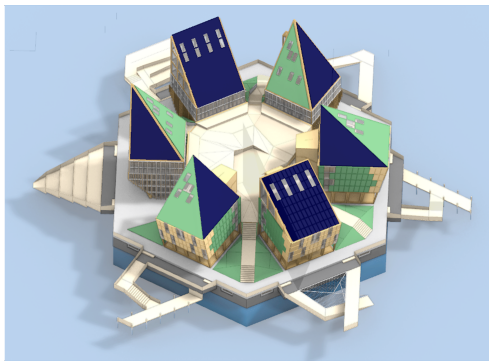


Figure 4.4: Platform Building

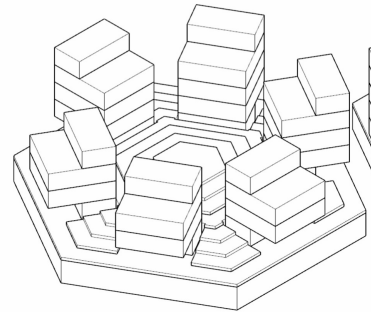


Figure 4.5: Piece model

For the proposed study, the loads are divided into three and studied individually:

- Thermal loads
- Electric loads
- Lighting loads

Generally speaking the factors that influenced energy consumption are:

- Climatic zone (ambient conditions)
- Intended use of the building (residential, industrial, tertiary)
- Presence of people
- Building parameters

Assumptions

In order to state a model which is both sufficiently general and accurate for describing all types of energy flow, we make the following assumptions and simplifications:

- The system in steady state.
- The steady state power, efficiency, and energy only, no other values are used for the system description.
- It is assumed that the costs are additive and that there are no perceptual changes in other factors such as plant capacity, unit cost of different energy sources, configuration of energy system etc.
- A time horizon of 1 h is used throughout this study.
- It is further assumed that the electrical load and the renewable sources are constant within each one-hour time step.
- The "Set point" of temperature and the "fraction of use" are estimated from literature, and in reference to the specific case, they, of course can be chance for the different locations, in particular as refer it was very useful in the America study.

Climatic zone

The period and the hours of the day in which the heating system can be switched on differs according to the climatic zone. The national territory of Italy is divided into six climatic zones based on the average daily temperatures. This makes it possible to evaluate each area's heat requirement to optimize consumption, CO₂ emissions into the atmosphere, and the economic impact of energy supply. The definition of the bands is done through day-degree (DD). They correspond to the sum, every day of the year, of the difference (only the positive one) between the temperature of the internal environment (fixed by convention at 20 ° C) and the average daily external temperature. This means that the higher this number, the colder the climate in that area. This indicator is evaluated from municipality to municipality. I.I.D.P.R. n. 412 of 26 August 1993 introduced, based on the calculation of the

degree-days, six climatic zones on the Italian territory to each climatic zone the relative range of degree days is associated.

| Climatic Zone | Day-Degree | Heating Period | Hours allowed per day |
|---------------|------------|-----------------------|-----------------------|
| A | <600 | 1 December - 15 March | 6h |
| B | 600-900 | 1 December - 31 March | 8h |
| C | 901-1400 | 15 November -31 March | 10h |
| D | 1401-2100 | 1 November - 15 April | 12h |
| E | 2101-3000 | 15 October - 15 April | 14h |
| F | >3000 | no limit | no limit |

Table 4.5: Italian Climatic Zones

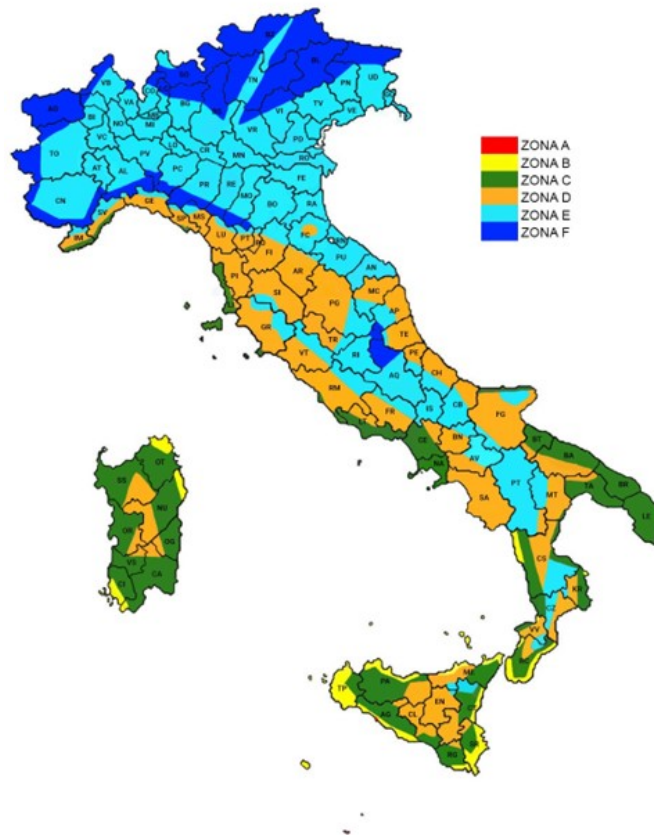


Figure 4.6: Italian Climatic Zones

| Climatic data input for load |
|------------------------------|
| Latitude |
| External temperature |
| Lighting hours |
| Solar radiation |

Table 4.6: Climatic data input for load

Intended use of the building

The interior spaces studied could be:

- Living spaces
- Office
- Auditorium
- Conference rooms/co working spaces
- Exhibition rooms
- Restaurant

In this work, only the following three final uses are considered:

- Living : spaces therefore used for daily residential use.
- Office : spaces used for office work.
- Support: space in which all the necessary auxiliaries from an energy and industrial point of view are put: such as the proposed storage systems, tanks, and desalination plants.

Presence of people

It is well known that people do not constantly occupy a space so contemporary factor and preliminary assumption need to be considered. [25]

- Living

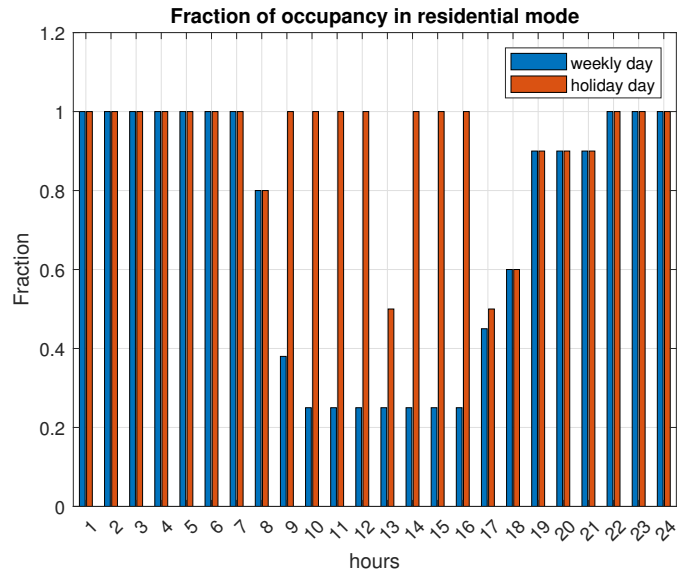


Figure 4.7: Occurrence in living space

- Office :

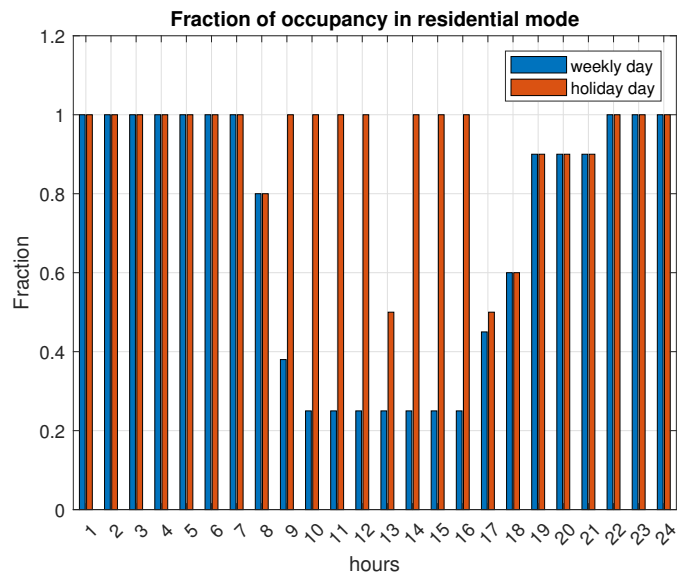


Figure 4.8: Occurrence in living space

- Support: as regards the support spaces, the constant presence of people is not foreseen but only the occasional presence for maintenance and control

operations. As these are quite difficult to predict, they are not considered in this first phase of the work.

Building parameters

Since this is a pre-feasibility study and not an executive project, the building parameters can be acquired from literature and the standards that establish limits for buildings in the "net zero emission" category. In the project's subsequent stages of the project, an analysis will be carried out for the choice of the material; consequently, the values will be replaced with those of the real project.

| Dimensional data input for thermal load |
|---|
| Height |
| Volume |
| Gross surface |
| Surface of each building element |
| Percentage of windows |
| Transmittance of each building element [W/m^2K] |
| Minimum hourly external ventilation rate (UNI 12831 -App.D) |

Table 4.7: Dimensional data input for thermal loads

4.3.1 Thermal load

To determine the thermal loads required by the utilities, it is necessary to evaluate the dispersions. This work is done in stationary conditions, thus neglecting the effects of thermal transients and hourly resolution. It was decided to follow the calculation method provided by the UNI EN 12831 standard for buildings with a limited height of the internal environments (height less than 5 m) for which "permanent regime" climate conditioning is provided (for which the system conditioning is always available). The hypotheses on which this method is based and which are therefore assumed in this thesis are:

- uniform distribution of internal and external temperature
- thermal losses calculated in permanent conditions: therefore thermo-physical properties and characteristics of the constant building elements.
- internal temperature of the air equal to the operating temperature

For each type of reference piece, a single thermal zone was considered for both winter and summer air conditioning as, according to Par.7.2 of UNI / TS 11300-1, zoning is not required if the following conditions co-occur:

- internal regulation temperatures for heating differ by no more than 4K;
- internal regulation temperatures for cooling differ by no more than 4K;
- the rooms are served by the same air conditioning system;
- if a mechanical ventilation system is present, at least 80% of the conditioned area is served by the same ventilation system with ventilation speeds in the different rooms that do not differ by a factor greater than 4;
- If humidity control is present, the internal relative humidity of the control differs by no more than 20 percentage points;

Consequently, the thermal contributions due to the heat exchange between adjacent rooms at different temperatures will be neglected, and only those due to the casing will be considered. For simplicity, in the absence of design data, in this first phase also, the envelope is considered "homogeneous" by considering the inequalities between the opaque and glazed elements and without considering the exchange with the ground exclusively.

The calculation procedure chosen refers to the quasi-stationary monthly calculation method from the European standard UNI EN ISO 13790. This procedure is based on the hourly balance between heat losses (transmission and ventilation) and heat gains (solar and internal). The calculation of the thermal energy requirement for heating is based on the following equation [26]:

$$Q_{thermal}[W] = (Q_{thermalloss} - Q_{gain})/\eta \quad (4.6)$$

$$Q_{thermalloss}[W] = H_{thermal}(T_i - T_e) \quad (4.7)$$

with:

- $H_{thermal}$: Thermal dispersion coefficient [W/K]

$$H_{thermal} = H_{transmission} + H_{ventilation} \quad (4.8)$$

with:

- $H_{transmission}$: Thermal dispersion coefficient by transmission;

$$H_{transmission} = 1.1(H_{t,casing} + H_{t,ground} + H_{t,roof}) \quad (4.9)$$

with:

$$H_{t,i} = A_{t,i}U_{t,i}e_{t,i} \quad (4.10)$$

Where i is the index for the casing, ground, and roof and where $e_{t,i}$ represents the correction factors due to the exposures but for simplicity

and to be able to consider all the homogeneous pieces, it is imposed unitary. The thermal transmission coefficient is multiplied by 1.1, so increased by 10% , to take into account the thermal bridges that will occur. This could be a very optimistic but realistic estimate if it is considered in project conditions.

– $H_{ventilation}$: Thermal dispersion coefficient by ventilation where

$$H_{ventilation} = NVc_{p,air}\rho_{air} \quad (4.11)$$

where N is choose in accordance with the use of building

the heat gains are:

$$Q_{gains} = Q_{sun} + Q_{int} \quad (4.12)$$

with:

– Q_{sun} : heat provided by the sun; The thermal flux of solar origin, Q_{sol} , expressed in W, is calculated with the following equation:

$$Q_{sol,w} = F_{sh,ob}A_{sol,w}I_{sol} \quad (4.13)$$

$$Q_{sol,op} = F_{sh,ob}A_{sol,op}I_{sol} \quad (4.14)$$

with:

- * $F_{sh,ob}$: reduction factor for shading relative to external elements for the effective solar collection area of the surface
- * $A_{sol,w}$: effective solar collection area of the glazed surface with a given orientation and angle of inclination on the plane horizontal, in the area or environment considered. It is obtained through the following equation:

$$A_{sol,w} = F_{sh,gl}g_{gl}(1 - F_F)A_{w,p} \quad (4.15)$$

with:

- $F_{sh,gl}$: reduction factor in solar gains related to use of mobile screens
- g_{gl} : solar energy transmittance of the transparent part of the component
- F_F : fraction of area relative to the frame, ratio of the projected area of the frame and the total projected area of the windows component
- $A_{w,p}$: the total projected area of the glazed component (the area of the compartment window)

* $A_{sol,op}$: effective solar collection area of the opaque surface with a given orientation and angle of inclination on the plane horizontal, in the area or environment considered. It is obtained through the following equation:

$$A_{sol,op} = \alpha_{sol,c} R_{se} U_{c,eq} A_c \quad (4.16)$$

with:

- $\alpha_{sol,c}$: solar absorption factor of the opaque component
- R_{se} : solar energy transmittance of the transparent part of the component
- A_c : projected area of the opaque component
- $A_{w,p}$: the total projected area of the glazed component (the area of the compartment window)
- * $U_{c,eq}$: equivalent thermal transmittance of the opaque component
- Q_{int} : heat provided by internal heat gains; The table below indicates human sensible and latent heat. The values can be used to calculate heat gain that need to be handled by air conditioning systems.

| Typical Application | Sensible Heat | Latent Heat |
|--|---------------|-------------|
| Theater-Matinee, Auditorium | 200 W | 130 W |
| Theatre-Evening, School | 215 W | 135 W |
| Office, Hotel, Apartments | 215 W | 185 W |
| Factory - light work | 240 W | 510 W |
| Factory - moderate work | 330 W | 670 W |
| Factory - heavy work, Gymnasium, Bowling | 510 W | 940 W |
| Restaurant | 240 W | 310 W |

Table 4.8: Heat gain for the different applications

So, the main input data considered in the calculations are:

- Dimensional data of the building
- Internal set conditions (confort conditions)
- Climatic data for thermal load

The conditions of comfort imposed come from Fanger theory and as a reference it is taken according to ASHRAE [27] [28]. Furthermore, the UNI EN 12831 standard suggests a method for calculating the project temperature based on the UNI 7730 standard, according to which the desired thermal quality inside the building can

be chosen between 3 categories (A; B; C) and the buildings in object of analysis belong to category A.:

| Use | Temperature | Humidity | Temperature range |
|----------------------------|-------------|----------|-------------------|
| residential, hotel, office | 25-26 °C | 50-45% | 1-2 °C |
| shop | 25-26 °C | 50-45% | 1-2 °C |
| theatre, bar, restaurant | 25-26 °C | 50-60% | 0.5-1 °C |
| workshop | 25-26 °C | 50-60% | 1.5-3 °C |

Table 4.9: Confort Condition in Summer

| Use | Temperature | Humidity | Temperature range |
|----------------------------|-------------|----------|-------------------|
| residential, hotel, office | 20-22 °C | 50-40% | 2 °C |
| shop | 20-21 °C | 35-50% | 2 °C |
| theatre, bar, restaurant | 20-21 °C | 50-60% | 2 °C |
| workshop | 15-18 °C | 50-60% | 3 °C |

Table 4.10: Confort Condition in Winter

The internal conditions imposed for the different spaces are shown below.

Living space

In the case of residential buildings, the objective is to maintain the conditions of comfort during the hours of occupation and to prevent the apartment from cooling and heating excessively during periods in which it is not used. The internal temperature set-points are shown based on the season and type of day considered.

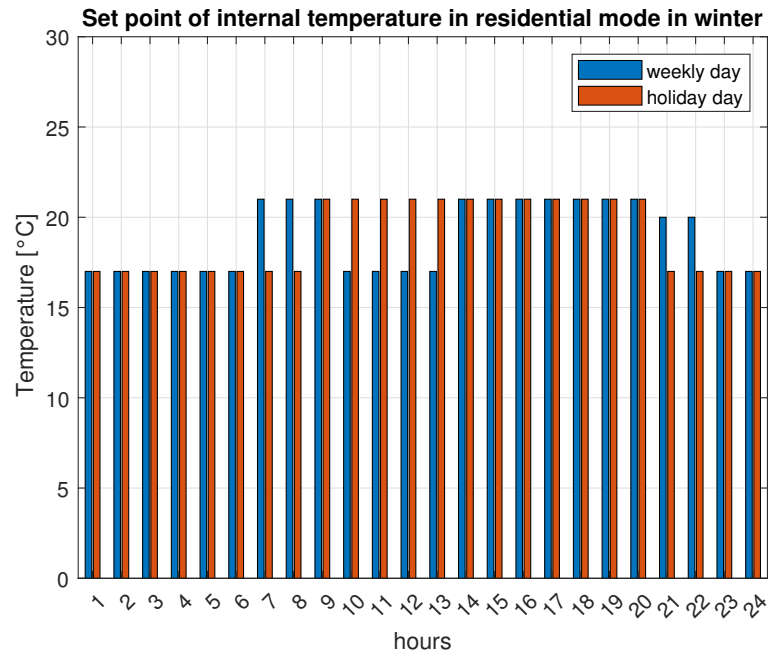


Figure 4.9: Internal Temperature set point for living space heating [25]

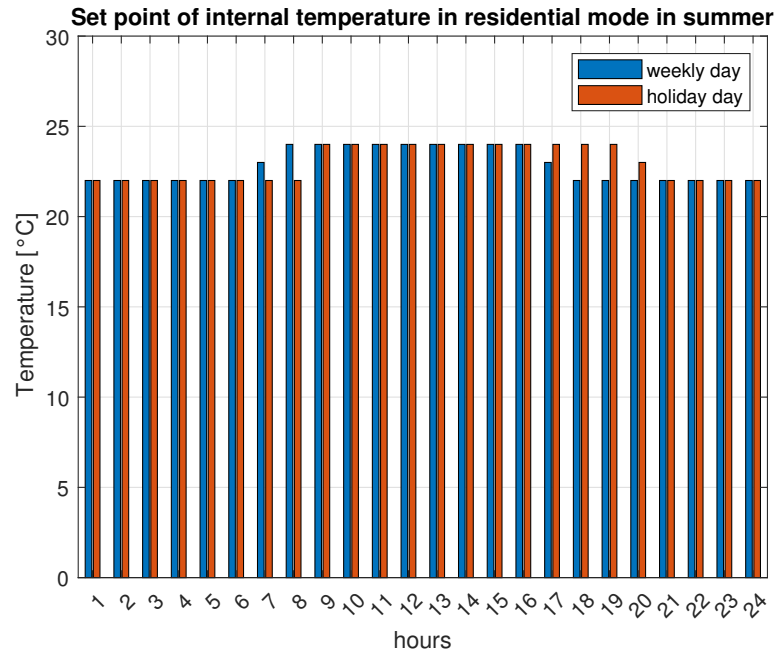


Figure 4.10: Internal Temperature set point for living space cooling [25]

Office space

For office buildings it is mandatory that during working hours, considered from 7:00 to 19:00, the temperature of 21-22 ° C is maintained while during the remaining hours the conditional system is switched off in winter and summer.

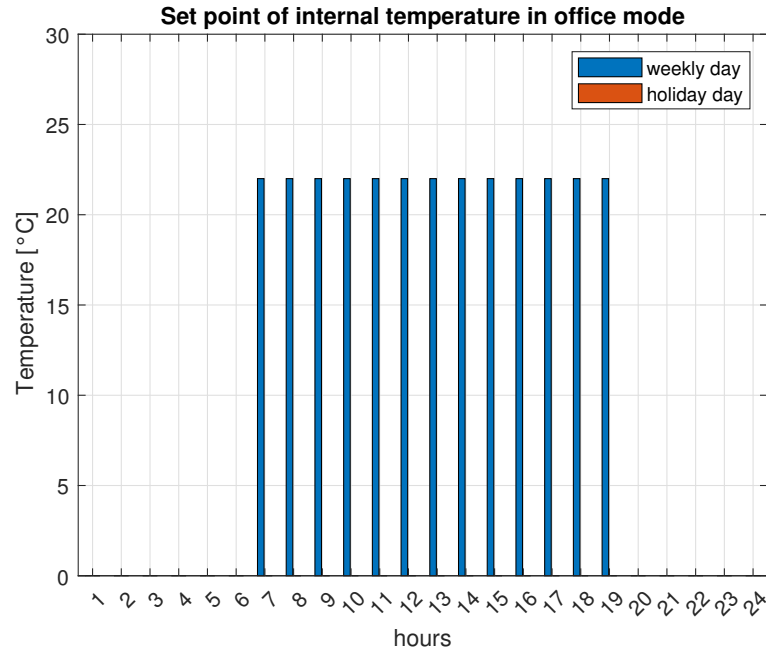


Figure 4.11: Internal Temperature set point for office space [25]

Support space

Regarding the third option envisaged for the possible pieces, in this initial phase, it was planned to have non-air-conditioned spaces, in which, however, the temperature does not drop below 10 ° C and does not go above 27 ° C in which to place the batteries for energy storage. These can be also spaces provided for cultivation or to install a desalinization.

4.3.2 Electric device load

The drivers of consumption due to electrical loads are the intended use of the buildings and the number of people expected. Specifically, the following assumptions are made to find a probability profile with a resolution of one hour was determined for each load on board the platform.

Residential spaces

It is assumed that the households are made up of 4 people and for each household there are the classic eletrodomestics, with the following usage profiles [29]:

- Refrigerator: Its load profile is a function of the external temperature but considering that it is assumed that the internal environments are air-conditioned, remaining prudent on the estimate of the load, it is assumed that it is always on and at nominal power. It is estimated that there is one refrigerator per household and its rated power is 300 W.
- Television: It is estimated that there is one television per household and its rated power is 120 W. It is hypothesized that it is active two hours in the morning from 7:00 to 9:00, two hours in the lunch break, from 12:00 to 14:00, and five in the evening from 19:00 to 23:00. Both on holidays and on weekdays.
- Dishwater: It is estimated that there is one dishwater per household and its rated power is 1132 W. It is hypothesized that it is active in the evening after dinner for three hours, from 20:00 to 23:00. Both on holidays and on weekdays.
- Washing machine: It is estimated that there is one wasching machine per household and its rated power is 979 W. It is hypothesized that it is active in three hours during the day, form 12:00 to 15:00, and three hours in the evening after, from 20:00 to 23:00. Both on holidays and on weekdays.
- Oven: It is estimated that there is one oven per household and its rated power is 1000 W. It is hypothesized that it is active in two hours during the day, form 12:00 to 14:00, and two hours in the evening after, from 19:00 to 21:00. Both on holidays and on weekdays.
- Microwave oven: is estimated that there is one oven per household and its rated power is 700 W. It is hypothesized that it is active in two hours during the day, form 12:00 to 14:00, and two hours in the evening after, from 19:00 to 21:00. Both on holidays and on weekdays.
- Computer: It is estimated that there is a computer per person with a nominal power of 70 W. Considering that nowadays the computer is also used as a television it is assumed that it is active during all hours of the day, therefore from 7:00 to 21:00 . This hypothesis is carried out both during weekdays and holidays, in the case of holidays perhaps an overestimation is made but being a low load it is a plausible assumption as it is a more conservative option and that simplifies the calculation procedure

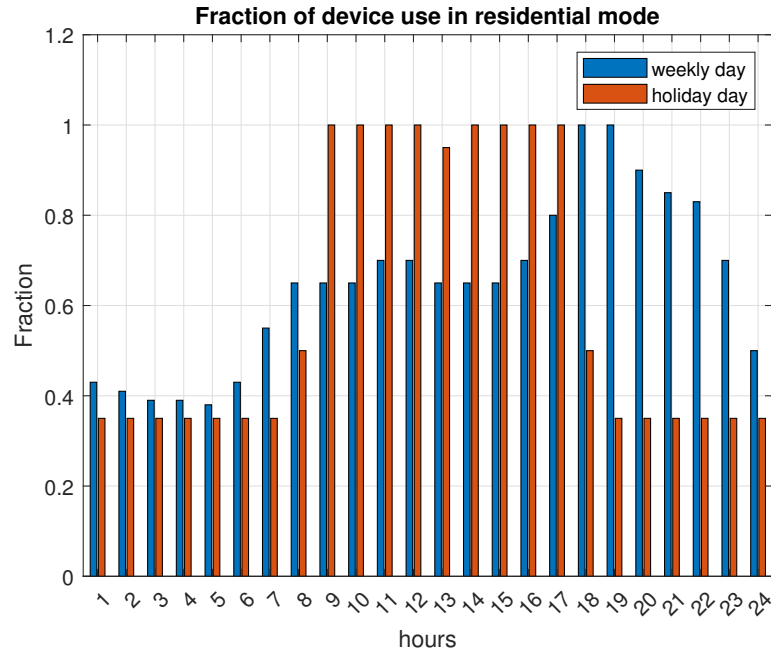


Figure 4.12: Use fraction of device load for residential [25] [30]

Office spaces

For each office, the people employed are known and the following devices are assumed:

- Refrigerator: Its load profile is a function of the external temperature but considering that it is assumed that the internal environments are air-conditioned, remaining prudent on the estimate of the load, it is assumed that it is always on and at nominal power. It is estimated that there is one refrigerator per office and its rated power is 300 W.
- Television: It is estimated that there is one television per for every 20 employed and its rated power is 120 W. It is hypothesized that it is active two hours in the morning from 7:00 to 9:00, two hours in the lunch break, from 12:00 to 14:00, and five in the evening from 19:00 to 23:00. Both on holidays and on weekdays.
- Dishwater: It is estimated that there is one dishwasher per office and its rated power is 1132 W. It is hypothesized that it is active in the evening after dinner for three hours, from 20:00 to 23:00. Both on holidays and on weekdays.
- Oven: It is estimated that there is one oven per office and its rated power is 1000 W. It is hypothesized that it is active in two hours during the day, from

12:00 to 14:00, and two hours in the evening after, from 19:00 to 21:00. Both on holidays and on weekdays.

- Computer: It is estimated that there is a computer per person with a nominal power of 70 W. Considering that nowadays the computer is also used as a television it is assumed that it is active during all hours of the day, therefore from 7:00 to 21:00.
- Printers: It is estimated that there are three printers per office with rated power of 500 W. It is hypothesized that they are active during all working time, from 7:00 to 21:00.
- Various: A load of 100 W is considered fixed during all 24 hours of the day.

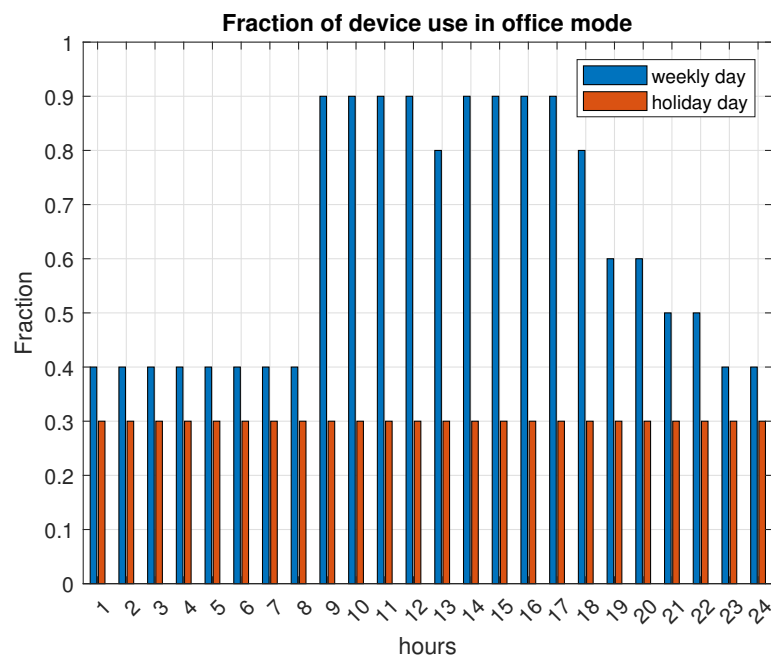


Figure 4.13: Use fraction of device load for office [25] [30]

Support spaces

As already explained, the presence of people within these spaces is not expected, at least at this study stage.

4.3.3 Lighting load

As drivers for estimating consumption due to lighting, it was decided to use the covered area to be illuminated and the intended use of the building. The covered area is considered as it is assumed that not all the base air of the piece is used for the use of the space. The fraction occupied by the thickness of the walls and all those areas that do not need lighting are therefore considered trivially. It is assumed that each bulb has an average power rating of 40 W in residential pieces and 75 W in office pieces, neglecting the different choices in terms of the use of the lamps that could be made. The following equation can be used to calculate the average number of bulbs needed to light up the dwelling floor area:

$$N_{bulbs} = \frac{I_{mean} S_{covered}}{L_{bulb}} \quad (4.17)$$

with:

- I is the buildings luminance level. Literature identifies the lux required for the different conditions of use of the space whose aim is to identify the lighting:
 - Corridors and passage areas normally from 50 to 150 lux per m² [31]
 - The bedrooms used from 100 to 150 lux [31]
 - Garages, storage rooms and the like would like around 100 lux [31]
 - The bathrooms would like to 150 lux, with the make-up areas going up to 400 lux [31]
 - The kitchens require 350 lux to ensure good visibility of the environment [31]
 - Studios or offices, on the other hand, require between 300 and 500 lux, depending on their intended [31]
 - External space 300 lux [32]
- S_{floor} : the floor surface (considered as a percentage of the base area of the piece)
- L_{bulb} : the lumen produced by a incandescent bulb (40 W in residential pieces and 75 W in office pieces)

The fraction of use considerate for the use of the lighting for the different use are:

Residential space

The covered area is considered as the 60% of the base surface.

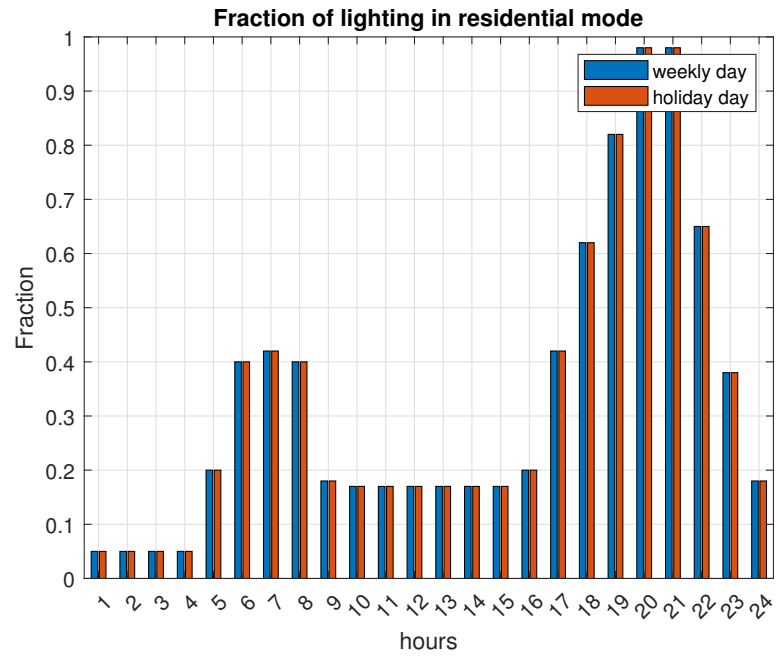


Figure 4.14: Use fraction of lighting in residential

Office space

The covered area is considered as the 70% of the base surface.

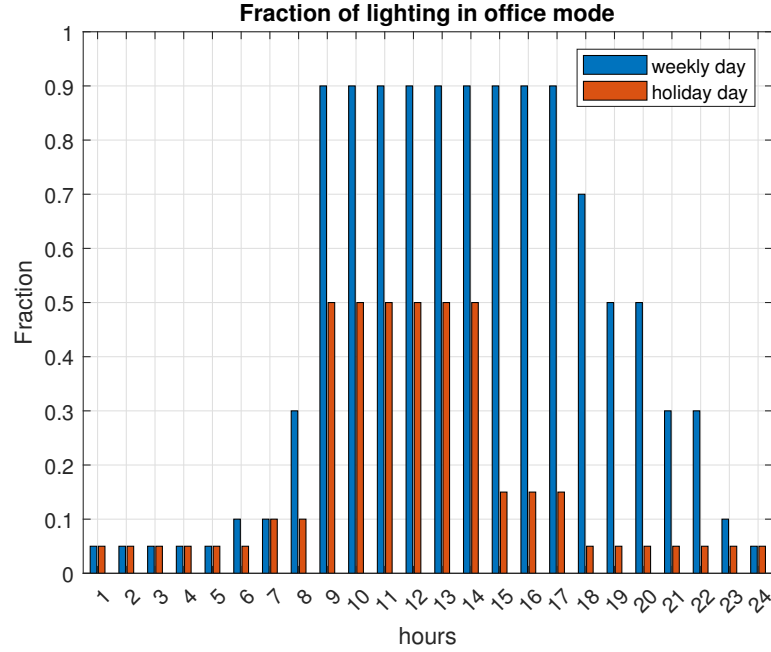


Figure 4.15: Use fraction of lighting in office

Support space

The covered area is considered as the 60% of the base surface. The fraction of lighting use, at this step, is considered the same of the office pieces.

4.3.4 Total load

To estimate the total load of the interconnected pieces the equation is the following [33]:

$$Load_{platforms} = \sum_{k=1}^u n_u Load_u \quad (4.18)$$

with:

- u kind of use
- n_u number of pieces with the u -use
- $Load_u$ load request from the single pieces with the u -use

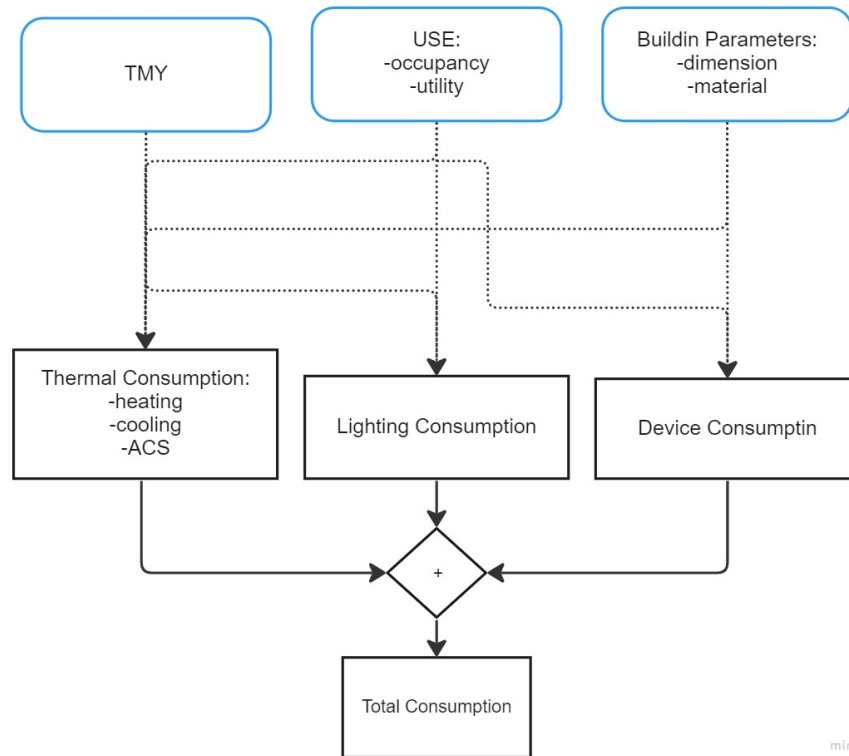


Figure 4.16: Algorithm consumption estimation

It was decided to report as consumption output beyond the annual profile also the daily one considering a weekday for each of the 2 seasons and a public holiday for each of the 2 seasons.

Weekday day load profile

- **Residential application:** From the statistical analysis carried out by the significant sample of Italian families, the average annual consumption for residential buildings is approximately 2800 kWh/year[34]. For residential application there are three peaks in the weekday load curve:
 - one around 8:00 in the morning: it maintains its position in the different seasons, decreasing its height passing from winter to summer
 - one in the central hours of the day: this is more distributed than the other two peaks but like the others it decreases its intensity in the transition from winter to summer
 - one in the evening: it tends to decrease in intensity and move towards the night hours going towards the summer

and three falls during the day:

- a nocturnal fall that covers the central hours of the night: it has a fairly stable shape but with higher withdrawals during the summer due to consumption for air conditioning
- diurnal fall
- afternoon fall: not much accentuated in the winter period as the consumption due to lighting shifts towards the evening hours
- **Office application:** There is a peak during the day climate conditioning is in fact provided only during the time in which the office is used.
- **Support application:** It is a random load and tendentially not high, it is not possible to predict a "typical" trend.

Holiday day load profile

- **Residential application** Two peaks are distinguished in the holiday load curve:
 - one in the late morning: it decreases in intensity passing from winter to summer
 - one in the evening: it tends to decrease in intensity and move towards the night hours going towards the summer

and two falls during the day:

- a nocturnal fall that covers the central hours of the night: it has a fairly stable shape but with higher withdrawals during the summer due to consumption for air conditioning
- afternoon fall: not much accentuated in the winter period as the consumption due to lighting shifts towards the evening hours
- **Official application** The load remains constant and almost zero as there are no spaces occupied during the holidays
- **Support application** It is a random load and tendentially not high, it is not possible to predict a "typical" trend.

| type of day | Winter | Spring | Summer | Autumn |
|-------------|----------|----------|----------|-----------|
| weekly | 8.38 kWh | 7.16 kWh | 7.35 kWh | 7.29 kWh |
| holiday | 8.97 kWh | 7.72 kWh | 7.41 kWh | 67.68 kWh |

Table 4.11: Typical daily consumption for residential application with 4 people

4.4 Productivity Analysis

The following assumptions:

- Steady state of the system and all technical and economic parameter
- the output of the PV array and the wind turbine is supposed to depend only on meteorological data linearly (and not on the facility's age)
- Weather and load data are constant within each 1-h time step
- Maintenance and breakdown interruptions are not considered: The possibility of power blackouts in an off-grid energy system is relatively high, as there are only a few devices to compensate for the breakdown of another one. Nevertheless, power blackouts have not been regarded. Power is therefore assumed to be supplied without interruption. The vulnerability of an off-grid energy system has to be regarded separately from this optimisation.
- The total PV electricity generation is estimated by applying full-load hours while only the global horizontal solar radiation has an influence on the hourly PV power output

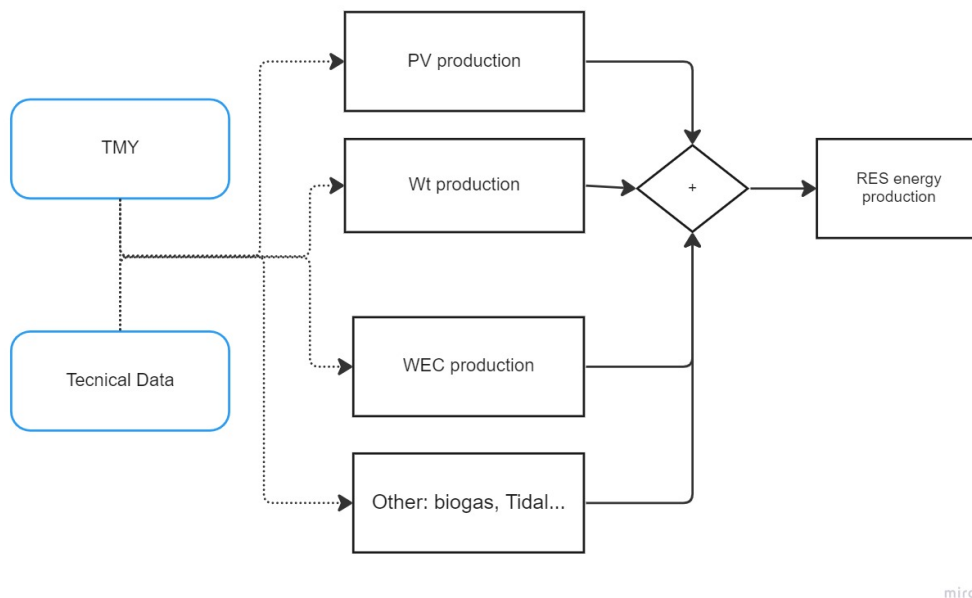


Figure 4.17: Algorithm RES productivity

4.4.1 PV productivity

The energy production of a PV module is dependent on its main characteristics and external factors.

- Solar irradiation
- Cell temperature
- Shading effects

The annual electricity output from PV modules was estimated using [35]:

$$E_{PV} = \eta_{PV}\eta_{auxiliary}A_{array}P_r I [kWh/year] \quad (4.19)$$

where:

- η_{PV} : efficiency of the PV
- A_{array} : Area of PV array (m²)
- I: Irradiance (kWh/m²)
- P_r : performance ratio
- $\eta_{auxiliary}$: efficiency of the auxiliaries

The PV efficiency and the performance ratio consider the losses experienced at the location, such as temperature losses, shading losses, cabling and transmission losses, mismatch losses, or even soiling losses. The annual availability of the PV system was defined as 95%, allowing for downtime for maintenance and unplanned outages. [36]. The photovoltaic generator produces DC power; therefore, when the hybrid energy system contains an AC load, a DC/AC conversion is required, so it is added to the efficiency of the auxiliary as inverter and Maximum Power Point Tracker.

The PV module efficiency for silicon technologies ranges from 13 to 21%. The PV efficiency is determinate in hourly resolution due to the its dependence on the external temperature:

$$\eta_{PV} = \eta_{stc}[1 + \lambda(T_c - T_{c,stc})] \quad (4.20)$$

In the figure, it is possible to notice the efficiency dependence on air temperature.

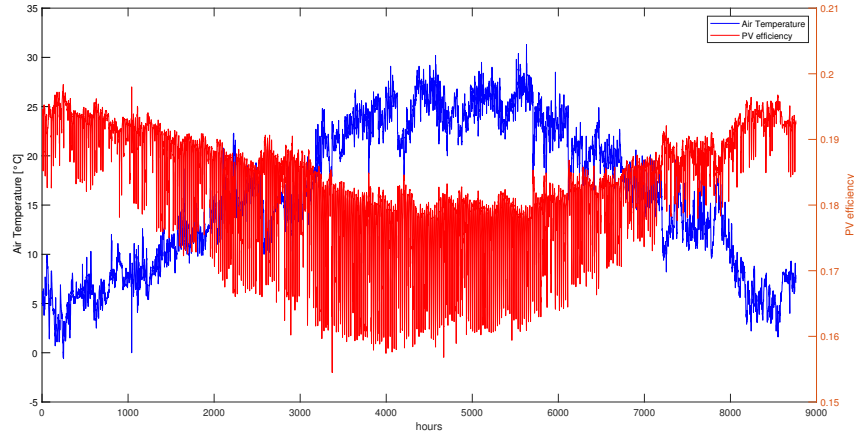


Figure 4.18: Air Temperature influence on PV efficiency

where:

- η_{stc} : module efficiency at STC
- λ : PV temperature coefficient of power
- η_{stc} : actual cell temperature
- $T_{c,stc}$: cell temperature at STC

Solar cells are temperature sensitive and rise temperature reduces the semiconductor band gap. The operating temperatures of the higher cells are reduced cell output, efficiency and duration, during operation conditions result in higher operating voltages. The actual cell temperature is given by [36]:

$$T_c = T_{amb} + \frac{NOCT - 20}{800} G_{inc} \quad (4.21)$$

with:

- T_{amb} : ambient temperature °C
- NOCT: nominal operating cell temperature
- The standard condition are 20°C and 800 W/m^2

A key role in maximizing the total annual produced energy is the tilt angle of the PV module: the theoretical optimum tilt angle is normally set to the site's latitude, as a rule of thumb. The optimum tilt angle determination is fundamental, as incorrect positioning does not maximize the power output.

4.4.2 WT productivity

To estimate the productivity of wind turbines, the power curve must be obtained as the nameplate data. In order to choose the best turbine for the proposed site, it is essential to evaluate not only the nominal power but, above all what are the cut-in and cut-off speeds. Each turbine has its own characteristic power curve. The power curve of a wind machine shows the relationship between the wind speed and the instantaneous electrical power delivered by the generator. A power curve of any wind turbine is structured as follows [35]:

- the cut-in wind speed is the minimum threshold to guarantee the start of the turbine
- the rated wind speed is the wind speed at which the machine reaches its rated power
- the cut-off wind speed is the maximum tolerated wind speed threshold: beyond which the wind turbine becomes safe and stops electricity production, to avoid the risk of damage

The purpose of the paragraph is to explain how to choose the turbine to install. Specifically, two turbines are compared: one with lower rated power and lower cut-in speed and one with higher rated power and higher cut-in speed. An analysis is then presented to choose which type of turbine for the site is the most favorable. The one that guarantees a greater total annual power is selected. The two power curves of the two turbines considered are shown, and the hourly profile of the hourly power depends on the wind speed that characterizes the site to identify which of the two turbines to install.

The two curves are taken from the reference in the bibliography [37].

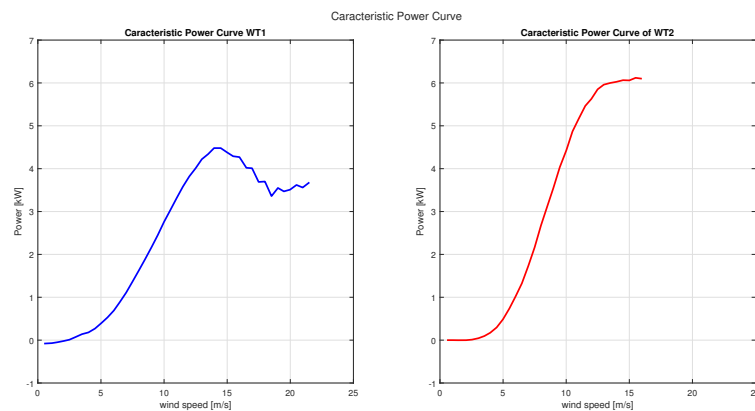


Figure 4.19: Power Curve of wind turbines

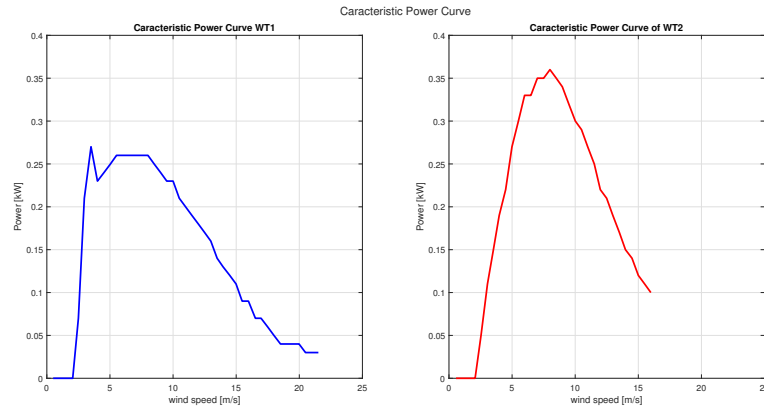


Figure 4.20: Power Coefficient of wind turbines

The extractable power of a turbine is determined as follow:

$$P_{WT} = \frac{1}{2} \rho C_p A v^3 [kWh/year] \quad (4.22)$$

where:

- ρ : air density (kg/m³)
- C_p : maximum power coefficient that is the ratio of the power extracted by a wind turbine to the power available in the wind. It has typical values between 0.25 and 0.45 with a maximum "theoretical" value of 0.593 (Betz limit)
- A : rotor area (m²)
- P_r : performance ratio

The aim of the performance ratio is to consider the power loss due to the maintenance, failure, regular inspection, power limitation, deterioration and other factors [38].

The data referring to the two microturbines of which the power curve is shown above enter the tool. A comparison is made between the two power profiles generated by these to be able to choose which type of turbine is best suited to the site in question. The turbine for which the annual power produced is higher is chosen.

4.5 Storage

The electricity produced by a renewable system does not perfectly follow the energy demand trend. Therefore, a storage system is necessary to compensate for this difference and ensure energy security with renewable sources and not only with traditional plants. All modeling and simulation are based on an hourly energy balance where the hybrid energy system supplies power to meet load demand (and possibly charge the batteries). For simplicity, the generator capacities were given as constant values, but the loads were varying. The initial battery energy level and the minimum allowable state of charge were set at 100% and 20% of the maximum allowable state of charge, respectively.

The dispatch strategy for a hybrid energy system is a set of rules for the interaction among various system components. It determines the energy flows from the various sources to the load, including the charging and discharging of the energy storage systems, on a time scale of hours, in such a way as to optimize system performance in terms of operating cost. In a system that has different renewable energy sources, the output from these renewable generators is generally subtracted from the hourly total load demand to determine the hourly net load. By observing the hourly operation of the proposed hybrid energy system configuration, there are five possible dispatch strategies to meet the net load. Suppose the net load is zero or negative in a particular hour. In that case, the battery charging strategy is used to absorb the surplus power (all or a fraction) generated by renewable generators. Alternatively, if the net load is positive, then all five dispatch strategies are used to operate and control the system. The summarized strategies that can be modeled are:

- Battery charging strategy
- Battery discharging strategy
- Load following strategy
- Cycle charging strategy
- Peak shaving strategy

For these analysis it is chosen to adopt the Battery charging strategy. Today, the known crucial technical solution for storage systems are:

- Mechanical energy storage (pump storage hydro-power plant, compressed air store and flywheel)
- Electrochemical energy storage (lead-acid, nickel metal and lithium-ion cells, high-temperature traction batteries, fuel cells and flow batteries)

The essential input data to determinate the typology of storage system and its dimension are:

- Available renewable energy generator power production capacity
- Hourly solar insolation
- Hourly demand load profile
- Battery bank capacity
- Unit cost of generation of different energy sources
- Minimum and maximum SOC of battery bank

Different storage models are proposed. The important criteria to choose the energy storage system are:

| Criteria | unit measure |
|---------------------------|--------------|
| Energy Density | kWh/m^3 |
| Power/Size | kW |
| Efficiency | – |
| Stability | – |
| Cyclability/Reversibility | – |
| Cost | <i>euro</i> |

Table 4.12: Storage property

Battery

To prevent overcharging of a battery, a charge controller is used to sense when the batteries are fully charged and to stop or decrease the amount of energy flowing from the energy source to the batteries.

- Battery charging efficiency
- Battery discharging efficiency
- Maximum capacity of battery, kWh
- Minimum state of charge of battery
- Maximum state of charge of battery
- Minimum energy stored in battery, kWh
- Maximum energy stored in battery, kWh

- Battery energy delivered directly to the load, kWh

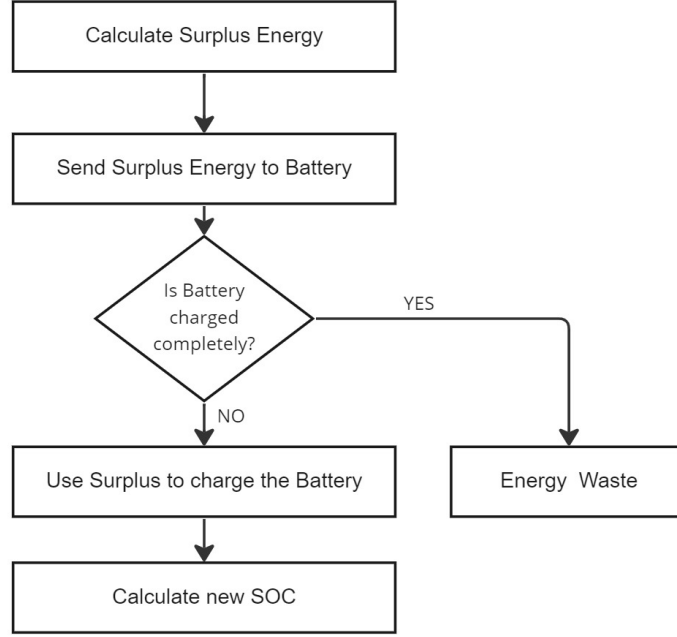


Figure 4.21: Battery charging algorithm

The depth of discharge is limited to 20% to 80% of the overall battery capacity; the depth of discharge represents the fraction of the battery that can be used without damaging the battery through internal irreversible processes, which shorten its capacity and durability. The battery state of charge (SOC) is the cumulative sum of the daily charge/discharge transfers. At any hour "t" the state of battery is related to the previous state of charge and to the energy production and consumption situation of the system during the time from "t-1" to "t". During the charging process, when the total output of all generators is greater than the load demand, the available battery bank capacity at hour "t" can be described by:

$$E_{battery(t)} = E_{battery(t-1)} + E_{surplus(t)}[kWh] \quad (4.23)$$

On the other hand, when the load demand is greater than the available energy generated, the battery bank is in discharging state. Therefore, the available battery bank capacity at hour t can be expressed as:

$$E_{battery(t)} = E_{battery(t-1)} - E_{surplus(t)}[kWh] \quad (4.24)$$

Meanwhile, the charged quantity of the battery is subject to the following constraints: The maximum value of SOC is 1, and the minimum SOC is determined by

maximum depth of discharge (DOD). For the system of this research, the working of the kind of battery will not be taken into account. Only the characteristic parameters, as the ration of energy input and output is taken into account: that is the round trip efficiency of the battery. The rest of the battery will be considered a black box.

At the end of the modelling of the storare system, knowing the profile of the wasted energy can be used to go into action all those auxiliary systems, such as the desalination plant. It is possible to fill a basin with drinking water by exploiting the energy that would otherwise be wasted.

4.6 Techno-economic analysis

The last task of the developed tool is to determine energy KPIs. In particular, it is chosen to report:

- Energy consumed per year
- Energy produced per year
- Energy load immediatly covered by renewable with and without storage
- Energy wasted with and without storage
- $LCOE_{theoretical}$: Theoretical Levelized Cost of Engergy
- $LCOE_{real}$: Real Levelized Cost of Engergy
- LCOS: Levelized Cost Of Storage
- $LCOE_{system}$: Levelized Cost of Engergy of yje system

Following the procedure for the determination the LCOE [39]. A general equation of the index includes the Capital Costs (CC), the annualized Operation and Maintenance ($O\&M$) cost, the Installation Cost, and the replacement cost of the system components throughout the system lifetime.

Costs of inverters, rectifiers, cable, and control system cost variables comprise only a small share of the system costs. For that reason, in the framework of this thesis, they are not considered [40]. In the proposed analysis different types of LCOE are reported to obtain a better comprehension of the energy system. In detail, in accordance with the reference [41] it is possible to define the following:

- the real LCOE, the cost of producing electricity from a technology, weighted on its actual productivity;
- the theoretical LCOE, the cost of producing electricity from a technology, weighted on its maximum theoretical productivity;
- the system LCOE, the cost of producing electricity in a system; thus, it is a weighted average of all of the LCOEs of the single technologies, also including the cost of storage;

The IEA [42] defines the LCOE of production technology as follows:

$$LCOE = \frac{\sum_{k=1}^t \frac{CC_k + O\&M_k + Fk + Carbon_k + D_k}{(1+ir)^k}}{\sum_{k=1}^t \frac{E_k}{(1+ir)^k}} \quad (4.25)$$

with:

- t: is the lifetime of the plant;
- CC: is the annual investment cost;
- O&M: is the annual cost of operation and maintenance;
- F: is the annual cost for fuel;
- Carbon: is the carbon cost;
- D: is the cost for decommissioning and waste management;
- E: is the electricity produced annually;
 - the total energy produced for the theoretical LCOE
 - the real usefull energy for the real LCOE
- ir: is the discount rate;

So, the two index obtained are:

$$LCOE_{theoretical} = \frac{\sum_{k=1}^t \frac{CC_k + O\&M_k + F_k + Carbon_k + D_k}{(1+ir)^k}}{\sum_{k=1}^t \frac{E_{k,produced}}{(1+ir)^k}} \quad (4.26)$$

$$LCOE_{real} = \frac{\sum_{k=1}^t \frac{CC_k + O\&M_k + F_k + Carbon_k + D_k}{(1+ir)^k}}{\sum_{k=1}^t \frac{E_{k,consumed}}{(1+ir)^k}} \quad (4.27)$$

The reference for each technology shows the theoretical and real LCOE, while in the present work, the theoretical and real LCOE already weighted by the RES is presented.

Regarding the storage, the equation considered is:

$$LCOS = \frac{\sum_{k=1}^t \frac{C_{cap} + O\&M_k + C_{rep} + C_{EL}}{(1+ir)^k}}{\sum_{k=1}^t \frac{E_k}{(1+ir)^k}} \quad (4.28)$$

where:

- C_{cap} is the annual capital cost of the investment;
- O&M is the annual cost of operation and maintenance;
- C_{rep} is the annualized cost for replacement;
- C_{EL} is the annualized cost for disposal and recycling;
- E_y is the annual electricity discharged;

In the equation considered, there is undoubtedly a surcharge since the part relating to the nominal power installed of the RES should be corrected in the capital cost, the real power used to store the energy of the RES in the capital.

Finally, the real LCOE of the considered system is determined. This value will result, due to the overestimation made in the LCOS, lower than the LCOS but higher than the LCOE of the RES.

Following a more specific description of the parameters described above:

- *CC*: Capital Cost: The investment cost includes the cost of plant, machinery and equipment, and the cost of studies and labor work. An estimation of specific investment costs per kW for each component of the hybrid plant separately and the values are presented in Table. The investment cost in present value, which is the time of the starting of the operation of the system, is formulated by the following equation:

$$CC = \sum_{n=1}^N n_i P_i S P_i \quad (4.29)$$

where:

- n_i : Number of the i-component
- P_i : Nominal Power by the i-component
- $S P_i$: Specif Prize by the i-component

Regarding the investment cost per kW [40] [43]:

| Component | Investment Cost per kW [euro/kW] |
|-----------------------------|----------------------------------|
| Wind Turbine (WT) | 2000 [44] |
| Photovoltaic Collector | 1070 |
| Floating PV | 700 [45] |
| Wave Energy Converter (WEC) | 2890 |
| Batteries | 450 [euro/kWh] |

Table 4.13: Investment Cost per kW for each component of the system [46] [47]

- O&M: annual operation and maintenance cost of the hybrid system. They include expenses for the labor salaries, maintenance and repair expenses of batteries, central inverter of the wind turbines and photovoltaic panels, and the annual premium for the facilities. In the calculations the annual *O&M* costs are generally considered to be stable and equal to a percentage of the

investment cost. These costs are considered to increase only by following the rate of inflation.

$$O\&M = O\&M_{\%}CC \quad (4.30)$$

where:

- $O\&M_{\%}$: $O\&M$ Cost as percentage of CC (4%)

To distinguish the different maintenance operations, instead of considering them as a percentage of the investment cost, it is possible to refer to the following values [43]:

| Component | $O\&M$ Cost per kW [euro/kW/year] |
|-----------------------------|-----------------------------------|
| Wind Turbine (WT) | 32 [44] |
| Photovoltaic Collector | 20 |
| Floating PV | 30 [45] |
| Wave Energy Converter (WEC) | 85 |
| Batteries | – |

Table 4.14: Operation and maintenance per kW for each component of the system [43]

- ir : Discount Rate (7%)
- t : life time (30 years)

4.7 Critical issues of the model and future improvements

A bottom-up approach generated a profile of energy demand and production.

Devices and actions resulting from triggered behaviors are simulated based on predefined probability profiles. The thermal demands of the system were simulated based on meteorological data and the technical characteristics of the building. The resulting load profiles exhibit a continuous shape, as you would expect. In detail, the loads that occur vary daily and present extreme load situations. As a result of the simulation, it was possible to reach an initial level of optimization of the system. To improve the accuracy of the calculated energy demands, a comparison with similar systems or, at best, even a prototype of the platform constructions should be performed. Furthermore, the efficiency of energy supply systems could be increased by installations that more specifically meet the energy needs of the hub. [48]

All steps of the tool have ample room for improvement. From the point of view of the typical meteorological year, it could be interesting to carry out more in-depth climatic analyzes not based only on history to take into account the future scenarios that can be foreseen.

From the view of resources and production, other forms of energy can be analyzed in a study of this type. For example, the energy of currents and the energy produced by biogas treatment could make an essential contribution. At the same time, we will have to wait longer to implement the system by adding other forms of renewable energy conversion that can be competitive (e.g., due to the difference in salinity).

As far as the estimation of energy consumption is concerned, the necessary improvements are the increase in the intended uses studied and the increase in the precision in determining consumption. To carry out the latter, it is necessary to include thermal zoning of buildings and increase the electrical devices considered.

One of the steps to pay more attention to improve the estimate is undoubtedly that of storage, specifically from different points of view. At the current state of the art, batteries for this type of system are the safest and most reliable solution: a necessary improvement is, therefore, the modeling of the battery: instead of considering it as a simple box in which to store energy when there is a surplus and from which to draw energy when there is an imbalance in demand, an algorithm could be developed which can charge the battery intelligently in such a way as to minimize the uncompensated loads and to optimize the satisfied loads.

From another point of view, it could be interesting to focus on other accumulation systems of a mechanical or thermal type. Since it is a thesis that deals with floating platforms, we want to mention a recent project carried out by the startup Ocean Grazer, a spin-off of the University of Groningen, in the Netherlands. These are the Ocean Batteries, and submarine batteries whose operation was developed from an evolution of the classic pumped hydroelectric plants. The core of the Ocean Battery lies in constructing a vast underwater tank capable of holding up to 20 million liters of water at low pressure. According to the calculations, this would be sufficient to contain a consideration of 10 MWh. According to the Dutch startup project, the underwater tank should be connected via a pumping system to an air chamber located at a higher level. The electricity generated on the surface would then be used to pump the water stored in the tank into the chamber located at the top: only when there is a demand for electricity that same water will be allowed to fall downwards (exploiting the natural pressure of the ocean water placed above the inner tube) and then towards the tank, activating the turbines suitably placed along the descent. An advantage of this storage system would undoubtedly be the space gained on the platform as the ocean batteries would be placed on the seabed. At the same time, their installation cost is one of the main problems. [49] [50] [51]

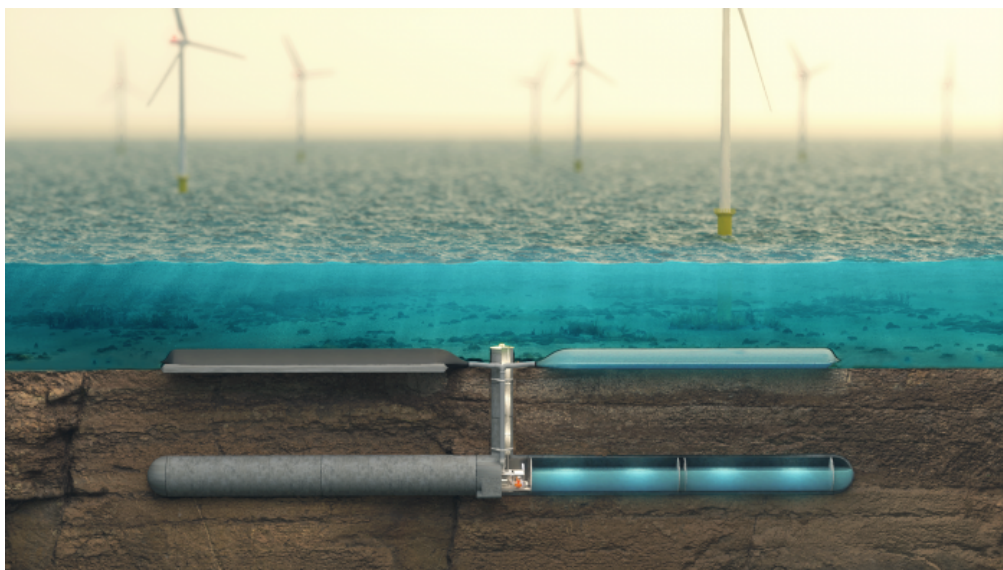


Figure 4.22: Ocean Battery

Chapter 5

Case study: Venice



Figure 5.1: Venice from the top

5.1 Venice overview

It is clear that in recent years the city of Venice has launched several requests for help. The last two aspects caused by mass tourism are: the depopulation and the denaturalization of the Venetian community. The site has the advantage of having a depth of fifty meters within 3km from the coast, figure, a factor that is of primary importance for the development of the platform, especially since this bathymetry facilitates anchoring and installation. Among the aspects in favor there is also the social one. Venice, in fact, is known for its universal paradigm of "city on water";

therefore, starting with this distinctive feature, recognized globally, we can go on to define an innovative and Italian solution to sea level rise.

5.1.1 Depopulation

In 1950 the historic center of Venice was inhabited by about 184,000 people. Today there are no more than 60,000 inhabitants in this area. Over the past 50 years, the historic center has lost almost two thirds of its inhabitants, meaning that on average 2,300 people a year leave this area of the city and head to the mainland [52].

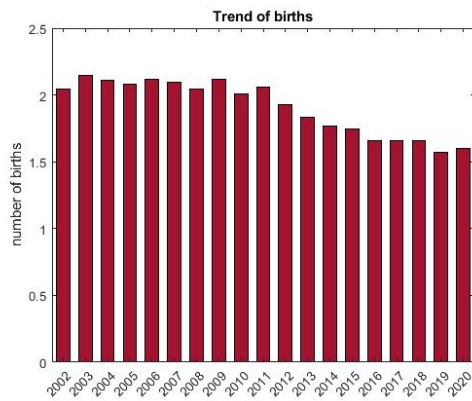


Figure 5.2: Births

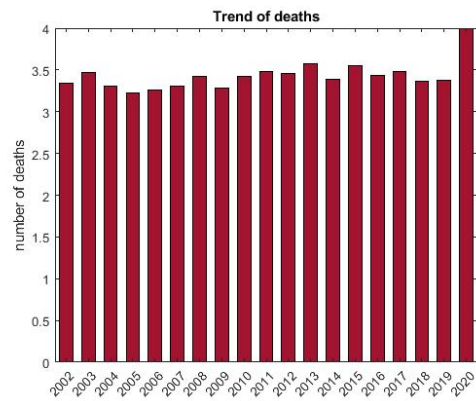


Figure 5.3: Deaths

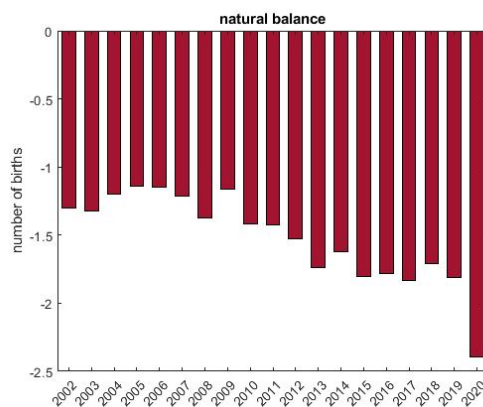


Figure 5.4: Natural balance

5.1.2 Sea Level

According to Climate-ADAPT [53], a partnership between the European Commission and the European Environment Agency, Venice is the second Italian city at risk of flooding and is the one with the largest urban area potentially affected by the rise of one meter in sea level within fifty years. In the affected area, works have already been carried out to contain water. In particular, launched in 2003, the MOSE [54] is a project consisting of barriers formed by rows of bulkheads, which allow the lagoon to be temporarily separated from the sea when a high water event is expected, located at the harbor mouths. It is part of a larger project that provides for the reinforcement of the coasts. The cost of the loan corresponds to 7,268 million euros.

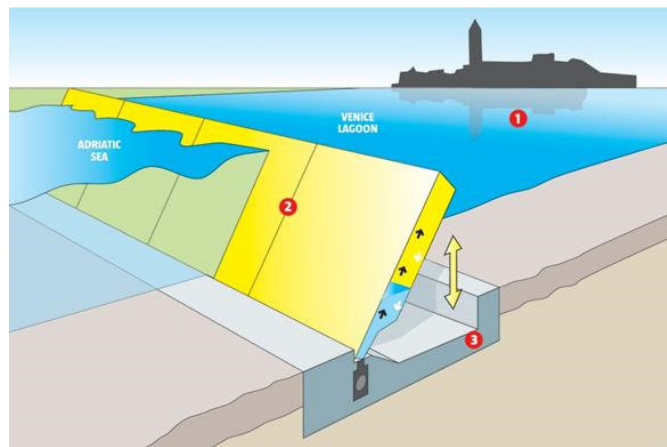


Figure 5.5: Mosè in Venice

The state of the art to date how to adopt a solution for the expansion of maritime cities is dredging, which is however financially very onerous and has a high impact on the marine and coastal environment. The solution of artificial islands has been studied in recent years as cheaper and more sustainable solutions with the funding allocated in Europe by the Horizon 2020 program.

5.2 Venice energy consumption

In the analysis [55] provided by Terna [56] the electricity consumption per inhabitant of the city of Venice is reported from the year 1963 to 2018. It is noted that this has a growing trend until 2012, then it decreased until the year 2015, now it is again uphill

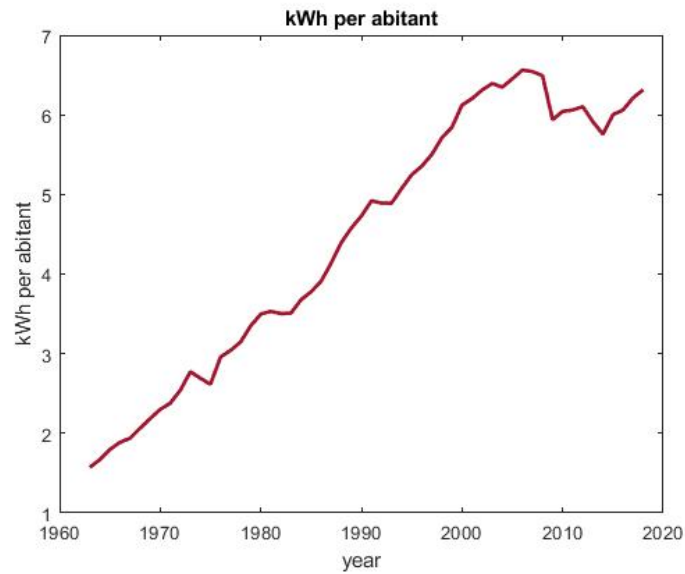


Figure 5.6: kWh per abitant

Based on the regional statistics for 2019, the gross installed power in the province of Venice is 2515 kW/h, of which 281.3 kW/h is renewable. While the net one is 2360.7 kW/h of which 275.7 kW/h of renewable.

In the following figure it is reported in kW the energy production of Venice province and its request along the period 2005-2022

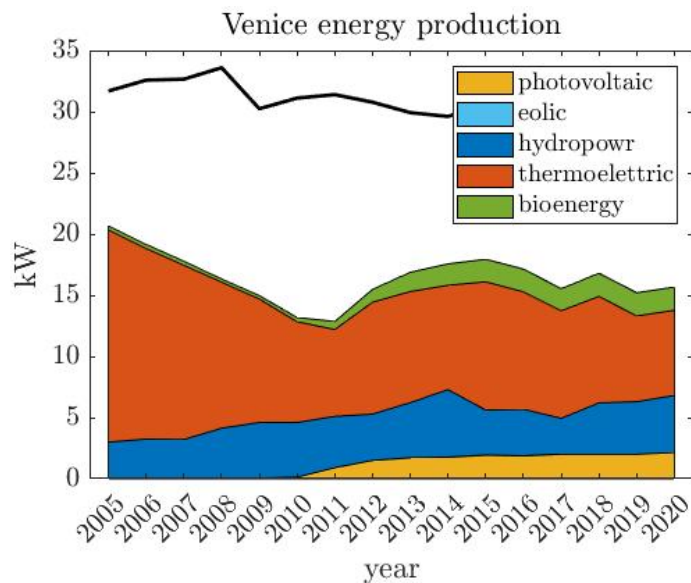


Figure 5.7: Venice energy production and request

Terna provides information about the distribution of consumption in the different sector, it is reported an average between the years 2001-2022: the industrial sector consumers the most (53,18%) followed by the tertiary sector (services) with a percentage of 26,66% and the domestic field that consumers the 18,08% of the electricity consumption. A little portion (2,3%) is for the agriculture.

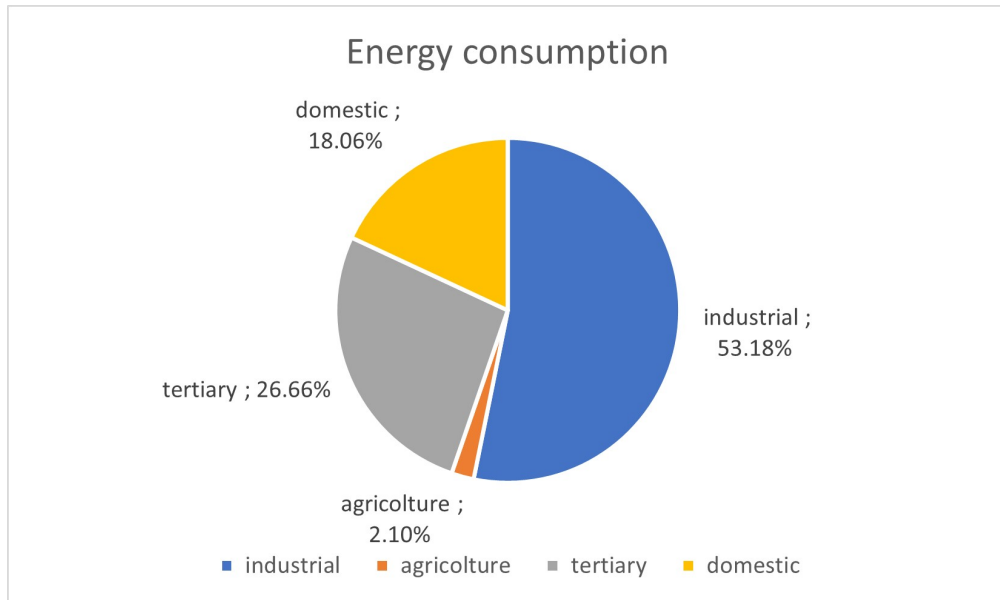


Figure 5.8: Energy consumption per sector

5.3 SeaForm

Analyzing the situation and the habits of the city, this lends itself very well to a possible site to build a floating city on its shore. After an investigation, it was chosen as the city for the installation of the prototype. The prototype aims to create three floating display platforms with smaller dimensions than those envisaged for the floating city. In order to present the results of the tool, the city of Venice was chosen as the site to already have the data on the energy resource for the exhibition pavilion. In order to demonstrate technological feasibility, following the first scale prototype for the city of Venice, which aspires to have both a testing role for the technology in a protected environment and commercial value for presentation and publicity, Seaform plans to implement at least one launch (full-scale) project.



Figure 5.9: Pavillon exposition

From the point of view of the project, on the other hand, possible configurations of the final project are reported. Specifically, the platform's substructure is hexagonal, with a diameter of 57 meters and an area of 2,107 square meters; it will be built in reinforced concrete for a total volume of 12,661 cubic meters. Its maximum dimensions were dictated by constructive constraints on the size of the shipyards in which it could be built. The next chapter of this thesis aims to report the results obtained from the tool implemented on Matlab to the explained case study. A set of 6 platforms to be installed on the Venice site is considered. Therefore, the climate of the data entered in the tool is those of the city of Venice. In particular, experimental data obtained directly from the measurements made by the sensors installed inside an off-shore platform was used.

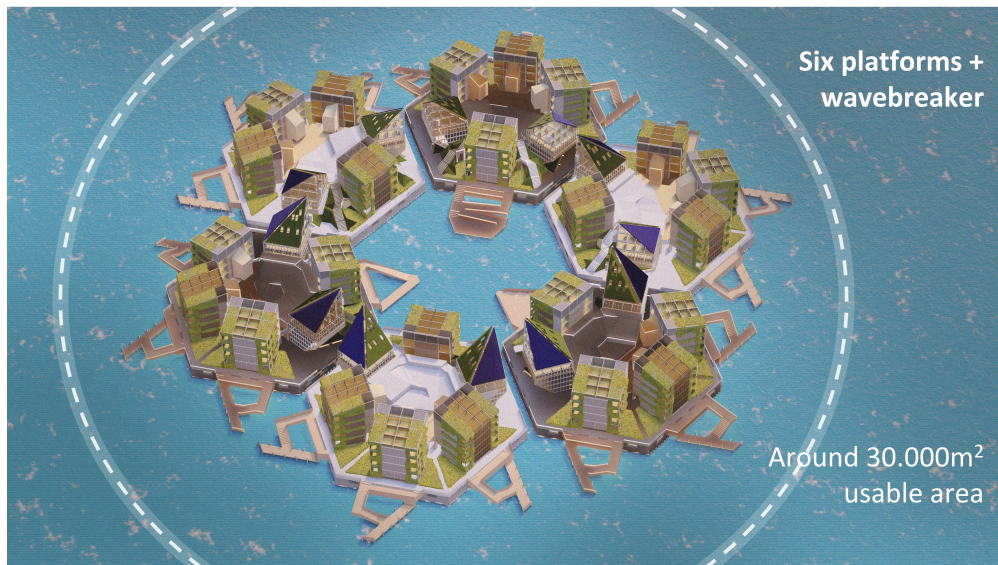


Figure 5.10: Six platform configuration

Chapter 6

Results

6.1 Typical meteorologic year

The meteorological data from which the typical year for the Venice case study was implemented were obtained from the ISMAR platform weather station of CNR [57], situated on the Adriatic costs with coordinates:

- 45 ° 18' 83.00" N
- 12 ° 30' 53.00" E

The platform is able to detect meteorological data thanks to different sensors: the obtainable parameters and the sensors used are shown in the table. The database of the station dates starts to 1983. In the case in question it was decided to analyze the meteorological data of the years 2012-2021.



Figure 6.1: ISMAR platform

| sensor | type of sensor | heigh |
|--------------------|----------------|--------|
| wind direction | t033 TDV | 20 m |
| wind speed | t031 TVV | 20 m |
| barometer | t011d TBAR-IVS | 12 m |
| ignometer | t003 TRH | 18 m |
| air temperature | t001 TTEP | 18 m |
| water temperature | t020 TTA | -2.2 m |
| solar irradiation | t055 TPIR | 18 m |
| rain gauge | t027 TP1K | 16 m |
| tide gauge | t039 TIDROM | 7 m |
| acquisition system | DA9000 | 12 m |
| wave gauge | t021 TLU16 | 8 m |

Table 6.1: Sensors of ISMAR

Following the procedure described above the Typical Meteorologic Year obtained for the site of Venice is reported:

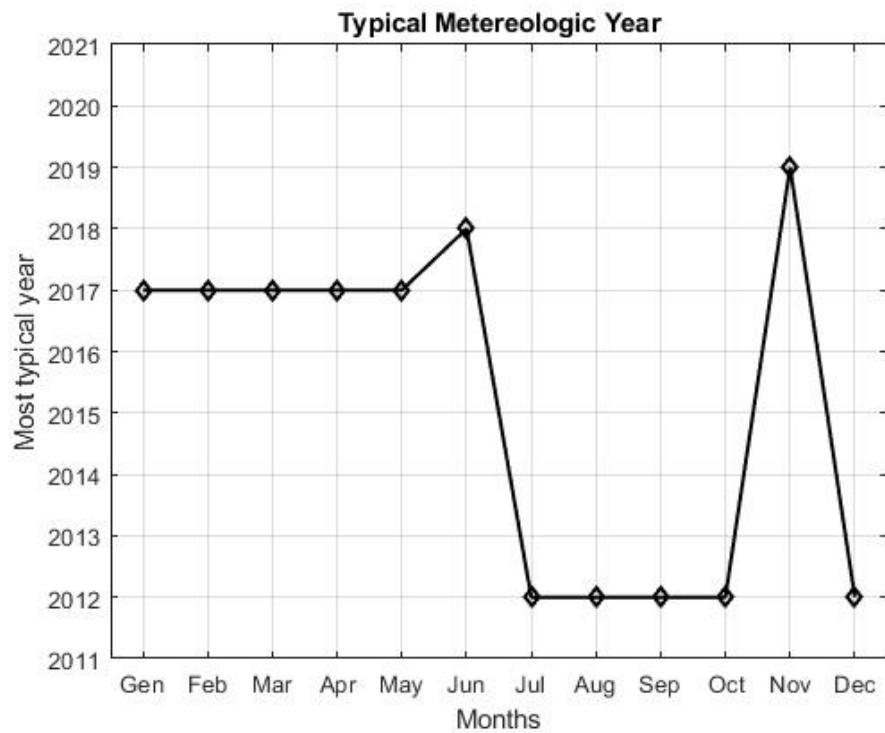


Figure 6.2: TMY

The trends of the 4 meteorological parameters used for the analysis of the site resource and for the estimation of the loads of the platform utilities are reported:

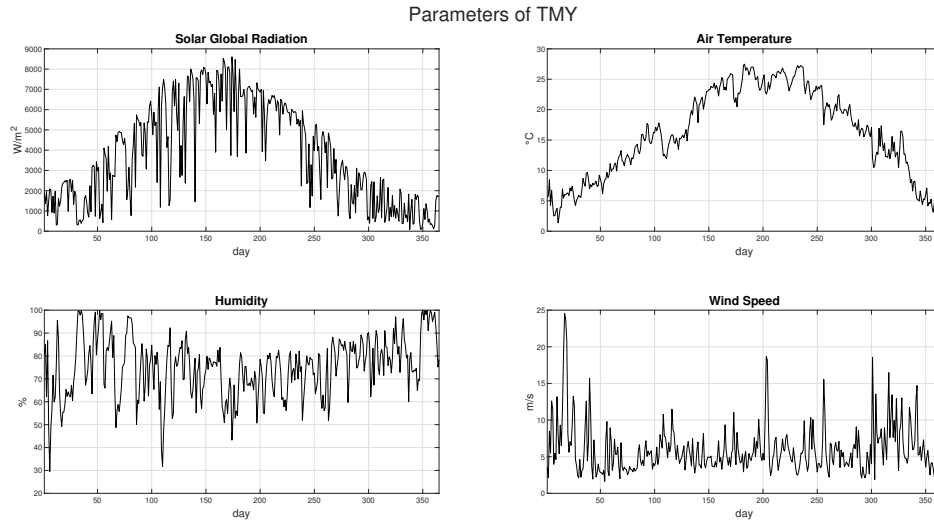


Figure 6.3: TMY Parameters profile

As expected, the trend of the closely related parameters, solar radiation and temperature is similar. The maximum temperature reaches is $28^{\circ}C$ in July while the minimum is $2^{\circ}C$ reaches in January. The hottest day of the year is July 2nd with an average temperature of 28. While the highest hourly temperature recorded is $31^{\circ}C$ on August 22nd. The coldest day of the year is January 11th with an average temperature of $1.36^{\circ}C$. While the lowest hourly temperature recorded is $-0.6^{\circ}C$ on the night of January 10th.

The humidity is very high, and, considering that both the meteorological platform and the platform under study are located in the sea, it is very predictable.

The maximum speed measured is 25 m/s during the month of January while the average annual wind speed is 4.85 m/s. The average wind speeds at the site are shown, with the maximum values of 9m/s and 7.6 m/s respectively in January and in November and with the minum values of 4.6 m/s in March.

Comparison between the TMY and the other years

The figures below compare the trends of the selected parameters in the ten years considered and the TMY. As it is possible to see, the TMY is a good trade-off between the stoical archive. Furthermore, the use of TMY, compared to the use of a real year, solves the problem of the lack of some data due to measurement errors and temporary malfunction of the sensor.

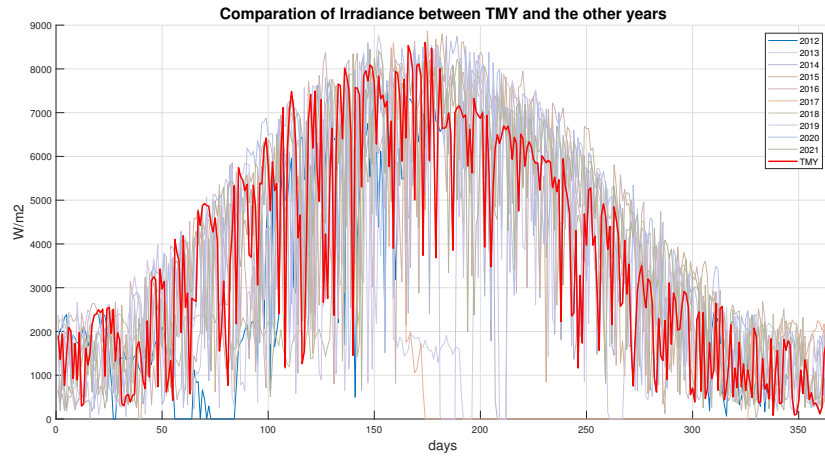


Figure 6.4: Comparison between Solar irradiation profile of TMW and the real years

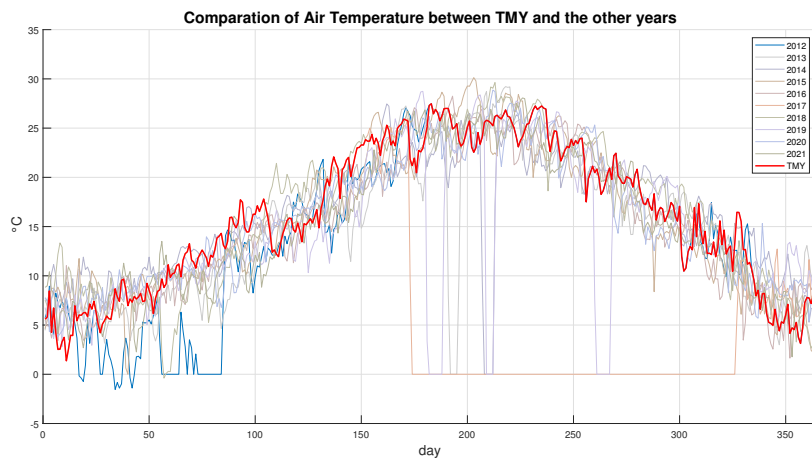


Figure 6.5: Comparison between Air Temperature profile of TMW and the real years

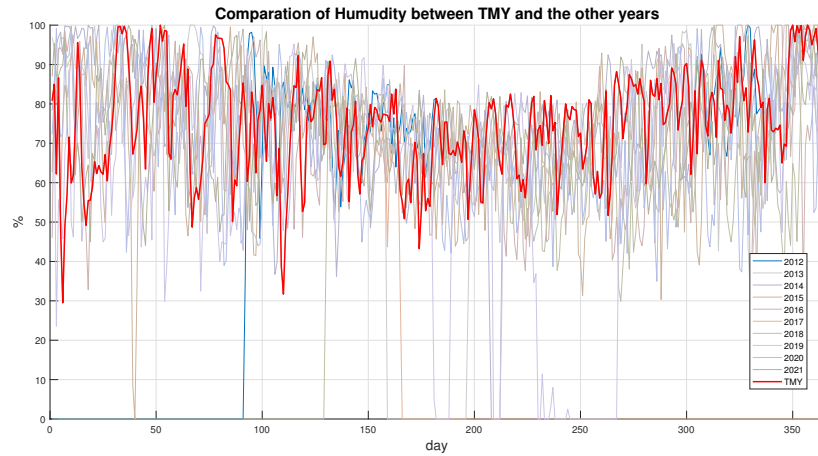


Figure 6.6: Comparison between Humidity profile of TMY and the real years

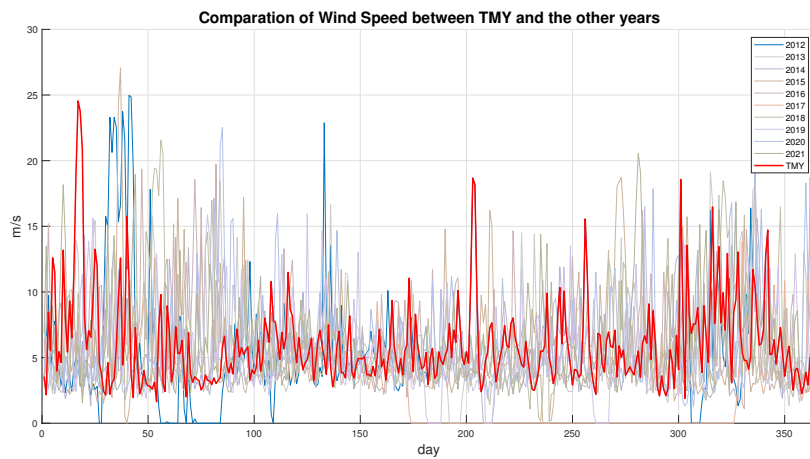


Figure 6.7: Comparison between Wind Speed profile of TMY and the real years

6.2 Resource Analysis

6.2.1 Sun

Data collection

Thanks to a Global Solar Radiation Transducer sensor installed at 18 m of height on the ISMAR platform, it is possible to obtain the data request. It is a very valid sensor for the most varied uses in the field of meteorology, thanks to the high standards of accuracy (10 W/m^2), which connotes it is equipped with a thermopile sensitive element. The sensitive element generates a voltage proportional to the measured radiation, which is acquired by signal conditioning electronics, which normalizes the output into a standard voltage, current signal. A double dome made of special optical glass optimizes the measurement characteristics and allows a wide measurement range of the solar radiation frequency ($0.3 - 3\mu\text{m}$).



Figure 6.8: Sensor solar

Potential

The total radiation of each month is shown: as expected, the month with the greatest amount of solar power is June with 200 kWh/m^2 while the month with the minimum is December with 27.59 kWh/m^2 . The total radiance in one year is 1380 kWh/m^2 , and the mean daily radiance in summer is and in winter is 5.406 kWh/m^2 and 2.12 kWh/m^2 , respectively.

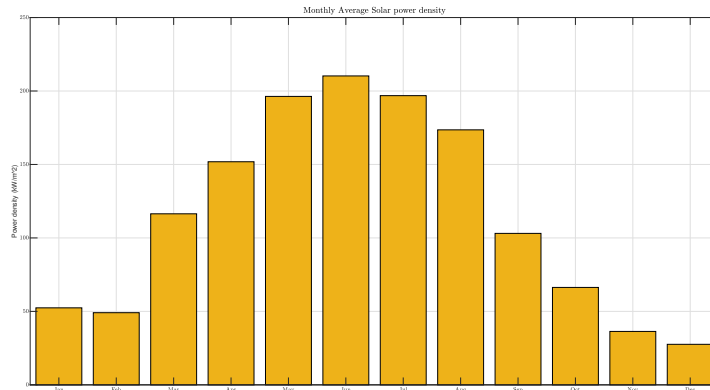


Figure 6.9: Monthly average

The typical days on which the daily analysis is carried out are chosen based on the trend of solar radiation and are:

- 15/06: Summer Typical Day
- 11/01: Winter Typical Day
- 17/04: Spring Typical Day
- 10/11: Autumn Typical Day

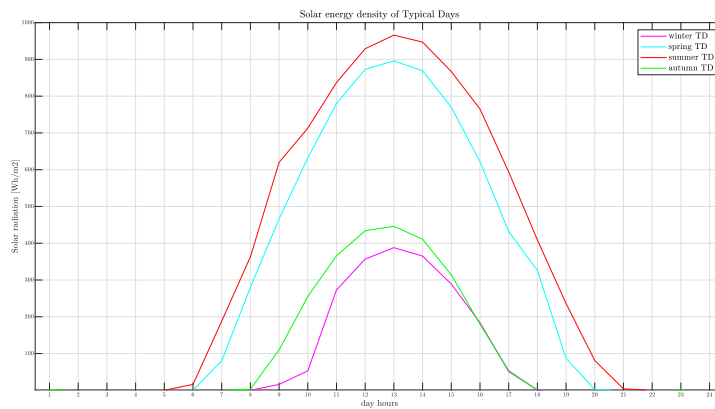


Figure 6.10: Solar power density TDAY

As can be seen, the summer and spring trend is very similar and the same regarding winter and autumn. Therefore, in this specific study, only two seasons will be considered regarding load profiles: summer and winter.

Then it is reported the daily total of Solar Power density for the 12 months of TMY.

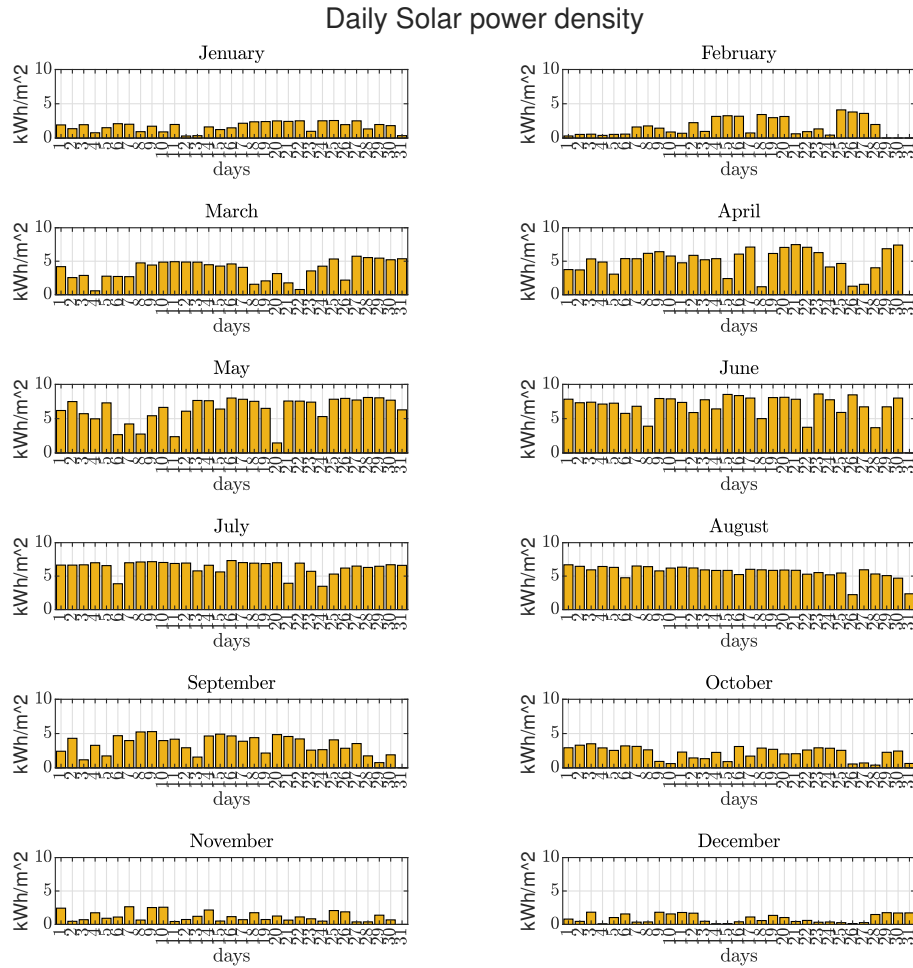


Figure 6.11: Daily irradiance

6.2.2 Wind

Data collection

To obtain wind speed data, a wind speed transducer is installed in the ISMAR platform, consisting of a swirling body that rotates on itself by exploiting the wind resistance of three conical elements (cups). Inside the rotating structure is a cylindrical magnetic element with six poles, and a Hall effect-sensitive element detects the rotating phenomenon by generating an impulse as every single pole passes. The dimensions of the cups and the lightness of the materials used were chosen to obtain a very low mechanical inertia and, consequently, to guarantee a high sensitivity of the measurement. The robust structure of the sensor guarantees its durability and adequate resistance even at high wind speeds. It has a sensitivity of 0.1 m/s.

The sensor is designed to ensure high performance in monitoring wind direction. The sensitive element consists of a balanced vane coupled to a magnet, whose position is detected using a hall effect device. This system allows us to detect with extreme precision the band's orientation concerning the angular degree at the point of origin and the angular direction of the wind with a resolution to the tenth degree. The dimensions of the vane and the lightness of the materials used have been designed to obtain a very low mechanical inertia and consequently guarantee a high sensitivity. The robust structure of the sensor guarantees its durability and adequate resistance even at high wind intensity. Furthermore, its simple and compact design facilitates installation and simplifies maintenance activities in the field. The sensor is supplied complete with power and signal cable (12m) and is also available with a heating element that can be powered at 24 V in alternating or direct current.



Figure 6.12: Wind speed sensor



Figure 6.13: Wind direction sensor

Potential

Regarding the direction, the wind rose is shown, to establish which could be the best orientation for the turbines. As you can see it is the north-north east quadrant.

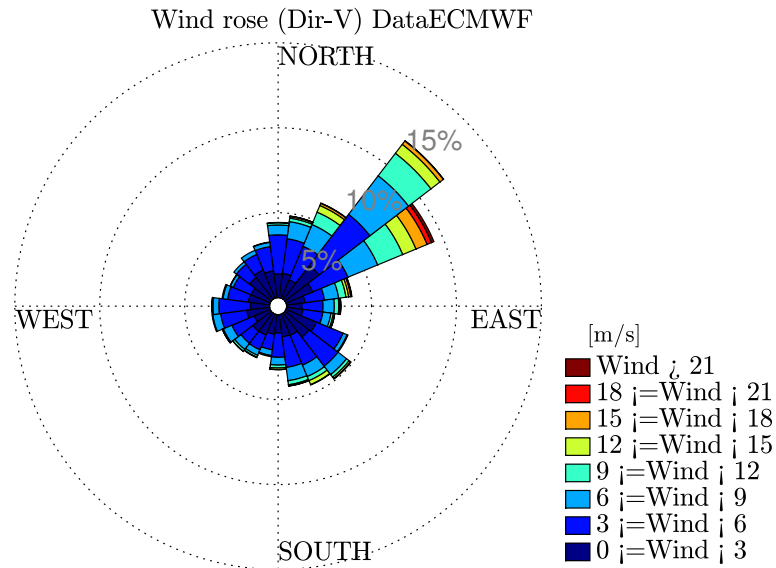


Figure 6.14: Wind rose

The maximum speed measured is 25m/s during the month of January, while the average annual wind speed is 4.85 m/s . The average wind speeds at the site are shown, with maximum values of 9m/s and 7.6 m/s , respectively, in January and November and minimum values of 4.6 m/s in March. The month with the highest average is January, for which there is an average speed of 7.29 m/s and theoretical maximum energy of 547.67kWh/m^2 . On the contrary, during March, there is a lower peak of 52.32kWh/m^2 maximum extractable energy. In fact, the average wind speed in that month is 3 m/s . It is interesting to note how, on a seasonal level, the two resources: solar and wind, are pretty complementary.

The average trend for each month is reported both from the wind speed and the theoretical maximum energy that can be extracted.

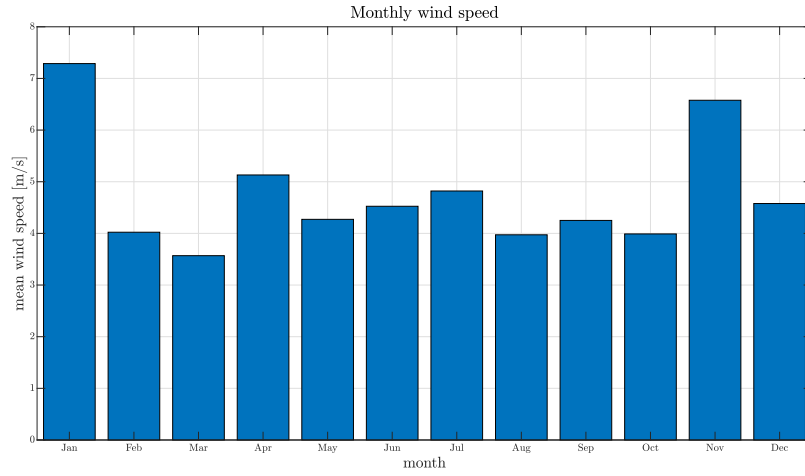


Figure 6.15: Monthly average daily wind speed

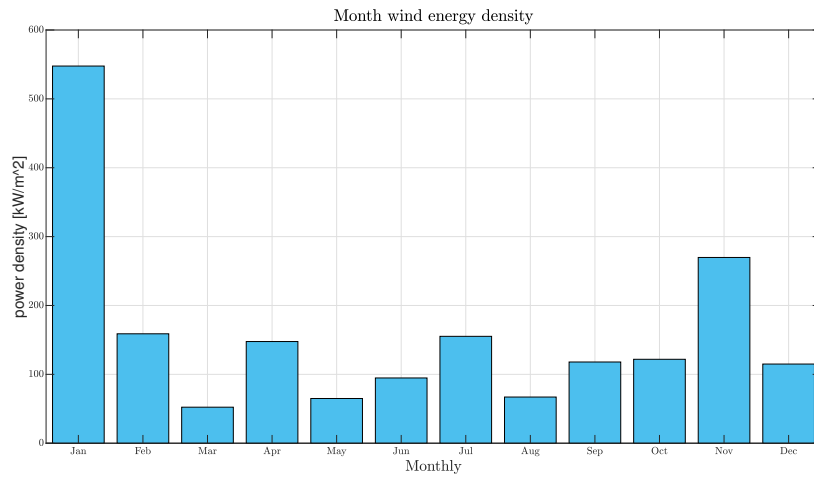


Figure 6.16: Monthly energy density

It is chosen to report the trend of the speed to notice that the site does not have an exceptionally high speed; having an overview of the average speed, it is possible to start making an assessment on the cut-in speed of the type of turbine to be installed.

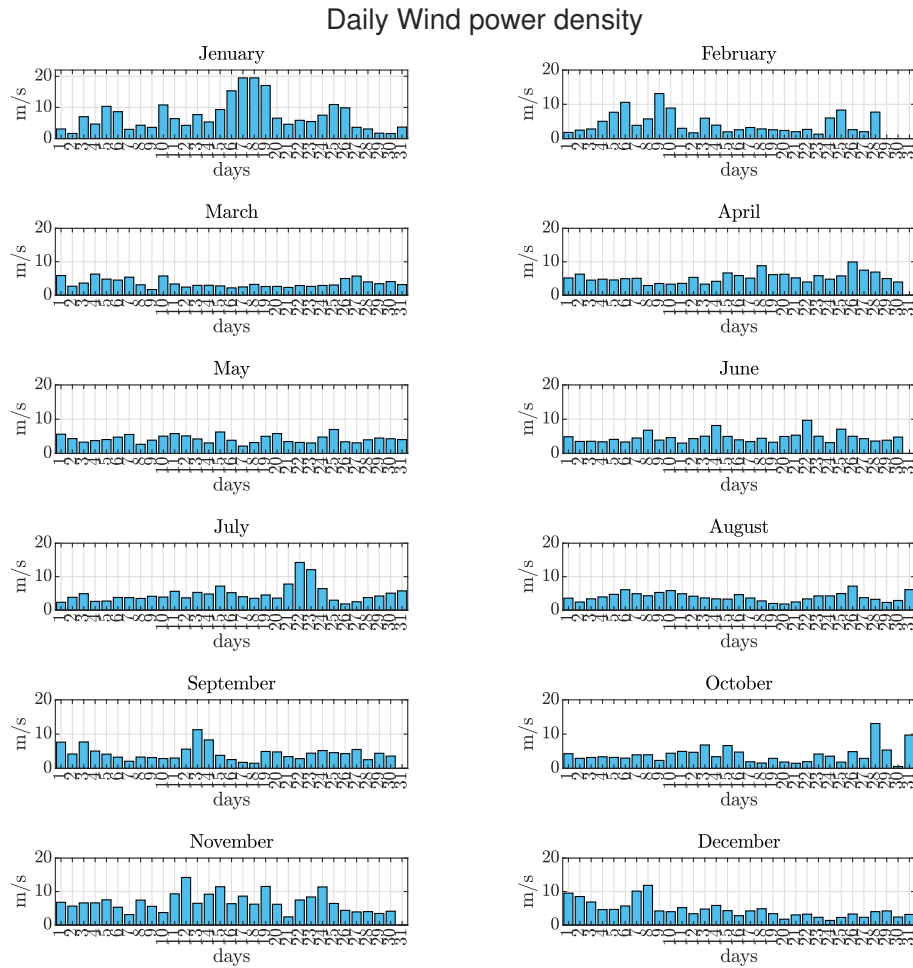


Figure 6.17: Daily average wind speed

Moreover, the typical days trend of power density are reported:

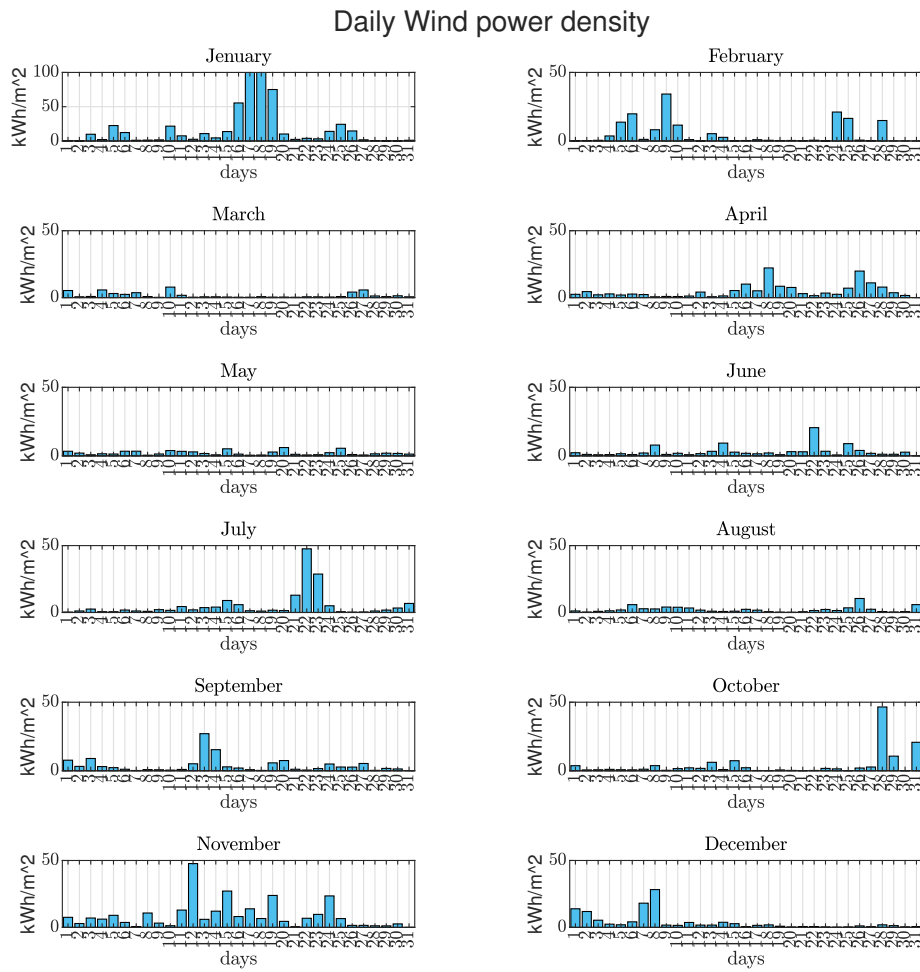


Figure 6.18: Daily average wind power density

The typical day profile of wind is also reported

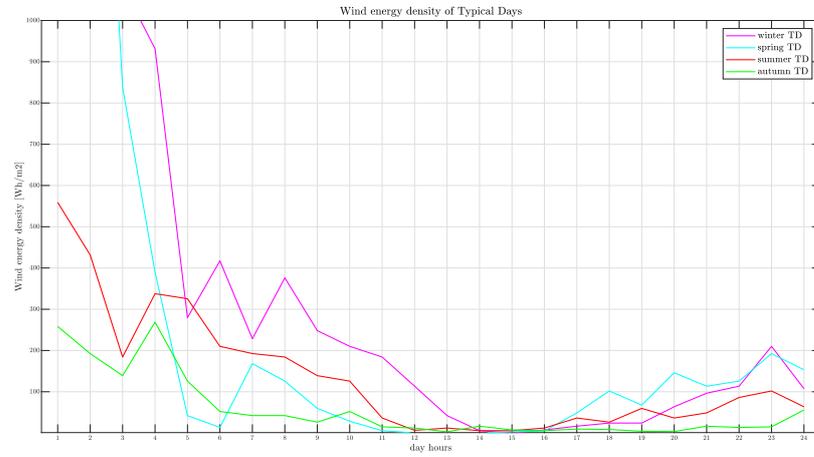


Figure 6.19: Wind power density TDAY

6.2.3 Wave

Data collection

The wave detection sensor is an ultrasonic sensor installed at about 8 meters above sea level and equipped with specific software for the calculation of the typical quantities of wave motion, such as the significant wave (understood as an average of 1/3 of the highest waves), the maximum wave and the average period. Processing is performed every 15 minutes. The published values were only subjected to the first validation level; given the instrument's position and the difficulty of detection, especially in rough sea conditions, invalid data may be present in the data series.



Figure 6.20: Wave sensor

Potential

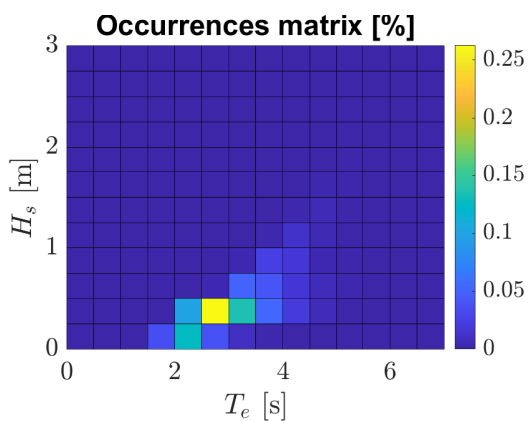


Figure 6.21: Wave occurrence scatter

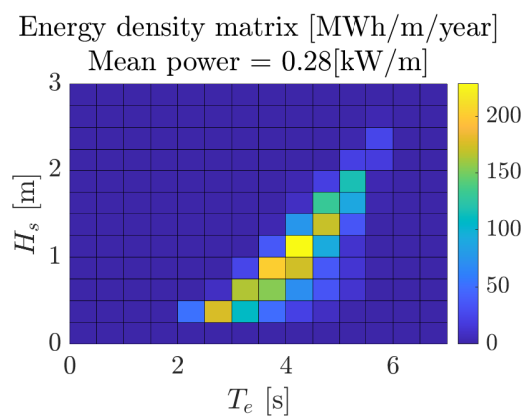


Figure 6.22: Energy wave scatter

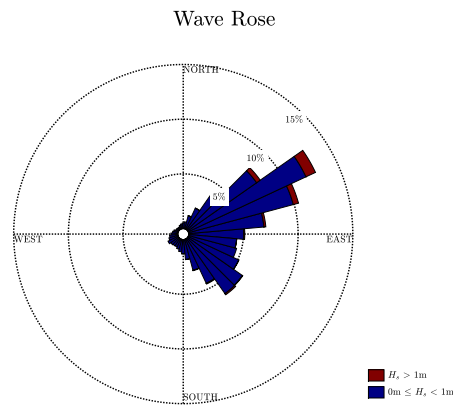


Figure 6.23: Wave rose

From the two matrices proposed for the study of waves, it is evident that the most energetic waves are less probably. Vice versa, the most frequent waves are the ones from which the extractable energy is less. [58]

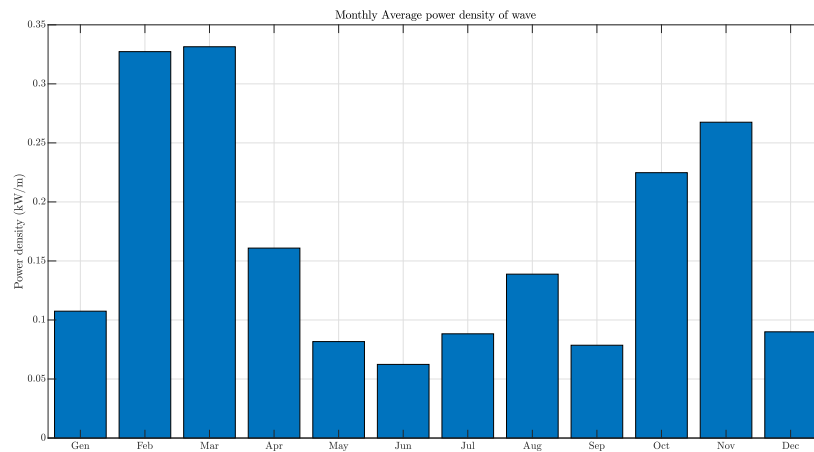


Figure 6.24: Monthly power density of wave

The power density of the waves is considerably lower than that due to the solar and wind resources. For this reason, the analysis for the case study of Venice will not continue with the analysis of the power produced by the waves. It will focus exclusively on solar and wind energy.

6.2.4 Renewable Resource

At this stage of the study no other possible energy sources were analyzed. The month trend of renewable power is reported.

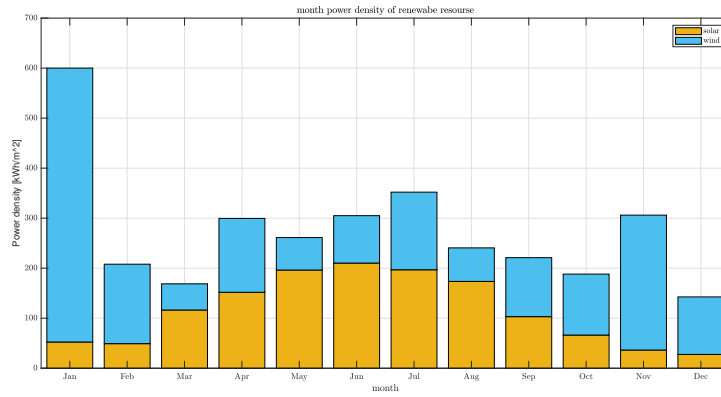


Figure 6.25: Montly renewable energy density

The total energy density for the site is around $3.3 \text{ MWh}/\text{m}^2$.

For the four typical day the hourly profile is also reported. It is interesting to notice as the wind power theoretically can be complemented with the sun power. The problem will be presented after with the productivity analysis.

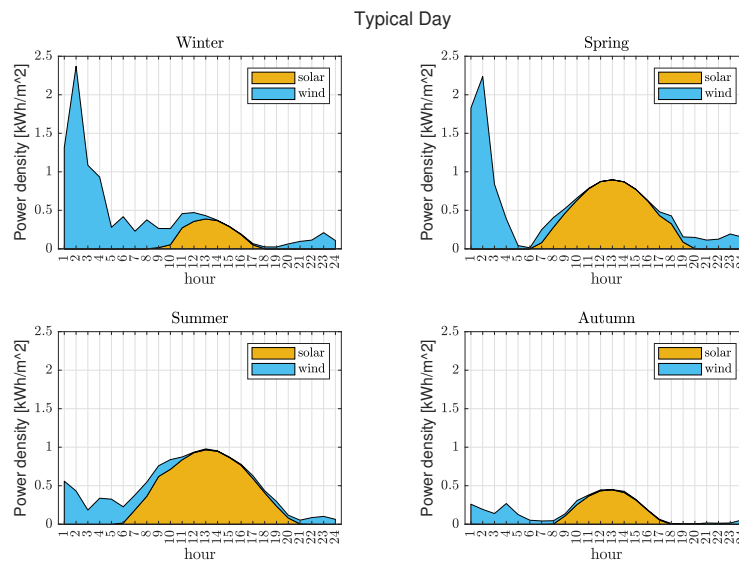


Figure 6.26: Renewable energy density of TDAYS

6.3 Estimation of consumption

This section of the thesis aims to show some application cases. Initially, the trend of the three types of loads is presented, in line with what is explained in the methodology section, for the three different uses that can accommodate a single piece. Each building, as explained, is modular: therefore, made up of several pieces. Each piece is assumed to be the same 10mx10mx4m size regardless of the relative position it occupies in the building and the activity that is carried out inside it. These assumptions are made in order to go and identify those configurations that are closest to energy independence by going quickly and efficiently to change the configuration of the platforms. However, they will be responsible for an overall overestimation of consumption. This is done to maintain conservative accounts.

6.3.1 External Temperature

The sensitive component of the sensor consists of a Pt100 platinum resistance thermometer with a response curve conforming to the DIN 43760 Class 1/3 standard and 4-wire connection. The sensor body is made of high-quality plastic material with stainless steel screws. The generously sized protection screen is made of non-hygroscopic and UV-stabilized plastic material, which reproduces an ideal measurement environment, ventilated and protected from direct sunlight. The sensor can be supplied with natural output (4 wires) or with normalized voltage, current or digital electrical outputs. The sensor is supplied complete with power and signal cable (4m).



Figure 6.27: Temperature sensor

6.3.2 Thermal load

Specifically, the data used for the calculation are shown in table x and they are according with the standard ones, reported in the legislation associated with climatic zone E [59].

| Data | Symbol | Value | Measure Unit |
|------------------------------------|-------------|-------|--------------|
| Wall trasmittance | U_{wall} | 0.26 | W/m^2K |
| Coverage trasmittance | U_{cov} | 0.22 | W/m^2K |
| Floor trasmittance | U_{floor} | 0.26 | W/m^2K |
| Windows trasmittance | U_w | 1.40 | W/m^2K |
| Dividers trasmittance | U_{div} | 0.8 | W/m^2K |
| Height | h | 4 | m |
| Wall Surface | S_{wall} | 160 | m^2 |
| Windows percentage for residential | po | 9 | % |
| Windows percentage for office | po | 2 | % |
| Windows percentage for facilities | po | 3 | % |
| Volume | V | 400 | m^3 |
| Floor surface | S | 100 | m^2 |
| Roof surface | S | 100 | m^2 |

Table 6.2: Building Parameters

The thermal loads profiles for the different pieces analyzed are reported:

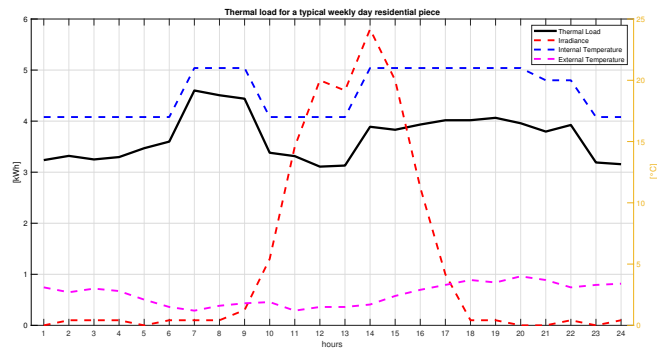


Figure 6.28: Thermal load profiles for residential piece in a Typical winter Day

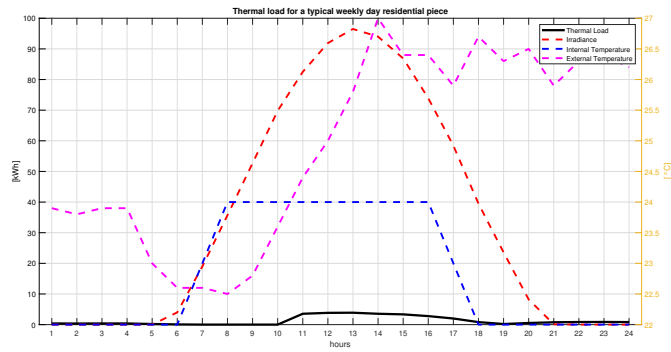


Figure 6.29: Thermal load profiles for residential piece in a Typical summer Day

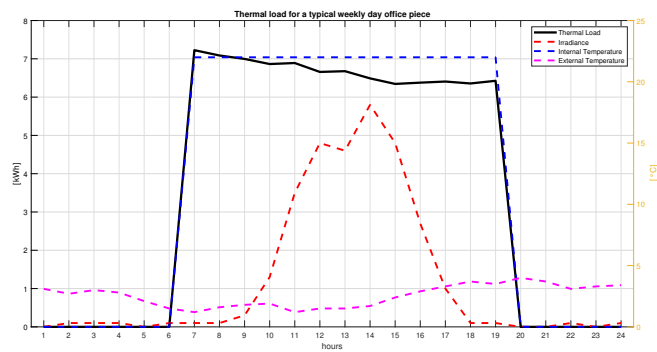


Figure 6.30: Thermal load profile for office piece in a Typical winter Day

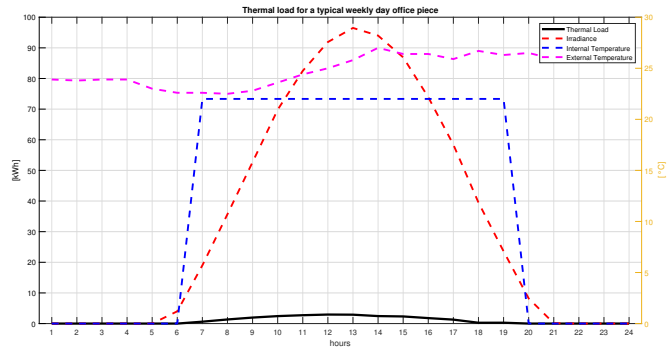


Figure 6.31: Thermal load profile for office piece in a Typical summer Day

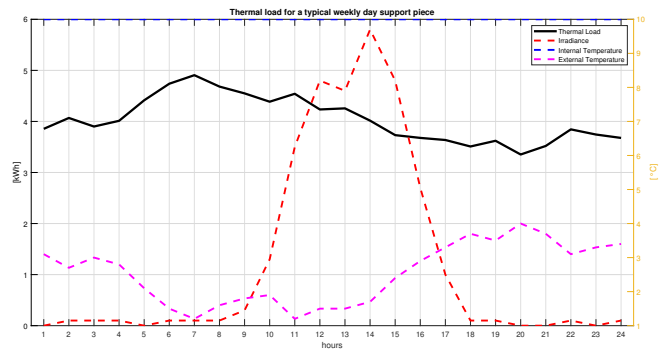


Figure 6.32: Thermal load profile for support piece in a Typical winter Day

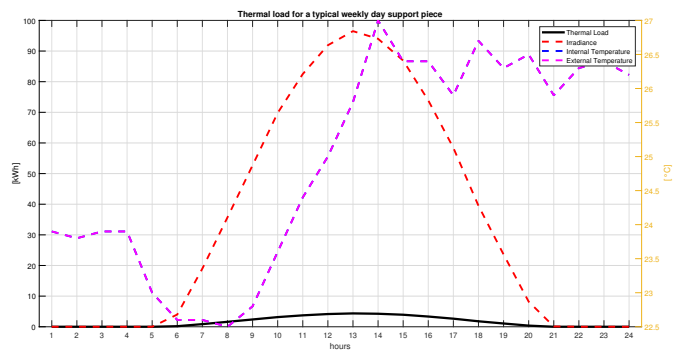


Figure 6.33: Thermal load profile for support piece in a Typical summer Day

6.3.3 Electronic devices load

The electronic devices loads profiles for the different pieces analyzed are reported:

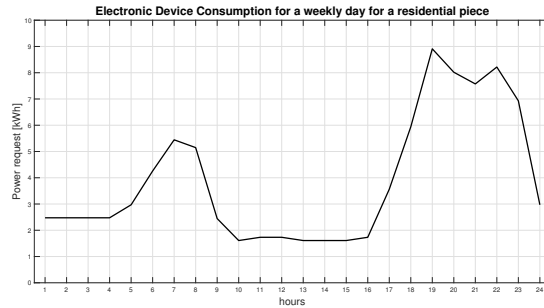


Figure 6.34: Electronic devices load profiles for residential piece in a Typical Day weekly

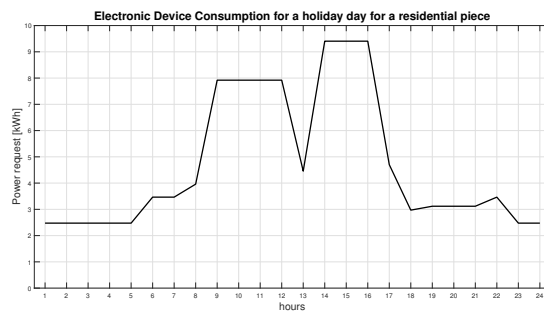


Figure 6.35: Electronic devices load profiles for residential piece in a Typical Day holiday

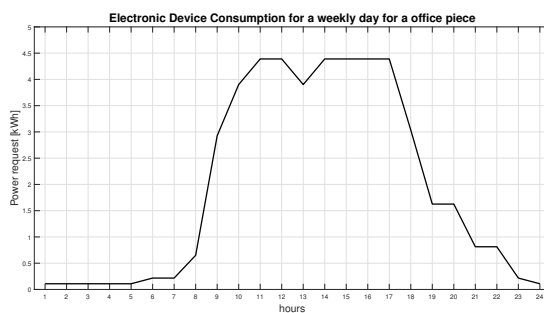


Figure 6.36: Electronic devices load profile for office piece in a Typical Day weekly

In a typical day of holiday the device consumption of the office is always null. As assumption the load of the support piece is always null.

6.3.4 Lighting load

The electronic devices load profiles for the different pieces analyzed are reported:

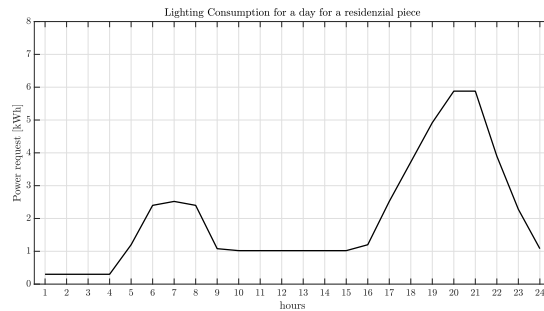


Figure 6.37: Lighting load profile for residential piece in a Typical Day weekly

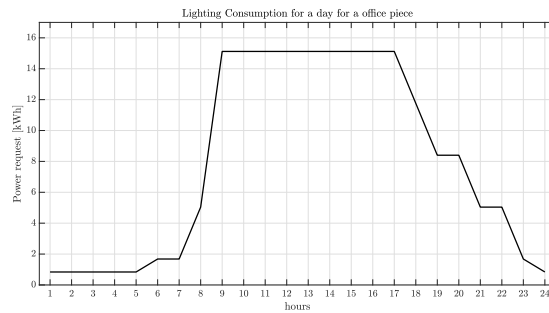


Figure 6.38: Lighting load profile for office piece in a Typical Day weekly

Regarding the external lighting load, it is expected that they follow the course of the dark hours of the place. The trend of the dark hours in Venice referring to 2022 it is reported and it is possible to see the normal decline during the summer months:

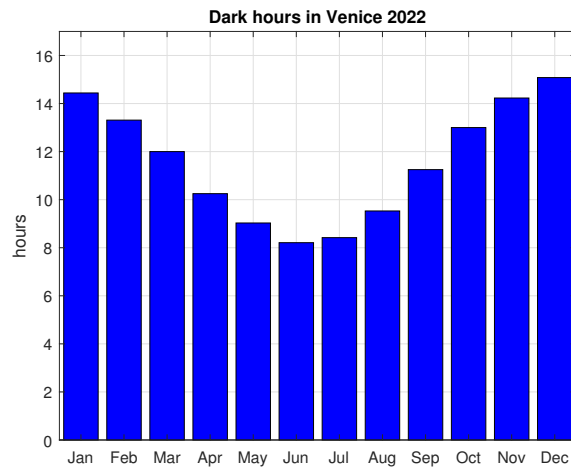


Figure 6.39: Dark hours in Venice 2022 [60]

6.3.5 Six uniform platforms case

As the first study tool developed, it was used to analyze a configuration of 6 platforms in which the three types of pieces are integrated. Specifically, each forum has the same structure, including four offices, eight residential, and nine support. The results obtained are commented on and presented below.

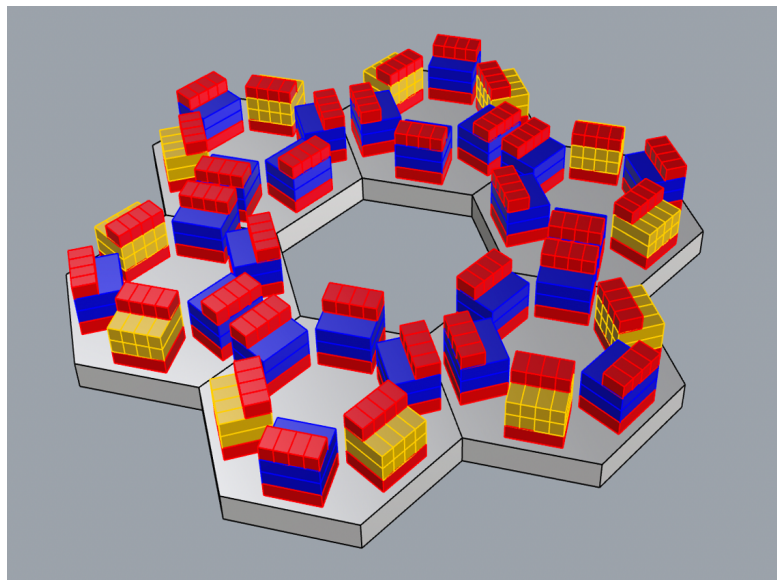


Figure 6.40: Configuration with pieces with different applications

6.3.6 Total load

The trend of the monthly load it is reported:

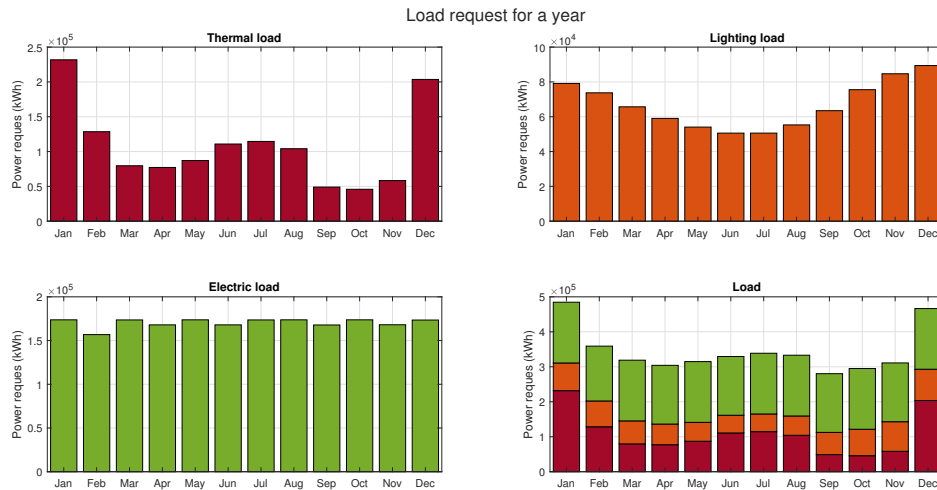


Figure 6.41: Total loads

The months in which the thermal demand, as could have been foreseen since it is an Italian climate zone E, is lower are March, April, May, September, and October. In contrast, the further months are, from the thermal point of view, the ones that require the most due to the substantial temperature differences between the outside temperature and the comfort temperature in winter and the high contribution from solar radiation in summer.

The electronic loads, as the tool has been estimated, are practically constant every day and undergo variations based on the season and the type of day (holidays and weekdays). Consequently, consumption differs monthly almost exclusively, as not all months have the same days.

The driver for the loads due to lighting, as already specified and as can be confirmed, is the dark hours.

A typical trend of daily loads is shown according to the season (winter or summer) and the type of day (working or weekday).

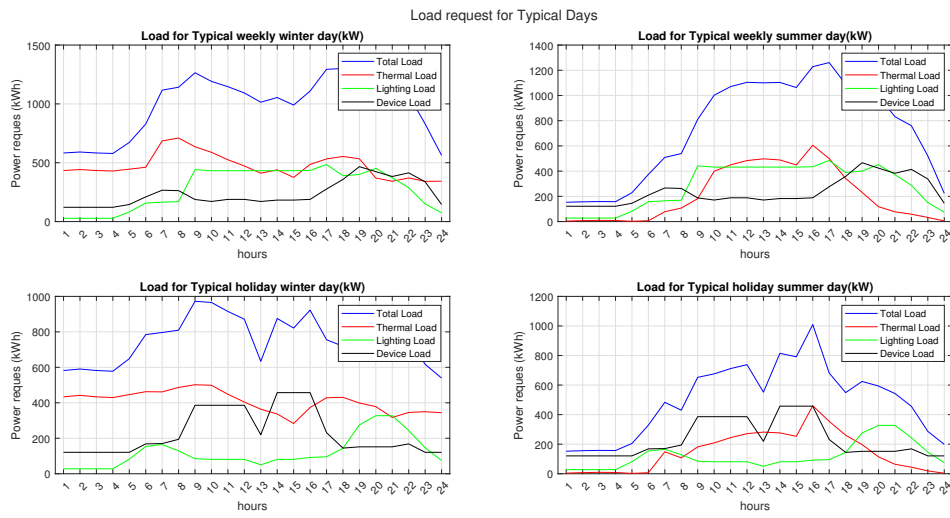


Figure 6.42: TDAY load case

6.4 Productivity Analysis

6.4.1 PV productivity

To carry out the productivity analysis of the photovoltaic panels of the case study, it was decided to proceed with panels with the following technical characteristic data:

| Data | Value |
|--|---------------|
| Standard efficiency η_{STC} | 0.18 |
| Inverter and MPPT efficiency η_{box} | 0.98 |
| Temperature coefficient of power λ | $-0.4\%/C$ |
| Cell temperature at STC | $25^{\circ}C$ |
| NOTC | $45^{\circ}C$ |
| Area of a panel | $1.7m^2$ |
| Performance ratio P_r | 0.7 |

Table 6.3: PV Technical Data

Considering that each building has an area of $120m^2$ for installing solar panels, the total available surface for photovoltaic panels is $4320m^2$.

The energy produced each month is shown below.

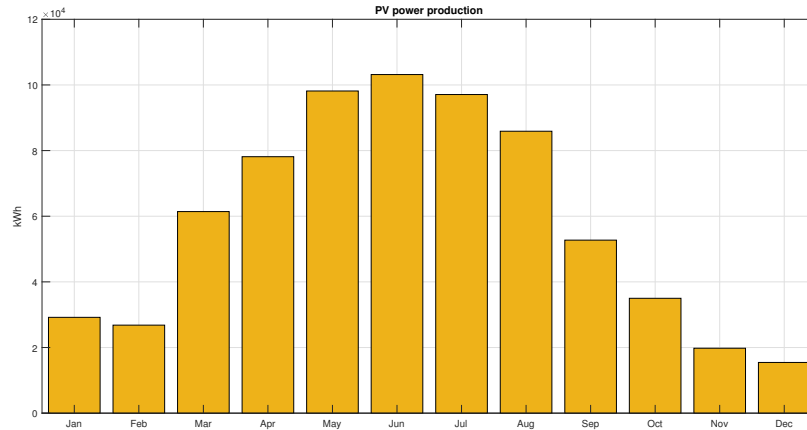


Figure 6.43: Monthly PV productivity

6.4.2 WT productivity

Reporting the trends of the two turbines explained in chapter 3, for the site in question, the preferable turbine is the one with the highest rated power and also the highest cut-in speed.

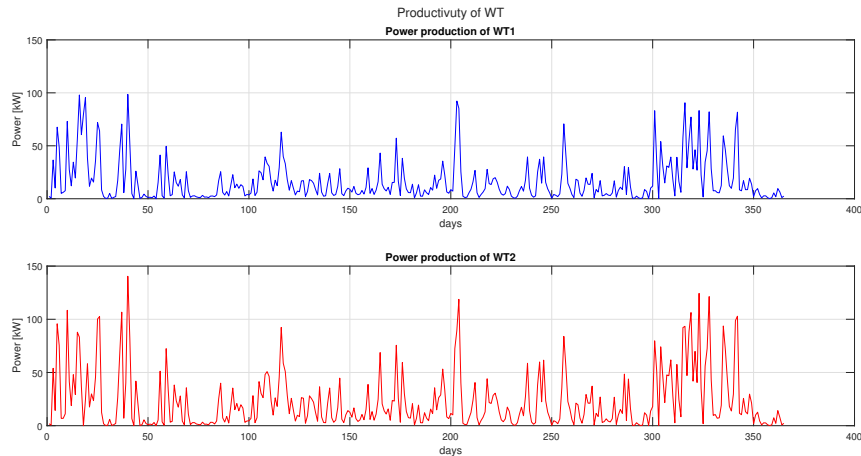


Figure 6.44: Annual production of wind turbines

To carry out the productivity analysis of wind turbine of the case study, it was decided to proceed with the second type presented in the "methodology", which have the following characteristic data:

| Data | Value |
|-------------------------|----------------|
| air density | 1.225 kg/m^3 |
| cut in speed | 2 m/s |
| cut out speed | 15 m/s |
| Performance ratio P_r | 0.90 |

Table 6.4: WT Technical Data

Assuming that each building has the possibility of hosting a turbine, the energy produced monthly is shown below:

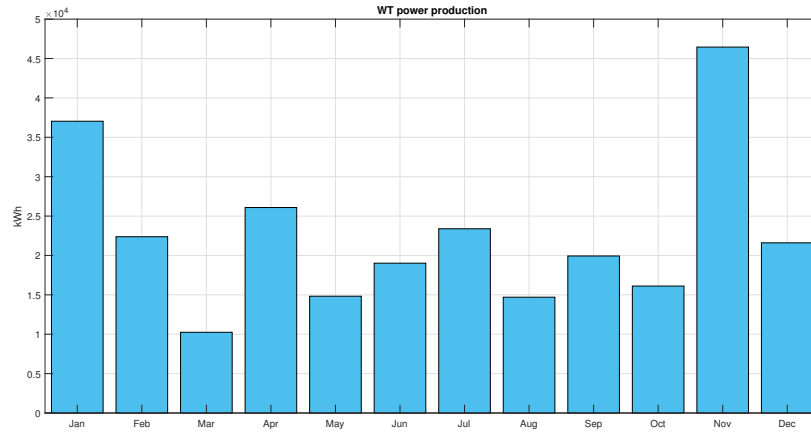


Figure 6.45: Monthly WT productivity

6.4.3 Renewable production

Summing the productivity of photovoltaic panels and wind turbines, it is possible to obtain the energy produced monthly. Since solar is the most abundant source in the chosen site, there will be a more lavish production during the summer season. In the winter months, the decrease in productivity due to solar energy is compensated for by the increase in wind productivity, due to higher winter speeds than in summer. For the case reported the RES power installed is around 1143 W (956 W of PV and 187 W of WT).

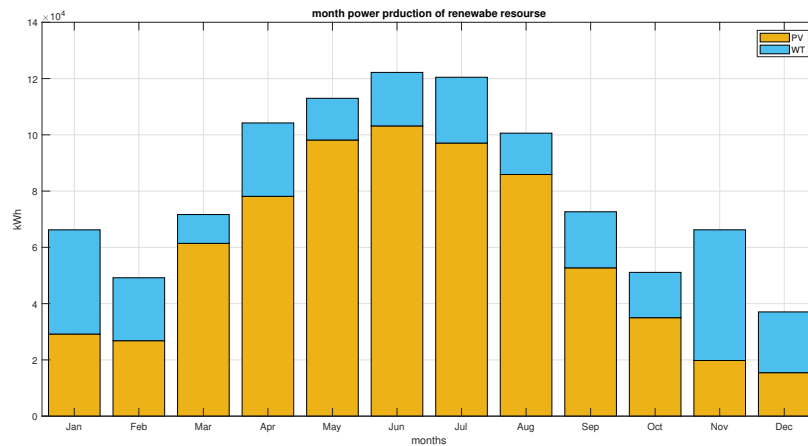


Figure 6.46: Monthly RES productivity

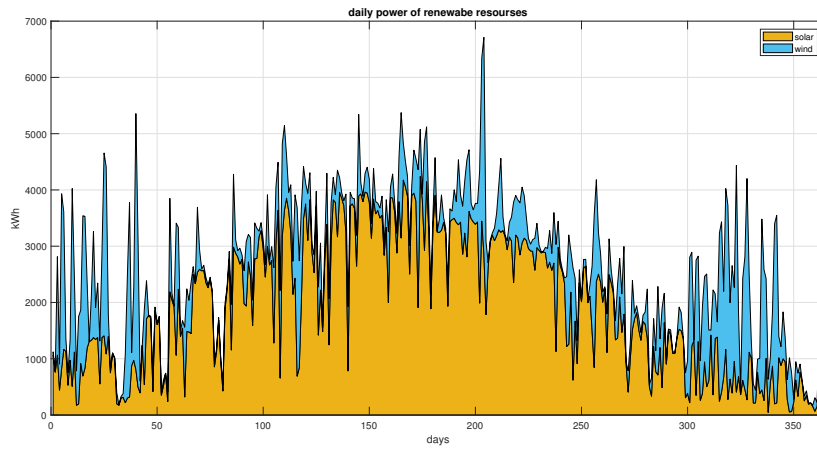


Figure 6.47: Daily RES productivity

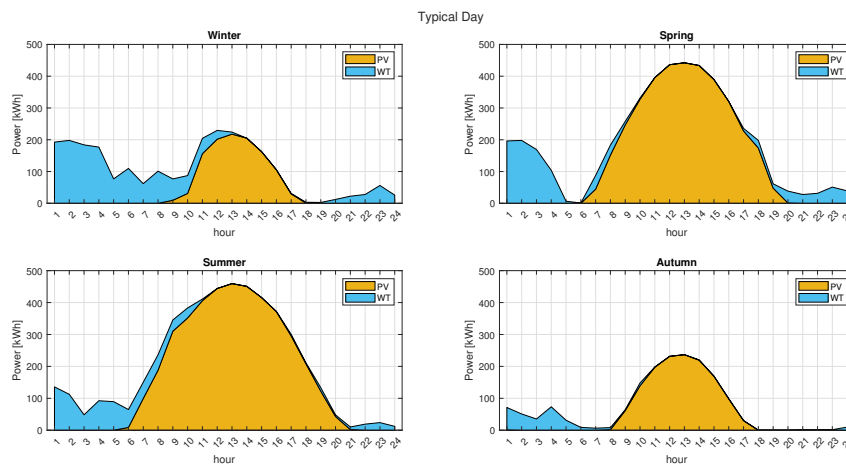


Figure 6.48: TDAYS renewable productivity

6.5 Storage and presentation of energy scenario

As already specified in the methodologies, the presence of a storage (battery bank) with the following specifications is therefore foreseen. For simplicity, the system is modeled considering a lithium battery storage system as the most common solution at the moment.

| Data | Value |
|-------------------------|-----------|
| Capacity | 605 kWh |
| System efficiency | 95% |
| DOD | 80% |
| Cycle durability at DoD | 7000 |
| Self discharge rate | 1 %/month |

Table 6.5: Battery bank specification: Li-ion [61]

Following the comparison between the energy produced and the energy request.

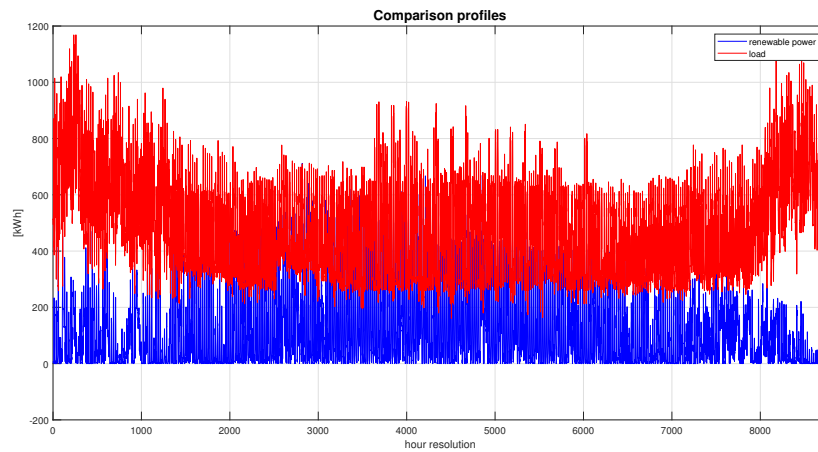


Figure 6.49: Comparison between renewable power and consumption in hour resolution

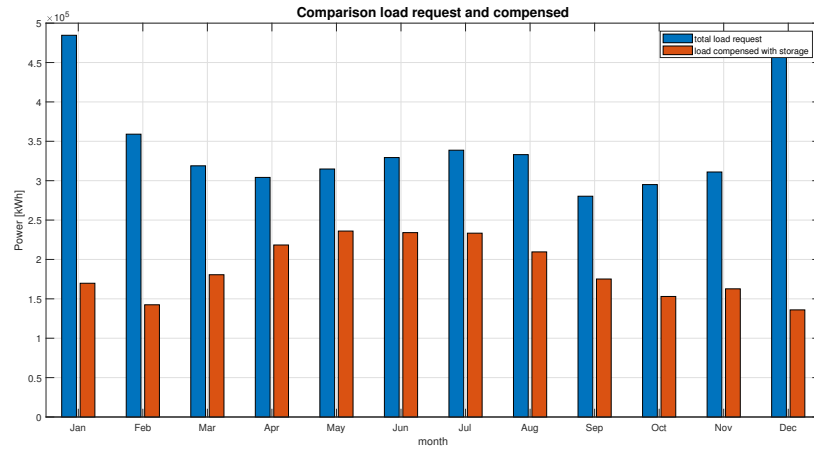


Figure 6.50: Monthly comparison between renewable power and consumption

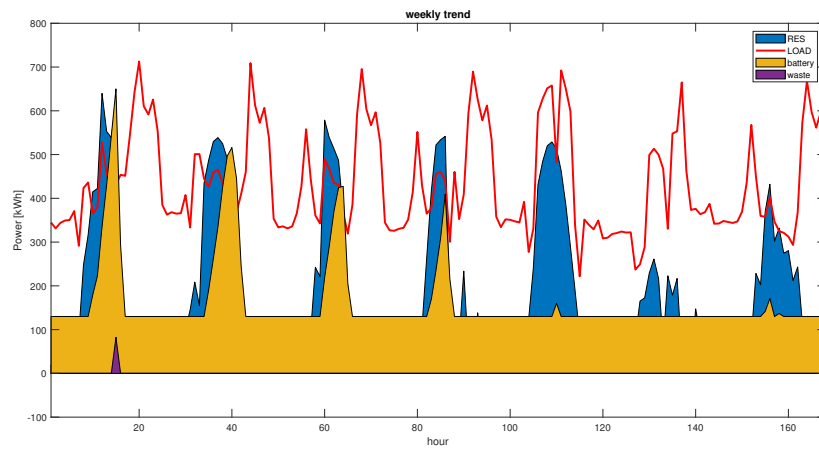


Figure 6.51: Characteristic spring weekly profile

Knowing the renewable energy profile that cannot be used as it is not used simultaneously by the platform and nest utilities, have wasted energy. All additional quests are planned to place them in the support pieces.

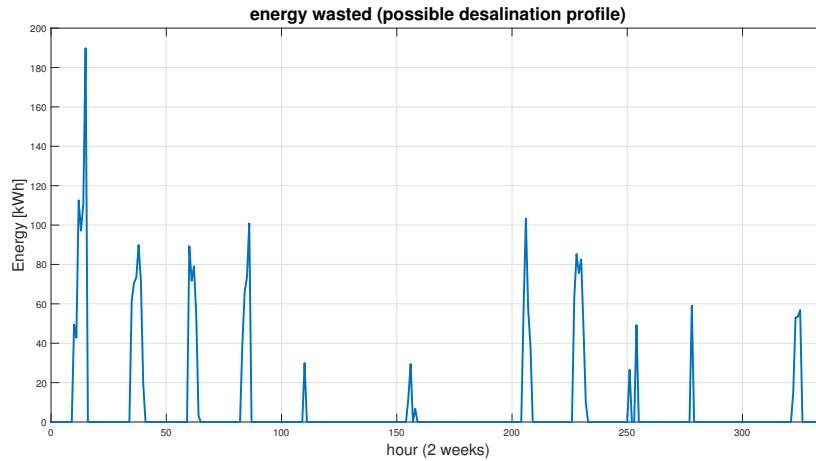


Figure 6.52: Waste energy profile

| | |
|------------------------------------|-----------|
| Total load request | 4.135 GWh |
| Total energy produced | 1.075 GWh |
| Total storage energy | 1.2 GWh |
| Total net load compensated | 1.05 GWh |
| Total load compensated | 2.25 GWh |
| Total energy wasted | 329 kWh |
| Total energy waste without storage | 0.017 GWh |

Table 6.6: Panoramic of energy scenario

| | |
|---|--------------------|
| Percentage of compensate load with storage | 54% |
| Area of a floating PV to compensate the load | 6200m ² |
| Percentage of compensate load without storage | 25% |
| Percentage of power waste with storage | 0% |
| Percentage of power waste without storage | 2% |

Table 6.7: Panoramic of energy percentage

As shown by the results, it is possible to cover only 54% of the expected consumption with this specific configuration. Consequently, other simulations must be carried out by changing the project configuration to find a more independent configuration. The appendix shows the results obtained from the study of two extreme configurations. Specifically, the analysis carried out was the following. It is clarified that we are far from energy independence exclusively with the support pieces.

It was decided to proceed by considering platforms exclusively for "energy" use (or "support"). On these platforms, the constraint of the buildings is removed, and therefore it is possible to increase the area of the photovoltaic panels. Specifically, we wanted to conduct a study to consider which of the office or residential use was more convenient. The result was that to power a platform used exclusively for residential use, one "energy" platform is required to cover 90% of consumption. In contrast, an energy platform is required to cover 100% of the consumption of two platform exclusively used as office. This result is very coherent given that the "office" consumption profile follows the typical trend of solar energy.

To compensate where it is impossible, not even with the aid of storage, to cover the energy needs, it is hypothesized to connect the floating city to a floating PV, given that it is the most profitable resource on the Venice site. The values obtained for the critical surface area in the examined case are unrealistic. For the other cases considered, the results obtained are already more realistic.

6.6 Techno-economic analysis

As regards the techno-economic analysis, the key performance indicator described in the methodology of the three cases are reported below: The following data are chosen to determinate the KPs:

$$LCOE = \frac{\sum_{k=1}^t \frac{CC_k + O\&M_k + Fk + Carbon_k + D_k}{(1+ir)^k}}{\sum_{k=1}^t \frac{E_k}{(1+ir)^k}} \quad (6.1)$$

- t: is the lifetime of the plant (30 years) ;
- CC: is the annual investment cost (tha data considered are reported in the metodology);
- O&M: is the annual cost of operation and maintenance (tha data considered are reported in the metodology);
- F: is the annual cost for fuel (it is not considered);
- Carbon: is the carbon cost (it is not considered);
- D: is the cost for decommissioning and waste management (it is not considered);
- E: is the electricity produced annually;
 - the total energy produced for the theoretical LCOE
 - the real usefull energy for the real LCOE
- ir: is the discount rate; (7%)

$$LCOS = \frac{\sum_{k=1}^t \frac{C_{cap} + O\&M_k + C_{rep} + C_{EL}}{(1+ir)^k}}{\sum_{k=1}^t \frac{E_k}{(1+ir)^k}} \quad (6.2)$$

- Ccap is the annual capital cost of the investment (the data considered are reported in the metodology);
- O&M is the annual cost of operation and maintenance (the data considered are reported in the metodology) ;
- Crep is the annualized cost for replacement (it is not considered);
- CEL is the annualized cost for disposal and recycling (it is not considered);
- Ey is the annual electricity discharged;

| Component | Investment Cost per kW [euro/kW] |
|-----------------------------|----------------------------------|
| Wind Turbine (WT) | 2000 [44] |
| Photovoltaic Collector | 1070 |
| Floating PV | 700 [45] |
| Wave Energy Converter (WEC) | 2890 |
| Batteries | 450 [euro/kWh] |

Table 6.8: Investment Cost per kW for each component of the system [46] [47]

| | CASE I | CASE II(appendix) | CASE III (appendix) |
|----------------------|---------------------|---------------------|---------------------|
| $LCOE_{real}$ | 74 <i>euro/MWh</i> | 122 <i>euro/MWh</i> | 123 <i>euro/MWh</i> |
| $LCOE_{theoretical}$ | 73 <i>euro/MWh</i> | 73 <i>euro/MWh</i> | 74 <i>euro/MWh</i> |
| LCOS | 256 <i>euro/MWh</i> | 233 <i>euro/MWh</i> | 205 <i>euro/MWh</i> |
| $LCOE_{system}$ | 220 <i>euro/MWh</i> | 253 <i>euro/MWh</i> | 233 <i>euro/MWh</i> |

Table 6.9: KPs of the different cases

The purpose of this section is to provide a basic comparison. Subsidies, fuel costs, or the price of CO₂ are not considered. The results obtained can be compared with the publication of bank Lazard [62]: which determines that utility-scale photovoltaics has an average LCOE starting from a minimum of 28-37 dollars per MWh (27-36 euros/MWh) to a maximum of 30-41 dollars/MWh (29-39 euros/MWh) based on the technology of the photovoltaic panels used. While for wind, the minimum LCOE is around 26 dollars/MWh (25 euros/kWh). In the indices presented, the contribution of the floating PV has not been added; therefore, once this technology is also sized, it will undoubtedly be necessary to add its contribution. The fact that real LCOE and theoretical LCOE are similar should indicate that the resource mix matches well with the load. In the applied case, instead the reason is that is not possible to compensate all the needs and the energy not instantly exploited is a low percentage. As regards the other two cases considered, the discrepancy between the theoretical and real LCOE is because the energy system has yet to be optimized, therefore is a need for a future improvement of the tool from this point of view.

Chapter 7

Conclusion and future work

This study shows the methodology used to perform an energy feasibility analysis of a system of interconnected floating platforms. In particular, a Matlab tool has been developed.

Having as input the site's meteorological data and the project's data to be carried out, it can provide an analysis of the production of resources of the site and an estimate of productivity and energy consumption. The tool is also developed to offer the value of the LCOE to carry out primary technical-economic analyses.

The tool's ultimate goal is to carry out energy assessments in the initial selection of the site and the project to be carried out. The new SeaForm project has the macro-objective of creating future living spaces that arise in the sea to cope with environmental problems.

In addition to the economic and legal analysis, it is, therefore, advantageous to evaluate how much the energy mix of the chosen site can correspond to the project to be implemented.

Venice was chosen as the first location for obvious social reasons. Consequently, the thesis reports the study of the possible configurations studied in this locality. The most relevant result is that to be completely self-sufficient from an energy point of view, the presence of "support platforms" is indispensable, whose existence is indispensable and exclusively for producing energy. The result was that one "energy" platform is needed to cover around 90% of the consumption of a platform used exclusively for residential use. In contrast, half of the energy platform is needed to cover all the consumption of a platform used exclusively for offices. This result is coherent, given that the "office" consumption profile follows the typical pattern of solar energy, which is the most exploitable resource on this site.

The future goal is certainly to implement the tool following the improvement presented in the paragraph "Criticalities of the model and future improvements". In particular, the design of the exhibition pavilion for the Venice Biennale 2024 is a new project that is currently starting. The pavilion will consist of 3 platforms: a "support", an "exhibition", and an "experience" with the intent to host a vertical farm. It will therefore be necessary to implement the tool by inserting these new uses of the spaces, defining the new set points.

Appendix A

Appendix

A.1 TMY parameter

The trends of other meteorological parameters as output of TMY, that can be important for a site analysis, are also shown below:

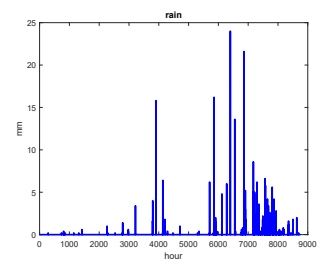
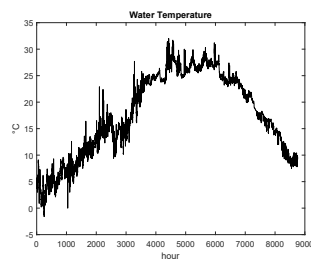


Figure A.1: TMY Water temperature

Figure A.2: TMY Rain profile

Sea surface temperature measurements are limited to the upper portion of the sea known as the near-surface layer. The sea surface temperature undergoes changes on a daily scale, but to a much lesser extent than the temperature of the overlying air mass due to the higher specific heat of the water than the air.

Note that October is the month with the highest number of cases with large amounts of rain. The figure also shows that, while the rain gradually decreases from January to July, it grows very rapidly after the summer, returning to maximum values in three months.

A.2 Other cases

The two cases in which the support platforms are considered are presented below. Therefore, this kind of platform is only used for energy generation, and the surface area of the installed solar panels is consequently increased.

CASE II: only residential platform

The installed nominal power rises to around 1.7MW due to that in this case there are 3 platforms with residential building and 3 support platforms. Following the comparison between the Power produced and the power request.

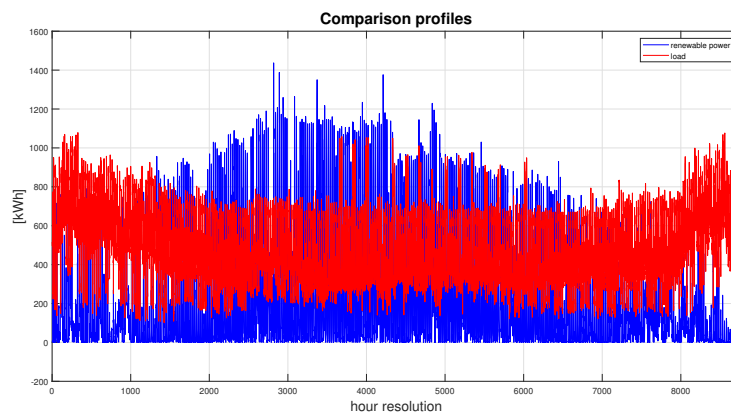


Figure A.3: Comparison between renewable power and consumption in hour resolution

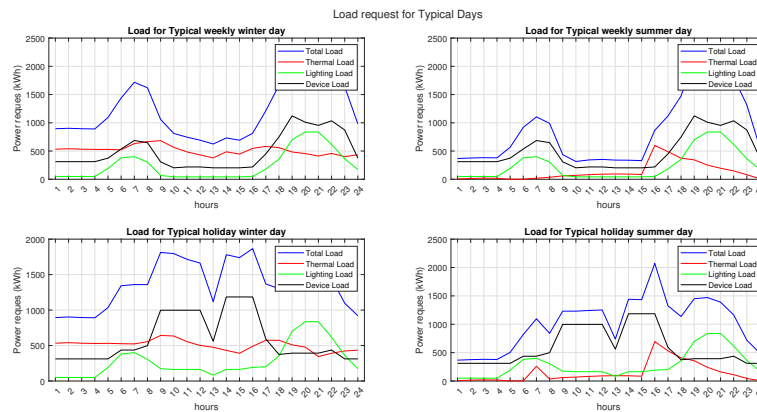


Figure A.4: Load consumption for typical days

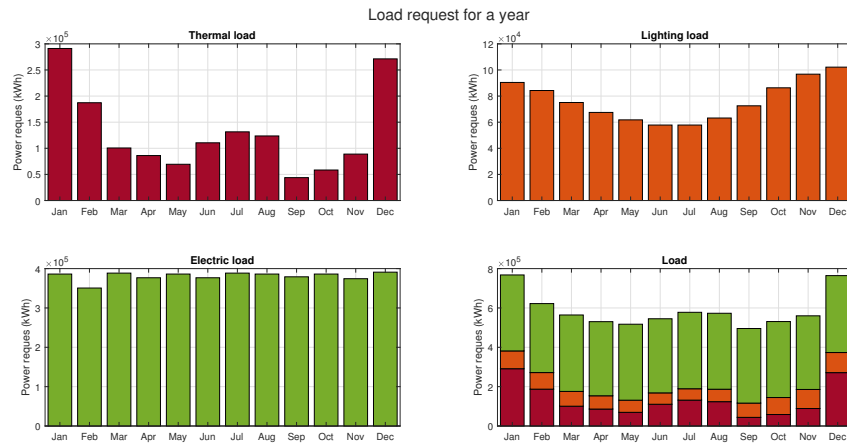


Figure A.5: Monthly load consumption

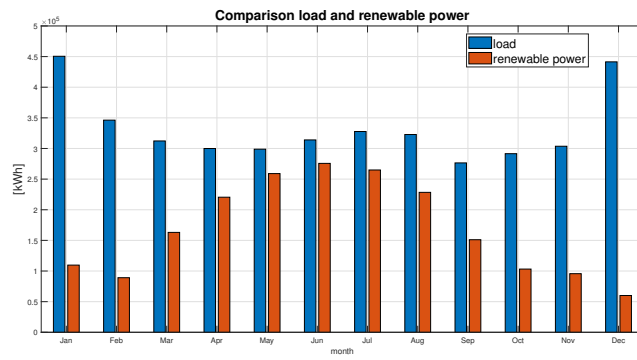


Figure A.6: Monthly comparison between renewable power and consumption

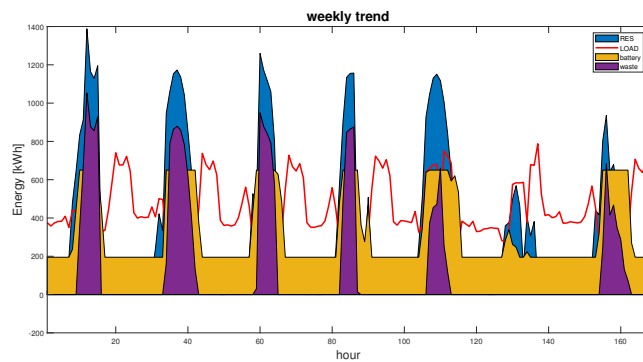


Figure A.7: Characteristic spring weekly profile

Knowing the renewable energy profile that cannot be used as it is not used simultaneously by the platform and nest utilities, have wasted energy. All additional quests are planned to place them in the support pieces.

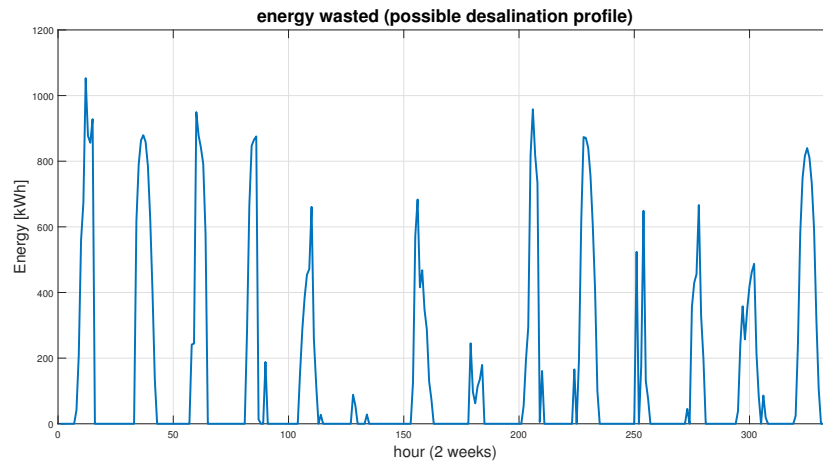


Figure A.8: Waste energy profile

CASE III: only office platform

The installed nominal power rises to around 1.4 MW due to that in this case there are 4 platforms with office building and 2 support platforms.

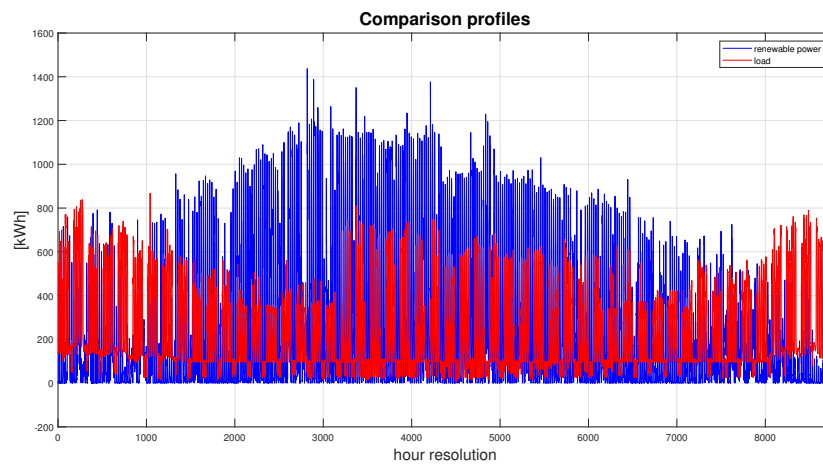


Figure A.9: Comparison between renewable power and consumption in hour resolution

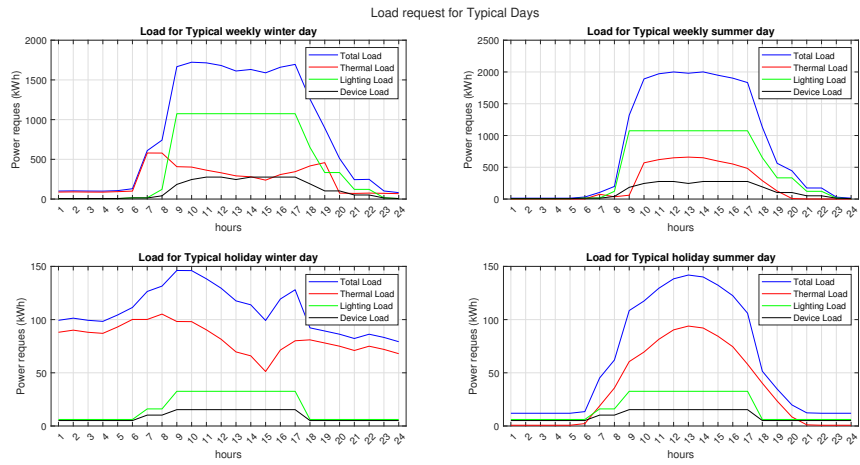


Figure A.10: Load consumption for typical days

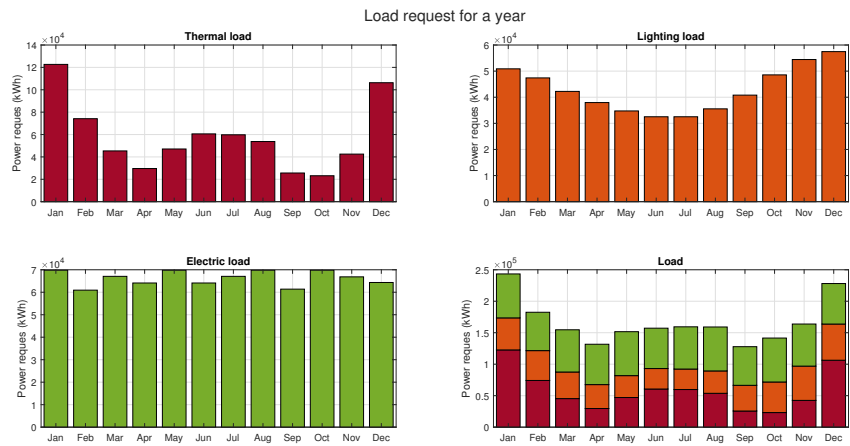


Figure A.11: Monthly load consumption

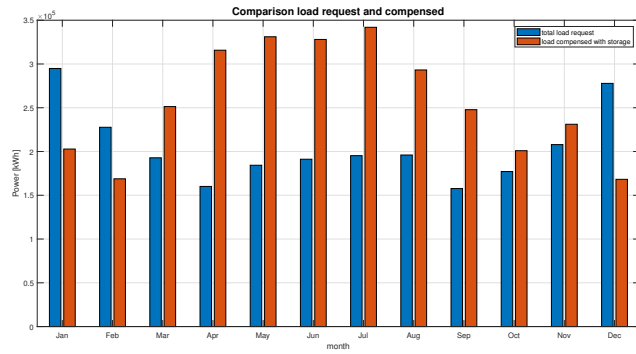


Figure A.12: Monthly comparison between renewable power and load consumption

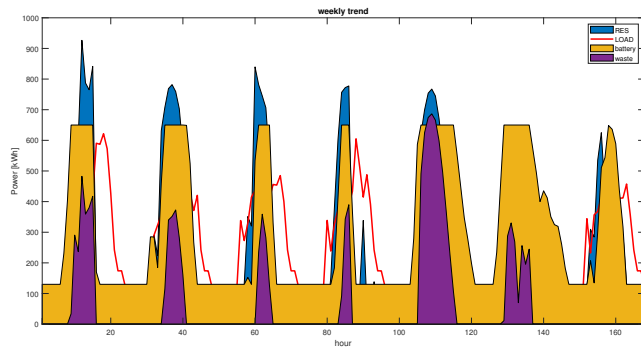


Figure A.13: Characteristic spring weekly profile

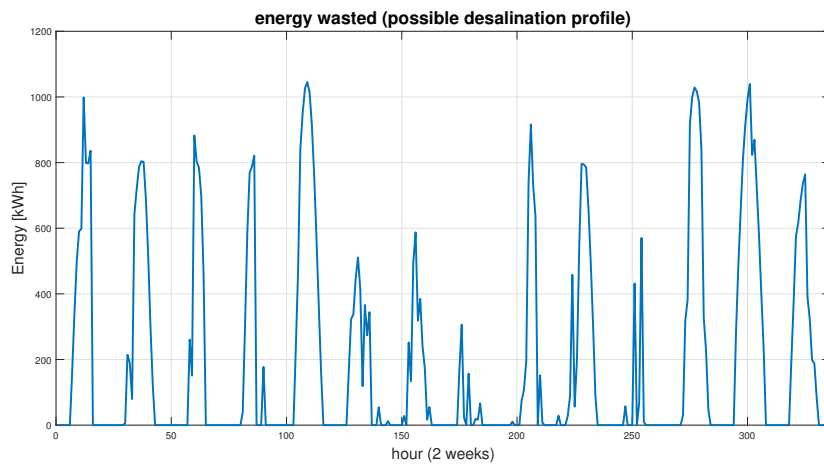


Figure A.14: Waste energy profile

| | CASE II | CASE III |
|----------------------------|-----------|-----------|
| Total load request | 3.68 GWh | 2.48 GWh |
| Total energy produced | 1.62 GWh | 1.44 GWh |
| Total storage energy | 2.05 GWh | 2.06 GWh |
| Total net load compensated | 1.12 GWh | 1.02 GWh |
| Total load compensated | 3.16 GWh | 3.07 GWh |
| Total energy wasted | 0.365 kWh | 0.423 GWh |

Table A.1: Panoramic of energy scenarios

| | CASE II | CASE III |
|---|--------------------|----------|
| Percentage of compensate load with storage | 86% | 124% |
| Area of floating PV to compensate | 1712m ² | – |
| Percentage of compensate load without storage | 30% | 41% |
| Percentage of power waste with storage | 31% | 21% |
| Percentage of power waste without storage | 23% | 29% |

Table A.2: Panoramic of energy percentages

Bibliography

- [1] «<https://buildingcue.it/oceanix-city-prima-citta-galleggiante/25865/>». In: () (cit. on p. 6).
- [2] «<https://maldivesfloatingcity.com/>». In: () (cit. on p. 6).
- [3] «<https://www.neom.com/en-us/regions/oxagon>». In: () (cit. on p. 7).
- [4] «<https://schoonschipamsterdam.org>». In: () (cit. on p. 8).
- [5] «<https://www.urbanrigger.com/about-us/>». In: () (cit. on p. 9).
- [6] «<https://oceanbuilders.com>». In: () (cit. on p. 9).
- [7] Thomas Bauwens. «Explaining the diversity of motivations behind community renewable energy». In: *Energy Policy* 93 (June 2016), pp. 278–290. ISSN: 03014215. DOI: 10.1016/j.enpol.2016.03.017 (cit. on p. 11).
- [8] F. Wittmann, C. Schmitt, F. Adam, and P. Dierken. «Evaluation of the energy demands for a floating O & M-hub». In: *Journal of Ocean Engineering and Marine Energy* 7 (2 May 2021), pp. 211–227. ISSN: 21986452. DOI: 10.1007/s40722-021-00191-1 (cit. on p. 11).
- [9] T Givler and P Lilienthal. *Using HOMER® Software, NREL’s Micropower Optimization Model, to Explore the Role of Gen-sets in Small Solar Power Systems Case Study: Sri Lanka*. 2005. URL: <http://www.osti.gov/bridge> (cit. on p. 11).
- [10] «<https://www.lumi4innovation.it/smart-grid-cose-e-cosa-significa>». In: () (cit. on p. 12).
- [11] Daniel Burmester, Ramesh Rayudu, Winston Seah, and Daniel Akinyele. *A review of nanogrid topologies and technologies*. Jan. 2017, pp. 760–775. DOI: 10.1016/j.rser.2016.09.073 (cit. on p. 12).
- [12] «<https://www.canaleenergia.com/interviste-video/microgrid-un-tema-attuale-anche-in-occidente-tra-isole-e-aree-isolate/>». In: () (cit. on p. 12).
- [13] S Wilcox and W Marion. *Innovation for Our Energy Future Users Manual for TMY3 Data Sets*. 1994 (cit. on pp. 15, 16).

- [14] Giovanni Murano, Politecnico Di Torino, and Paolo Baggio. *Definizione degli anni tipo climatici delle province del Nord Italia*. 2010 (cit. on p. 15).
- [15] Abdulsalam Ebrahimpour and Mehdi Maerefat. «A method for generation of typical meteorological year». In: *Energy Conversion and Management* 51 (3 Mar. 2010), pp. 410–417. ISSN: 01968904. DOI: 10.1016/j.enconman.2009.10.002 (cit. on p. 15).
- [16] I J R Hall, R R Prairie, H E Anderson, and E C Boes. *Generation of Typical Meteorological Years for 26 SOLMET Stations*. 1978 (cit. on p. 17).
- [17] *The IPCC Special Report on Renewable Energy Sources and Climate Change Mitigation* (cit. on p. 18).
- [18] Elaine K. Hart, Eric D. Stoutenburg, and Mark Z. Jacobson. «The Potential of Intermittent Renewables to Meet Electric Power Demand: Current Methods and Emerging Analytical Techniques». In: *Proceedings of the IEEE* 100.2 (2012), pp. 322–334. DOI: 10.1109/JPROC.2011.2144951 (cit. on p. 18).
- [19] H. Lund. «Large-scale integration of optimal combinations of PV, wind and wave power into the electricity supply». In: *Renewable Energy* 31.4 (2006), pp. 503–515. ISSN: 0960-1481. DOI: <https://doi.org/10.1016/j.renene.2005.04.008>. URL: <https://www.sciencedirect.com/science/article/pii/S0960148105000893> (cit. on p. 18).
- [20] Christina E. Hoicka and Ian H. Rowlands. «Solar and wind resource complementarity: Advancing options for renewable electricity integration in Ontario, Canada». In: *Renewable Energy* 36.1 (2011), pp. 97–107. ISSN: 0960-1481. DOI: <https://doi.org/10.1016/j.renene.2010.06.004>. URL: <https://www.sciencedirect.com/science/article/pii/S0960148110002600> (cit. on p. 18).
- [21] F. Monforti, T. Huld, K. Bódis, L. Vitali, M. D’Isidoro, and R. Lacal-Arántegui. «Assessing complementarity of wind and solar resources for energy production in Italy. A Monte Carlo approach». In: *Renewable Energy* 63 (2014), pp. 576–586. ISSN: 0960-1481. DOI: <https://doi.org/10.1016/j.renene.2013.10.028>. URL: <https://www.sciencedirect.com/science/article/pii/S0960148113005594> (cit. on p. 18).
- [22] Lucy Cradden, Hakim Mouslim, Olivier Duperray, and David Ingram. «Joint exploitation of wave and offshore wind power». In: Sept. 2011 (cit. on p. 18).
- [23] Gordon Reikard, Bryson Robertson, and Jean-Raymond Bidlot. «Combining wave energy with wind and solar: Short-term forecasting». In: *Renewable Energy* 81 (2015), pp. 442–456. ISSN: 0960-1481. DOI: <https://doi.org/10.1016/j.renene.2015.03.032>. URL: <https://www.sciencedirect.com/science/article/pii/S0960148115002141> (cit. on p. 19).

- [24] F Cumo, F Nardecchia, A D' Angelo, B De, Lieto Vollaro, and C Romeo. *Misure energetiche di un edificio a elevate prestazioni. Confronto tra dati derivanti da calcolo e dati effettivi* MINISTERO DELLO SVILUPPO ECONOMICO (cit. on p. 27).
- [25] «<https://www.energy.gov/eere/downloads/reference-buildings-building-type-midrise-apartment>». In: () (cit. on pp. 30, 37, 38, 40, 41).
- [26] Marco Citterio and Gaetano Fasano. *Indagine sui consumi degli edifici pubblici (direzionale e scuole) e potenzialità degli interventi di efficienza energetica* (cit. on p. 33).
- [27] «ASHRAE, Procedures for Commercial Buildings Energy Audit,» in: () (cit. on p. 35).
- [28] «ANSI/ASHRAE RP-669/SP-56. Atlanta, GA: American Society of Heating, Refrigerating and Air- Conditioning Engineers, Inc., 2004». In: () (cit. on p. 35).
- [29] S Sibilio, A D' Agostino, M Fatigati, and M Citterio. *Valutazione dei consumi nell'edilizia esistente e benchmark mediante codici semplificati: analisi di edifici residenziali* (cit. on p. 39).
- [30] G Fasano, C Romeo, M Zinzi, P Signoretti, D Iatauro, G Centi, B Di Pietra, and E Costanzo. *Sviluppo di metodologie, strumenti di misura ed analisi dei consumi energetici degli edifici* MINISTERO DELLO SVILUPPO ECONOMICO (cit. on pp. 40, 41).
- [31] <https://www.pgcasa.it/articoli/illuminazione/quantilumen-occorrono-per-illuminare-una-camera14147> (cit. on p. 42).
- [32] «<https://areasosta.com/domande-frequenti/quantilux-per-strada>». In: () (cit. on p. 42).
- [33] Xin Shen, Zhao Luo, Jun Xiong, Hongzhi Liu, Xin Lv, Taiyang Tan, Jianwei Zhang, Yuting Wang, and Yinghao Dai. «Optimal Hybrid Energy Storage System Planning of Community Multi-Energy System Based on Two-Stage Stochastic Programming». In: *IEEE Access* 9 (2021), pp. 61035–61047. ISSN: 21693536. DOI: 10.1109/ACCESS.2021.3074151 (cit. on p. 44).
- [34] «ArticoloMaggioreEvoluzioneCurveCarico». In: () (cit. on p. 45).
- [35] Ajai Gupta, R. P. Saini, and M. P. Sharma. «Steady-state modelling of hybrid energy system for off grid electrification of cluster of villages». In: *Renewable Energy* 35 (2 Feb. 2010), pp. 520–535. ISSN: 09601481. DOI: 10.1016/j.renene.2009.06.014 (cit. on pp. 48, 50).

- [36] D. O. Akinyele, R. K. Rayudu, and N. K.C. Nair. «Grid-independent renewable energy solutions for residential use: The case of an off-grid house in wellington, New Zealand». In: vol. 2016-January. IEEE Computer Society, Jan. 2016. ISBN: 9781467381321. DOI: 10.1109/APPEEC.2015.7380969 (cit. on pp. 48, 49).
- [37] «<https://github.com/NREL/turbine-models/tree/master/Distributed>». In: () (cit. on p. 50).
- [38] Yanhui Qiao, Yongqian Liu, Yang Chen, Shuang Han, and Luo Wang. «Power Generation Performance Indicators of Wind Farms Including the Influence of Wind Energy Resource Differences». In: *Energies* 15 (5 Mar. 2022). ISSN: 19961073. DOI: 10.3390/en15051797 (cit. on p. 51).
- [39] Philipp Beiter, Walt Musial, Patrick Duffy, Aubryn Cooperman, Matt Shields, Donna Heimiller, and Mike Optis. *The Cost of Floating Offshore Wind Energy in California Between 2019 and 2032 Cost and Performance Results Data*. URL: www.nrel.gov/publications. (cit. on p. 56).
- [40] IEEE Industry Applications Society, Denki Gakkai (1888). Sangyō Ōyō Bumon, Chōllyōk Chonja Hakhoe, Zhongguo dian gong ji shu xue hui, IEEE Power Electronics Society, European Power Electronics, Drives Association, Institute of Electrical, and Electronics Engineers. *The 2014 International Power Electronics Conference - ECCE ASIA - IPEC-Hiroshima 2014 : Power Electronics for Peaceful World : May 18th-21st, 2014, International Conference Center Hiroshima*, p. 3370. ISBN: 9781479927050 (cit. on pp. 56, 58).
- [41] Riccardo Novo, Francesco Demetrio Minuto, Giovanni Bracco, Giuliana Matti-
azzo, Romano Borchiellini, and Andrea Lanzini. «Supporting Decarbonization Strategies of Local Energy Systems by De-Risking Investments in Renewables: A Case Study on Pantelleria Island». In: *Energies* 15 (3 Feb. 2022). ISSN: 19961073. DOI: 10.3390/en15031103 (cit. on p. 56).
- [42] «<https://www.iea.org/reports/projected-costs-of-generating-electricity-2020>». In: () (cit. on p. 56).
- [43] Riccardo Novo, Francesco Demetrio Minuto, Giovanni Bracco, Giuliana Matti-
azzo, Romano Borchiellini, and Andrea Lanzini. «Supporting Decarbonization Strategies of Local Energy Systems by De-Risking Investments in Renewables: A Case Study on Pantelleria Island». In: *Energies* 15.3 (2022). ISSN: 1996-1073. DOI: 10.3390/en15031103. URL: <https://www.mdpi.com/1996-1073/15/3/1103> (cit. on pp. 58, 59).

- [44] Alessandro Bianchini, Galih Bangga, Ian Baring-Gould, Alessandro Croce, José Ignacio Cruz, Rick Damiani, Brent Summerville, David Wood, and Alice Orrell. «Current status and grand challenges for small wind turbine 1 technology». In: *Christian Navid Nayeri* 8 (), p. 14. DOI: 10.5194/wes-2022-34. URL: <https://doi.org/10.5194/wes-2022-34> (cit. on pp. 58, 59, 105).
- [45] Hassan Gholami and Harald Nils Røstvik. «Levelised cost of electricity (Lcoe) of building integrated photovoltaics (bipv) in europe, rational feed-in tariffs and subsidies». In: *Energies* 14 (9 May 2021). ISSN: 19961073. DOI: 10.3390/en14092531 (cit. on pp. 58, 59, 105).
- [46] Aikaterini Anastasopoulou, Sughosh Butala, Bhaskar Patil, John Suberu, Martin Fregene, Juergen Lang, Qi Wang, and Volker Hessel. «Techno-economic feasibility study of renewable power systems for a small-scale plasma-assisted nitric acid plant in Africa». In: *Processes* 4 (4 Dec. 2016). ISSN: 22279717. DOI: 10.3390/pr4040054 (cit. on pp. 58, 105).
- [47] Michael Taylor, Andrei Ilas, and Pablo Ralon. *Renewables: The True Costs* (cit. on pp. 58, 105).
- [48] F. Wittmann, C. Schmitt, F. Adam, and P. Dierken. «Evaluation of the energy demands for a floating O & M-hub». In: *Journal of Ocean Engineering and Marine Energy* 7 (2 May 2021), pp. 211–227. ISSN: 21986452. DOI: 10.1007/s40722-021-00191-1 (cit. on p. 60).
- [49] W A Prins. *An energy efficiency study on the Ocean Battery together with hydrogen conversion*. 2021 (cit. on p. 61).
- [50] *Revenue maximization of distributed Ocean Battery systems through Model Predictive Control* (cit. on p. 61).
- [51] <https://www.green.it/ocean-battery/> (cit. on p. 61).
- [52] <https://www.comune.venezia.it/> (cit. on p. 63).
- [53] «<https://climate-adapt.eea.europa.eu/>». In: () (cit. on p. 64).
- [54] «<https://www.mosevenezia.eu/>». In: () (cit. on p. 64).
- [55] *DATI STATISTICI SULL'ENERGIA ELETTRICA IN ITALIA* (cit. on p. 64).
- [56] «<https://www.terna.it/it/>». In: () (cit. on p. 64).
- [57] «<https://www.comune.venezia.it/it/content/3-piattaforma-ismar-cnr>». In: () (cit. on p. 69).

- [58] Sara Oliveira-Pinto, Paulo Rosa-Santos, and Francisco Taveira-Pinto. «Assessment of the potential of combining wave and solar energy resources to power supply worldwide offshore oil and gas platforms». In: *Energy Conversion and Management* 223 (Nov. 2020). ISSN: 01968904. DOI: 10.1016/j.enconman.2020.113299 (cit. on p. 84).
- [59] G Centi, D Iatauro, S Morigoni, C Romeo, P Signoretti, and L Terrinoni. *Valutazione delle prestazioni energetiche (EP) negli edifici nZEB MINISTERO DELLO SVILUPPO ECONOMICO* (cit. on p. 87).
- [60] «<https://miocalendario.com/albe-tramonti/?citta=VE>». In: () (cit. on p. 92).
- [61] Verena Jülch. «Comparison of electricity storage options using levelized cost of storage (LCOS) method». In: *Applied Energy* 183 (Dec. 2016), pp. 1594–1606. ISSN: 03062619. DOI: 10.1016/j.apenergy.2016.08.165 (cit. on p. 99).
- [62] «<https://www.lazard.com/>». In: () (cit. on p. 105).